3-19-2014

Design, Simulation, Prototype, and Testing of a Notched Blade Energy Generation System

Henry Cabra
University of South Florida, hcabra@mail.usf.edu

Design, Simulation, Prototype, and Testing of a Notched Blade Energy Generation System

by

Henry Cabra

A dissertation submitted in partial fulfillment
of the requirements for the degree of
Doctor of Philosophy
Department of Electrical Engineering
College of Engineering
University of South Florida

Major Professor: Sylvia W. Thomas, Ph.D.
Paris Wiley, Ph.D.
Jing Wang, Ph.D.
Susana Lai Yuen, Ph.D.
Lennox Hoyte, Ph.D.

Date of Approval:
March 19, 2014

Keywords: Cross-flow turbine, permanent magnet, brushless motor, miniaturized-turbine, power generation

DEDICATION

I dedicate my dissertation work to my wife Paula, my daughter Sophia, immediate and extended family, and friends for their support.

ACKNOWLEDGMENTS

I would like to express infinite thanks to God, my Wife, my Daughter, and my family because they are the inspiration and the reason for my life; they have stood by my side always to support, encourage, and wait for me patiently over the past years, sacrificing dreams and time for this goal, which is our goal.

I would like to express my profound appreciation to my PhD supervisor Dr. Sylvia Thomas, whose guidance, support and encouragement helped me in all my research.

I would like to thank Dr. Lennox Hoyte, Dr. Paris Wiley, Dr. Jing Wang, and Dr. Susana Lai Yuen for their support as my dissertation committee members.

I am also very grateful to my brother in law, Alex Lezama, for his wit and ingenious support in the assembly of the prototypes, as well as with the formatting of the final manuscript.

Furthermore, I would like to thank all AMBIR group members, especially my friend Samuel Perez for his personal and professional support.

Finally, I would like to thank Mr. Bernard Batson, the USF Graduate School, and the Electrical Engineering Department.

TABLE OF CONTENTS

LIST OF TABLES

LIST OF FIGURES

ABSTRACT

This dissertation addresses the design, simulation, prototype, and test of a new energy generation system, which transforms rotational motion into electricity by the use of an innovative turbine-generator. The system is divided in two assembled subsystems that interact to finally transform kinetic energy into electricity. The first subsystem is a miniaturized notched impulse turbine system, and the second one is a millimeter permanent magnet generator (PMG) assembled into the turbine.

The conversion of biomechanical energy to electric energy, using clean and free energy produced by a living organism, is being increasingly researched [1]–[11]. These are all viable options, but advantages and disadvantages of each type of energy conversions should be evaluated individually to determine key factors such as efficiency as an energy harvesting method, the implementation cost, size, and the final applications where they will be used.

Through this dissertation, a new option of green energy conversion is made available; focusing on the use of turbines to extract energy from microfluidics, with diverse application in biomedical, military/aerospace, and home areas. These systems have the potential of converting mechanical movement energy, and hydraulic energy into electric energy that may be sufficient for self-powering nano/micro devices and nano/micro systems. A flow, with constant pressure, a magnetic generator, and a novel impulse turbine design are combined to form a self-contained miniaturized generator system. The turbine consists of two main parts: a bearingless rotor and the enclosure or

casing; while the miniaturized magnetic generator is a permanent magnet brushless machine, consisting of permanent magnets in a ring configuration and radial coils. A permanent pressure, from microfluidic pressure system, is the force used to move the blades. This rotational motion of the turbine is transformed into electricity using magnetic induction, formed by permanent magnets on the rotor and nine coils fixed in the holder of the turbine. The electricity is generated when the magnetic field rotates and moves past the conductor, which induces a current according to Faraday's Law [1–3]. The system has potential uses not only in medical equipment, but in automotive applications, home appliances, and aquatic and ventilation systems.

CHAPTER 1: INTRODUCTION

1.1 Overview

The research work presented in this dissertation states the design, mathematical model, simulations, and tests of a new energy system, which is a miniaturized system that transforms rotational motion into electricity by the use of innovative subsystems that interact to finally transform kinetic energy to electricity. The dissertation work incorporates a new turbine model, which includes notched blades, and a special turbine casing, designed to work in immersed micro flow fluid systems. In addition, an electromagnetic system is attached inside of the turbine, to finally convert the variable magnetic field to electricity, which is produced from permanent magnets (attached on a rotor) that rotate and induce currents into coils that are fixed inside the turbine casing. The final design could be used to create new systems, replace old, inefficient and toxic devices or could be adapted to biomedical and vehicular applications, and to military and aerospace systems. In addition, with small design modifications and utilization of biocompatible materials, this notched blade energy generation system can be used for in vivo and many other applications.

1.2 Dissertation Organization

This dissertation in energy generation uses a battery-free system capable of operating in bio/medical, environmental, aquatic/marine, and many other micro-fluidic applications is organized into five chapters, with the first and fifth corresponding to

introduction and conclusions respectively. Chapters two through four describe the primary contributions of the work developed in this dissertation.

Chapter 2 provides the theoretical background to support the design of the notched blade energy generation system. This chapter summarizes the hydrodynamics laws applied in turbine designs, electromagnetic theories which explain the interactions of magnetic field and coils to produce electricity, and concludes with a description of permanent magnet machines used as generators or motors.

Chapter 3 presents the final computer aided-designs (CAD), detailing the geometries of the designs of the notched blade turbine and the magnetic generator system. Chapter 3 also shows the step-by-step development of a new mathematical model created to explain the physical behavior of the complete system.

Chapter 4 presents the simulations, assembly, tests, and the analysis of results of three different prototypes. This chapter describes how the scaled prototypes were assembled and tested, and explaining the differences and updates of each, until the best model is found.

1.3 Contributions

This dissertation is an original work, which has led to the discovery of a miniaturized system capable of producing electrical energy by the use of a novel cross-flow turbine. Unlike the impulse turbines, such as Pelton wheel [15]–[19], the core of the system is a miniaturized cross-flow turbine [16], [20], [21] which is a hybrid system that combines action and reaction turbine characteristics and takes the benefits of an initial impulse jet (jet stream of fluid) and the internal pressure to move the totally immersed notched blade rotor. The assumption of immersion, which is crucial to the design,

derives from the need to allow future compatibility with closed micro fluidics systems, such as the circulatory system, for which a Pelton design would not be appropriate given their requirement of air in the rotor chamber [15], [18], [19]. Despite similarities in the way the impulse applied to the blades, there are significant differences that make the design of this system a unique development. The notched blade turbine can use one or two motor-generators assembled inside of the turbine to convert the rotational movement into electricity by magnetic induction. This novel system is currently undergoing a patent process through the University of South Florida Patent Office.

The turbine rotor is the first innovation of the model. The rotor includes six notched blades supported in a central hub, and two disks in the internal rotor cavity, increasing the internal pressure and optimizing the flow to have an impact on each blade. The rotor design is a new immersed cross flow model never used before. Rotors of traditional impulse turbines consist of several blades joined to a common hub. The blades are separate pieces assembled in a common center (hub) to form the rotor. The blades of this design are different compared to all turbines reported [1], [3], [4], [6], [15]–[17], [22]–[27], because the rotor structure is one piece divided in three parts: a cylindrical central hub, two discs on top and bottom of rotor, and nine miniature notched blades connected around the cylindrical hub, and supported by the rotor discs. The miniaturized notched blades have a semicircular curvature, complemented with a notch in the internal edge of each blade, fixed by three sides, top, bottom, and center, of the rotor, to spin about the central axis of the rotor (hub).

The second innovation, the miniaturized casing, was developed to channel a continuous flow through the system, help maintain a constant velocity, and direct the jet

stream to the tip of the rotor blade. These conditions create an environment conducive to increased rotor rotation. Traditional impulse turbines [6], [15], [16], [18], [19], [28]–[30], such as the Pelton system, have an orientation and fixed position, and do not require a pressure around the rotor chamber, because the fluid jet is created by the nozzle prior to reaching the blades; in general the fluid is in free flow after blades are impacted. Our system, however, fulfills a different function compared to the one found in the Pelton casing, which is only to protect the surroundings from water splashing. This special casing and miniaturized notched blades are designed to optimize the fluid injected at the inlet, contain and control the pressure of the working fluid through the turbine, and maintain volumetric pressure on the surface of the blades that are not receiving the initial fluid stream directly. Also, considering biomedical applications and systems that provide flow pressure into the turbine blades, the distance between the blades and the stator walls were increased to prevent drastic alterations and changes in pressure and flow of the system where implants may occur. This prevention is not addressed by the Pelton system [15], [18], [19].

The third innovation in this research is the adaptation and assembly of a brushless machine model, which was inspired by the principles and shape of a micro hard drive disk motor. The rotational parts of the brushless machine (ring of permanent magnets) are attached on the rotor, while the static parts (coils) are attached inside of the turbine casing. The importance of incorporating a brushless machine in this design is to provide the mechanism by which the system will convert mechanical energy to electricity.

In summary, the final result of this research is a miniaturized system capable of producing electrical energy by the use of a novel notched blade turbine. The turbine has an attached magnetic system that induces electric current in coils when a fluid rotates the turbine rotor.

1.4 Current State of the Art

The conversion of mechanical energy to electricity using the clean and free energy produced by small flow of water, and microfluidics systems is being researched and will be a transformative innovation to energy problems, and an alternative to create self-powered micro and nano portable devices, as well as to replace invasive and toxic devices, used as power supplies. [[3], [5], [8]–[10], [31]].

Models such as the macro hydroelectric systems are used to develop new micro and nano energy systems moved by any kind of flow, because these are the more common way to produce clean energy, on demand around the world, and one of the main parts of those systems is the turbine [19], [25], [32], [33]. Computer-aided manufacturing (CAM) and microfabrication processes are being used in miniaturization of traditional turbines models, which could be used to develop tiny power supplies and/or self-powered systems, but precision in the assembly of parts, requirements of size and shape, and adaptability to applications are still waiting to be solved, and this is precisely the core goal of this research.

Some so called micro turbines, with sizes minor of one square meter, have been developed. They have good responses and applicability in small generators systems such as farms, small towns or houses [6], [28], [33]–[35]. These kind of systems use the small water fall force to produce an amount of energy of median power, capable of

powering home machines, or small industrial equipment, but cannot be used on portable devices.

The use of computer-aided manufacturing (CAM), 3D printers, and the microfabrication processes have open new possibilities in the scaling down of macro systems, which can be used in portable devices. Currently, research groups are working on microfabrication processes to develop micro and nano generator systems to be used in portable devices, medical and environment applications, and communication systems [1], [3], [7], [11], [22], [27], [36]–[44].

Energy harvesting has become increasingly interesting to engineering, material sciences, and the medical profession, as an answer to the proliferation of commercial portable devices, and medical and military applications. Efforts to develop alternative micro and nano generators systems have resulted in many promising technologies; including the use of piezoelectric semiconducting nanowires to convert energy from sources such as body movement or blood flow to electrical energy when they are twisted or deformed [45]. The use of MEMS power generators, using micro fabricated permanent magnets oscillating around a central shaft, due to the motion of the thorax during breathing, inducing a voltage across a micro fabricated planar coils [3], [7], [46]; and the use of a “magnetic spring” placed in a daypack to generate power, which with the human motion vibrates easily at off resonance conditions [43]. In addition, there are research teams studying the possibility of producing energy using physiological systems, such as the respiratory system, urinary system, circulatory system [22] and the motion system in animals and humans [5].

1.4.1 Micromachines Used as Generators

The use of turbine to electric energy generation is not recent [28]. In 1750 Leonhard Euler [47], directed experiments on the mechanics of reaction wheels, and his results have been applied in modern water turbines. In 1826, Jean-Victor Poncelet, proposed the idea of an inward-flowing radial turbine, and years later developed the Francis, Pelton, Kaplan, Cross flow and Banki turbines, and new turbines with origins in modifications of all these models [16], [29], [30], [32]. Towards the end of the past century and during the 21th century, there has been increasing scholarly interest in the conversion of biomechanical energy, present in living organisms, to electricity [3], [22], [39], [48].

The development of a simple impulse turbine for nano hydropower was reported by Nakanishi [6] as a hydraulic turbine, to be utilized in mountainous areas, as a hydropower of small water resources. The impulse turbine used by Nakanishi has inexpensive components, and this model is easy to build, having similarities with a cross flow turbine. Experimental results on a turbine prototype determined that the maximum efficiency of the rotor is 0.56, and the nozzle position is the key factor to improving the output power of this turbine.

Dr. Martinez and Dr. Chowdhury from University of Windsor designed a MEMS system power generator [3], Figure 1.1. The system comprises an asymmetrical circular rotor and microfabricated NdFeB permanent magnets in alternating polarity. The voltage in this system is induced in the coils by the oscillations of permanent magnets during breathing and the motion of the thorax. The generator has a length x, width area of 4x4

mm^2, 12 pole pairs in the rotor, 179 coil turns, and can generate 59.73 mW_{RMS} output power per coil, and with 9.0 V_{RMS} open circuit voltage per coil.

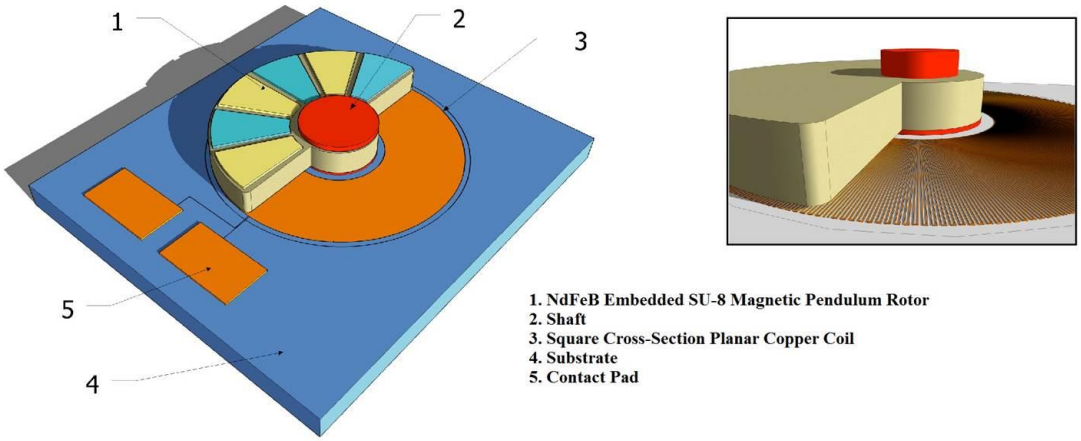

Figure 1.1 A conceptual 3D model of a single stator generator. From Martinez et al. [3]

Seoul National University developed a radial microturbine [27]. Using MEMS technology they fabricated a stack of five wafers, using photolithography, DRIE, and bonding processes. The design used 31 stator blades and 24 rotor blades, reporting a maximum rotation speed of 11,400 rpm and a flow rate of 16,000 standard cubic centimeters per minute (sccm) achieved in performance tests.

Reynaerts, Peirs, and Verplaetsen have introduced an axial turbine for electric power generation [1]. This turbine is a miniature gas turbine that generates electrical energy from fuel. Fig. 1.2 from Reynaerts et al. [1] and [49] shows details of this design. The turbine was produced with electro-discharge machining (EDM), with a rotor diameter of 10 mm, and the housing has a diameter of 15mm and is 25mm long. The turbine was made of stainless steel using die-sinking electro-discharge machining. It

was tested to speeds up to 160,000 rpm, generating a maximum mechanical power of 28 W with an efficiency of 18%.

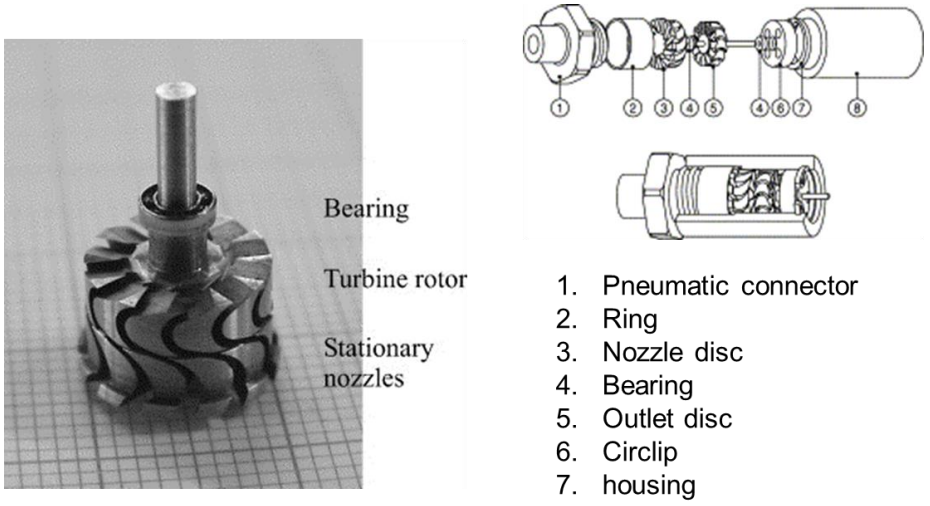

Figure 1.2 Left side: Nozzle disc, turbine rotor, and bearings. Right side: microturbine design. From Reynaerts et al. [1] and [49].

The design, fabrication, and characterization of a rotary micromotor supported on microball bearings is another micromachine reported by Ghalichechian, Modafe, Beyaz, and Ghodssi [50], design shown in Fig 1.3. They designed a rotary micromotor to be used in centrifugal micropumps, which could be applied to fuel-delivery and cooling applications. Micro fabrication was used to develop the micromotor, where stator and rotor fabricated separately are assembled with microballs coated with a silicon carbide (SiC) film to reduce the friction. Microballs housing coated with SiC and fabricated on the stator, plus Microballs housing coated with SiC and etched in the rotor, produced a response 44 times higher than the velocity previously reported in linear micromotors.

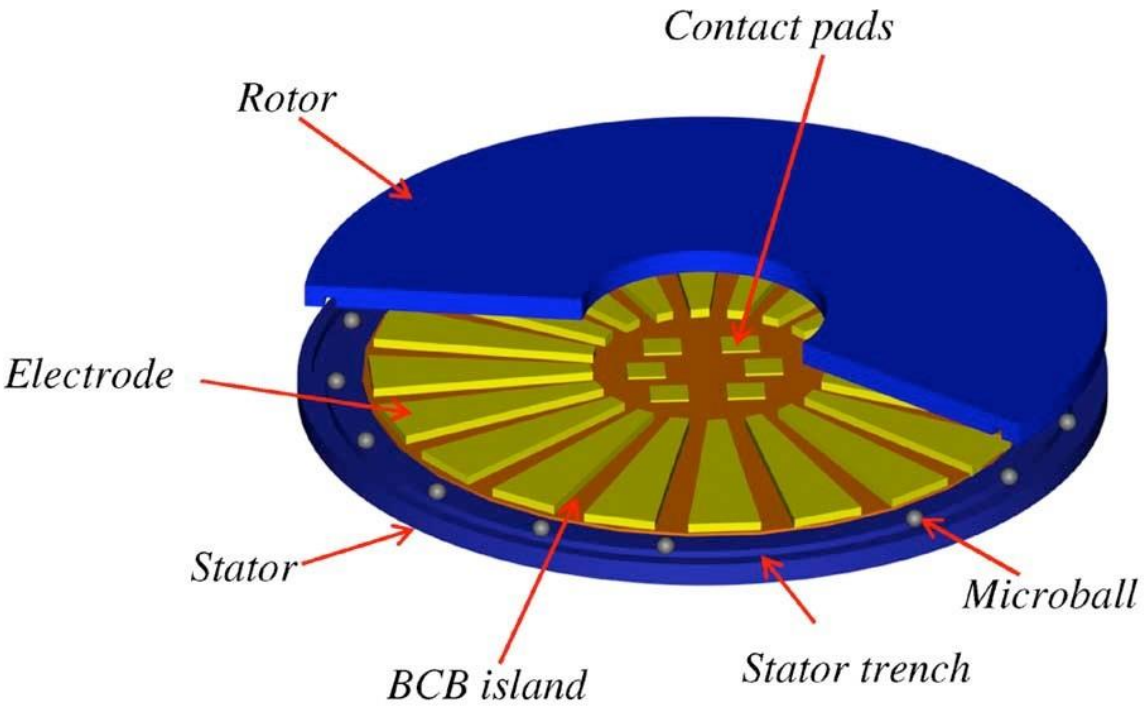

Figure 1.3 Simplified 3-D schematic of the rotary micromotor. From Ghalichechian et al. [50].

The MEMS Rotary Engine Power System project results were presented by Fernandez-Pello, Pizano, and other members from the Berkeley Sensor & Actuator Center of the University of California at Berkeley [11]. An integrated generator design using nickel-iron alloy electroplated in the engine rotor poles, served as the generator rotor. 4 Watts of power at 9300rpm was generated using a 12.9 mm diameter Wankel engine.

The project challenge was the design of an efficient and clean micro engine to transform hydrocarbon fuel to electricity, and the goal was to develop an electrical power output of 90 milliwatts from the 2.4 mm engine.

Kinetron Company offers different rotational micro generators such as water turbine generators for converting Kinetic energy in electricity [51], [52]. These use permanent magnets rotating within coils in a miniature variant of a conventional electrical generator. The smallest devices have millimeter sizes and rotational speed of 5000 rpm, and can produce 2.6 Volts at a frequency of 580 Hz, generating around 15 mW of power, according with the model used. Figure 1.5 shows a CAD model of micro generator, and one water generator offered by Kinetron Company. The pictures in Figure 1.5 were taken of Kinetron web-page [51]. Also, all information about Kinetron products can be found in the same reference.

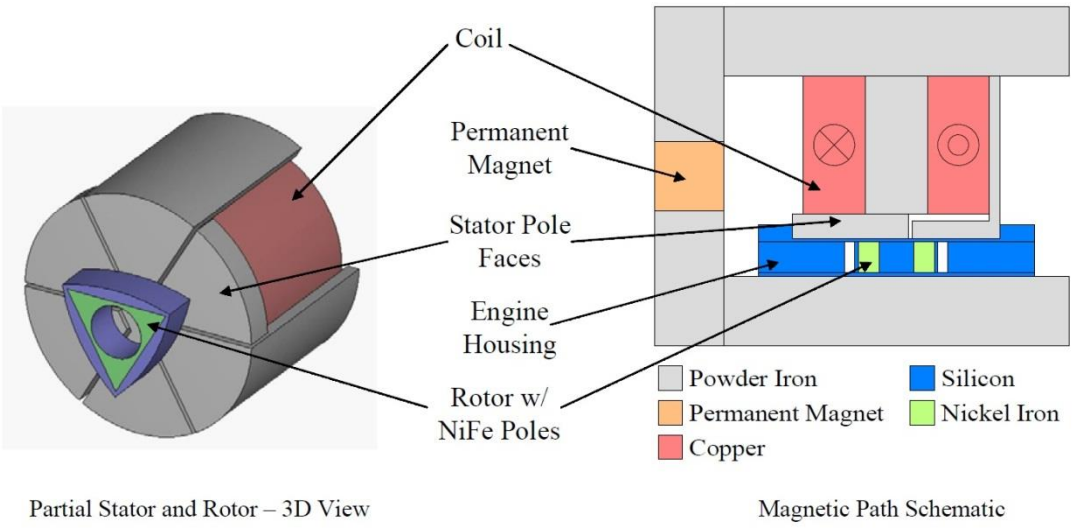

Figure 1.4 Integrated electric generator schematic. From Fernandez-Pello et al. [11]

1.4.2 Permanent Magnet Generators

Chen, Pan, and Liu reported [40] "the analysis and the prototype of a micro-electromagnetic generator" measuring 9x9x1 mm^3. The generator is constituted by multilayer silver microcoils of different shapes, and multipolar planar permanent magnet

of 1.4T of residual induction. The generator produces a maximum theoretical induced voltage of 218.127 mV in the microcoil, when the permanent magnet (PM) is moving at 1395.34 rad/s relative to a microcoil. The PM has an outer diameter of 9 mm, a thickness of 700 μm, fabricated by sintered Nd/Fe/B (neodymium/ferrum/boron), while the microcoils were fabricated using low-temperature co-fired ceramic (LTCC) technology. Figure 1.6 from Chen et al. [40] is showing the different coil shapes and the permanent magnets used in this design.

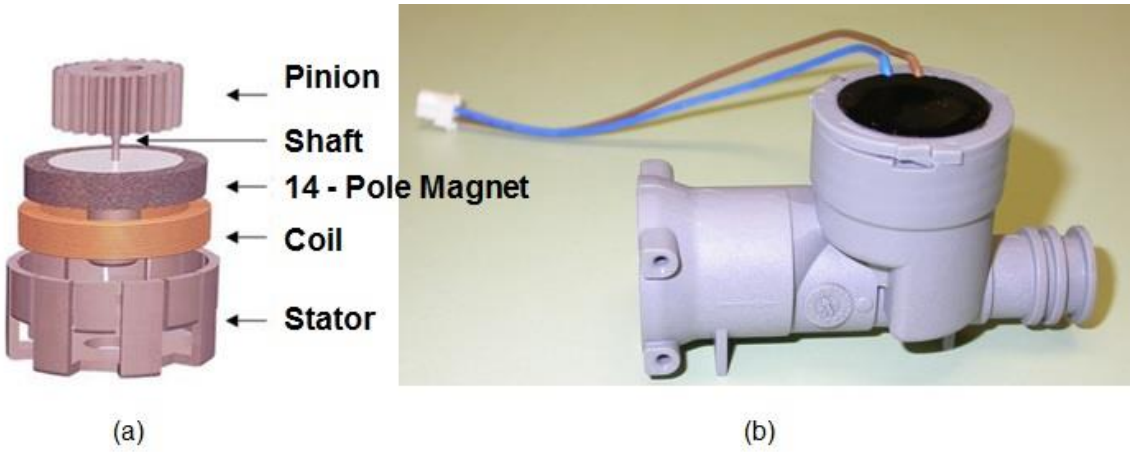

Figure 1.5 Kinetron Company micro generator. (a) 3D drawing of micro generator; and (b) the water turbine generator. Public Domain image [52].

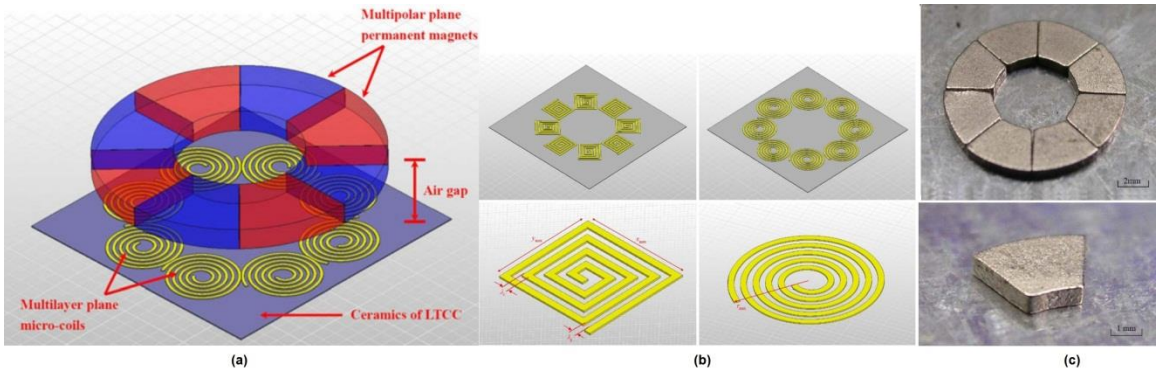

Figure 1.6 In-plane electromagnetic micro-generator. (a) Diagram of the micro-generator; (b) the diagram of a square-shaped, and circle-shaped micro-coils; (c) The multipolar permanent magnet.

The modeling, design, fabrication, characterization of permanent-magnet (PM) generators, to be used in microscale power generation systems was presented in 2006 by Das et al. [53], [54]. The generators were synchronous machines, three-phases of axial-flux, with eight-pole, and constituted by surface-wound stator and PM rotor. The machines were modeled as a set of continuous planar layers. The open-circuit voltage predictions were established with 3-D finite-element analysis simulation results. The devices were fabricated using a combination of microfabrication and precision assembly. The stators were fabricated using electroplated windings. The mechanical-to-electrical power conversion reported was of 2.5 W with a rotational speed of 120 000 rpm, but using a resistive load. However, after passing by a transformer and rectifier output, the electrical power delivered was of 1.1 W of dc electrical power. The results and conclusions of Das et al. [53], [54] contributed to determine that indeed watt-level power production is achievable using miniaturized magnetic machines and demonstrated the viability of scaled PM generators to be used in small applications.

Cordero et al. [38] presents the development of a micro-rotational electromagnetic generator for high speed applications. The generator uses a rotor composed of 20 NdFeB 6x2x1 mm permanent magnets with multiple-poles orientation and axial flux; and a stator with dimensions of 25 mm in diameter and 2 mm thick. The stator has 10 stacked micro-fabricated planar copper-clad polyimide coils. The planar micro-coils were manufactured by photolithography, whereas the permanent magnets were assembled in the rotor using a CNC-machined slotted disk, and produced 5.8 mW when the rotor moved at 4000 rpm. The experimental results are shown by Cordero et al. [55].

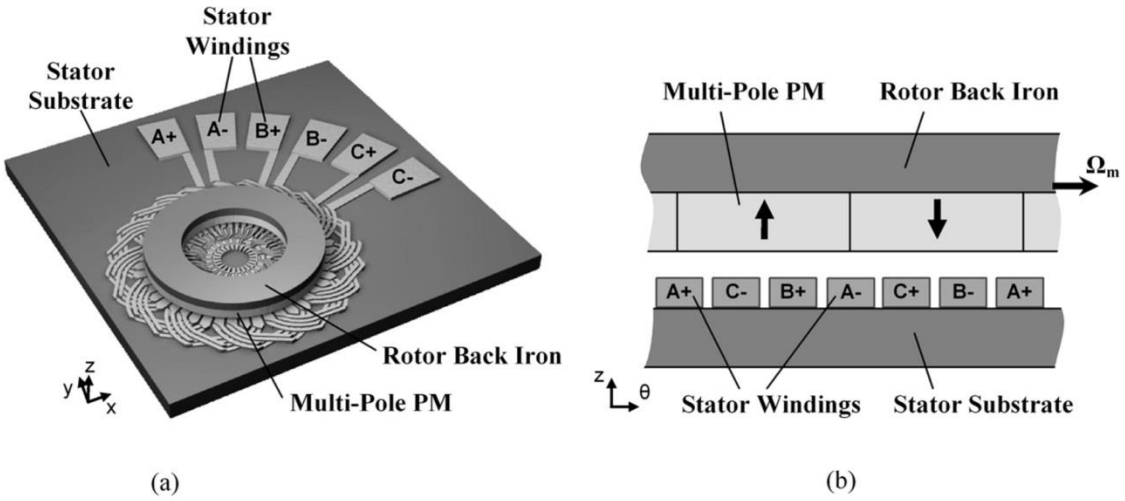

Figure 1.7 PM generator: (a) perspective view and (b) cross section area. From Das et al. [53], [54].

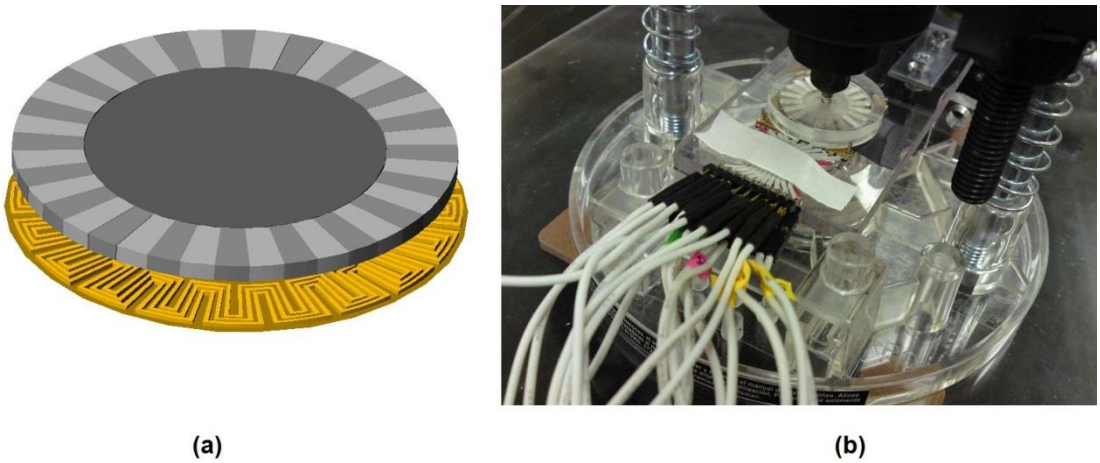

Figure 1.8 Micro-rotational electromagnetic generator for high speed applications. (a) Schematic of the micro-rotational generator; (b) device on testing apparatus. From Cordero et al. [38].

1.4.3 Implantable Devices Used in the Physiological System

In recent decades, implantable devices that use micro motors and micro turbines have been developed as medical alternatives to treat heart failure and other kinds of human physiology problems. Ventricular assist devices (VADs) are one example, and

many models were presented by Timms Danniels in 2011 as “a review of clinical ventricular assist devices” [35]. The review briefly shows rotary devices such as left VADs or LVADS, which are clinically available, being in lab tests, or in clinical trials with humans and animals. Products such as the HeartWare [56], ‘HVAD’ [57], Thoratec ‘HeartMate IXVE/IP’ [58], Thoratec ‘IVAD/PVAD’, Abiomed ‘BVS5000/AB5000’ [59], Thoratec ‘HeartMate II’ [60], Jarvik Heart ‘Jarvik 2000 FlowMaker’ [61], [62], Berlin Heart‘InCOR’, WorldHeart ‘Levacor’ [57], Terumo ‘DuraHeart’ [63], Abiomed ‘Impella’ [64], and CircuLite ‘Synergy’ [65], are miniature ventricular assist devices, which use rotary axial and/or mixed flow, and are used in pumps to control the flows of air or liquids into the body.

Figure 1.9 Ventricular assist systems. (a) Thoratec IVAD™ Ventricular Assist Device; (b) HeartWare® Left Ventricular Assist Devices (LVAD); and (c) Abiomed AB5000™ Ventricular Assist Device.

The pictures in Figure 1.9 are from [66], [67]. The Thoratec IVAD™ is an implantable cardiac assist device pneumatically operated, that can provide left, right or biventricular support, which can deliver up to 7.2 l/min. The housing is made of titanium and is a compact size to accommodate a wide range of patients, including those who were previously unable to receive an implantable, pulsatile device [57], [68]. The HeartWare® [56] Left Ventricular Assist System (LVAS) is a third-generation

continuous radial flow blood pump, implanted in the pericardial cavity for the treatment of advanced heart failure. The device has the capacity to produce of up to 10 liters per minute of blood flow using a rotational speed of between 2,000 and 3,000 revolutions per minute. The rotor is suspended within the pump housing through a combination of passive magnets and a hydrodynamic bearing [57], [68]. The ABIOMED AB5000™ [59] Circulatory Support System can provide left, right, or biventricular support for patients whose hearts have failed but have the potential for recovery. The AB5000 can be used to support the heart, giving it time to rest and potentially recover native heart function. The AB5000 can provide flow rates of up to 6 liters per minute [57], [59], [68].

In conclusion, there have been several energy generation systems investigated for various applications, but due to structural and functional restrictions and limitations that prevented the systems from being used under low pressure, with low flow rates, in closed environments, and while being immersed, the miniaturization, versatile, and bio functionality of these systems have been very limited.

This dissertation work addresses these issues through the design, simulations, prototyping, and testing of a novel hybrid action-reaction turbine with notched blades and casing shape designs capable of producing continuous energy generation.

CHAPTER 2: BACKGROUND AND LITERATURE REVIEW

2.1 Mathematical Background

The main purpose of this chapter is to support the design of the turbine and the conversion of Kinetic energy to electricity. The following sections describe the theories, laws, and concepts that have been used, and define the bases of the operation and behavior of the complete system. Through thermodynamic laws, electromagnetic theories, mathematics and physics concepts, it is possible to derive the relations between mass flow rate, cross section areas, velocities, forces, and torque, to arrive at the mechanical and electrical power.

As mentioned in chapter 1, the miniaturized turbine-generator presented in this dissertation is comprised of two systems, the turbine and the permanent magnet generator (PMG). The theoretical concepts and the fundamental laws of physics, including equations and assumptions, plus previous design models of turbines, coils, and the configuration of permanent magnets attached to these turbines, are presented throughout this chapter to support the final results of this dissertation.

The models developed, prototyped, and tested make use of three basic principles of fluid flow: the principle of conservation of mass, from which the continuity equation is derived, the principle of conservation of energy that yields

the energy equation, and the principle of conservation of momentum, used to derive the momentum equation [69]–[74]. Also, Newton's second law for rotation, Bernoulli's and Pascal's law, Poiseullie's equation, Euler's equation, Faraday's, and Maxwell's equation complement the background used to support the mathematical models [12]–[14], [69].

2.2 Equations Governing Flow and Pressure

The principle of fluid machines is centered on the utilization of useful work due to the force applied by a fluid jet, impacting and moving, over a series of blades attached to a rotating wheel that spins about an axis. The equations of flow and pressure in a tube flow system, such as in Figure 2.1, are defined through the equations of continuity of steady flow (mass conservation) and momentum equations [15], [69]. These equations may be written as follows:

$$\sum \rho V \cdot A = 0 \tag{2.1}$$

$$-\rho_1 A_1 v_1 + \rho_2 A_2 v_2 = 0$$

$$\rho_1 A_1 v_1 = \rho_2 A_2 v_2 \tag{2.2}$$

The variables $\rho_i,\ A_i,\ and\ v_i$ are density, transversal area, and velocity respectively. The principles of conservation of mass and momentum, which predicts that a fluid of constant volume and flow rate, with density ρ, and flowing during a period of time through an area, produces simultaneously an increase in the mean velocity and a decrease in pressure at the outlet of the system.

To determine the rate of change of momentum in Figure 2.1, it is important to analyze the momentum of fluid entering and leaving in the stream conical pipe in the time Δt. The volume of the fluid in time Δt, is moved a distance $v_i \Delta t$, and the momentum equations can be written as

$$Momentum\ of\ fluid\ entering = mass \times inlet\ velocity$$

$$\dot{m}_i v_{in} \Delta t = \rho A_i v_{in} v_{in} \Delta t = \rho A_i v_{in}^2 \Delta t \quad 2.3$$

$$Momentum\ of\ fluid\ leaving\ = mass \times outlet\ velocity$$

$$\dot{m}_o v_n \Delta t = \rho A_n v_n v_n \Delta t = \rho A_n v_n^2 \Delta t \quad 2.4$$

If equations 2.3 and 2.4 are combined with Newton's second law, is possible to find the total force supplied by the fluid. The law states that the force is equal to the rate of change of momentum [69], [70], [73], and can be written as

$$F = \frac{(\rho A_n v_n^2 \Delta t - \rho A_i v_{in}^2 \Delta t)}{\Delta t} \quad 2.5$$

The equation 2.5 defines the force inside of the conical pipe, when it is acting in the direction of the flow of the fluid. The volume flow rate (Q) will be considered constant through the system, if the fluid is incompressible, density ρ is constant, and one dimensional [69], [70], [73]. The expression governing Q will be written as

$$Q = A_i v_{in} = A_n V_n \quad 2.6$$

where nozzle area is defined as

$$A_n = \pi * \left(\frac{D_n}{2}\right)\ (m^2) \quad 2.7$$

Therefore the Q and A_n equations can be used to rewrite the force equation

$$F = Q\rho(v_n - v_{in}) \quad 2.8$$

The Bernoulli equation defines the fluid dynamic relationship between fluid velocity (v), fluid pressure (p), and height (h) [69], [70], which describe the behavior of fluids in a tube, but some assumptions such as flow viscosity = 0 (internal friction), constant density (ρ), steady flow, and Incompressible flow, must be defined to assure the applicability of this equation. The analysis of forces and velocities in a turbine could

be developed using similar shapes and variables, shown in Figure 2.1 and 2.2, and reported by [69], [74]–[77].

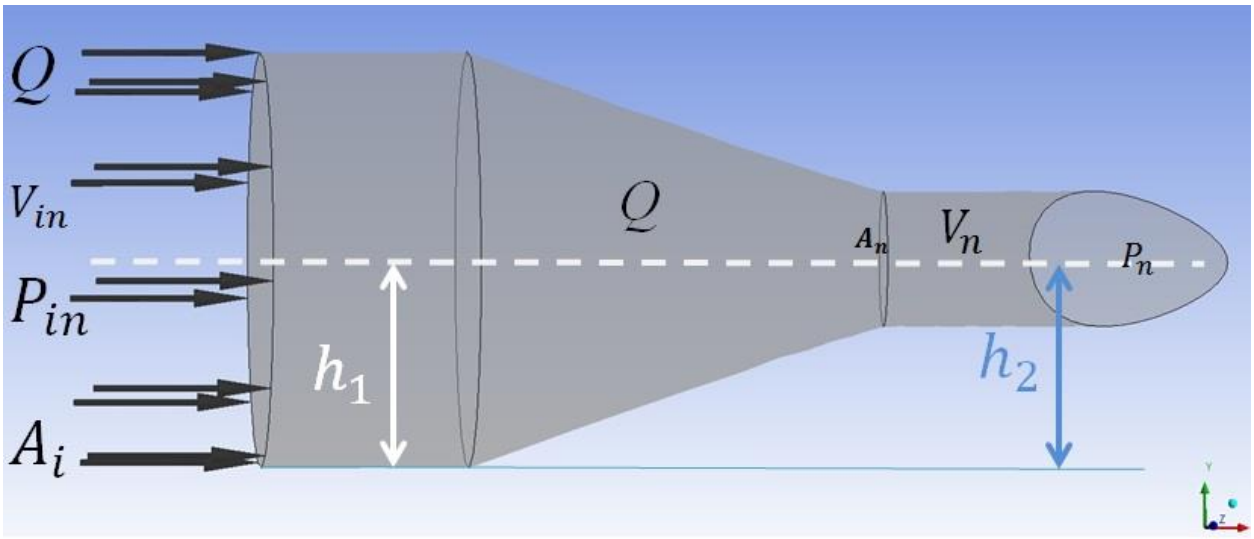

Figure 2.1 Pipe tube in gradual contraction.

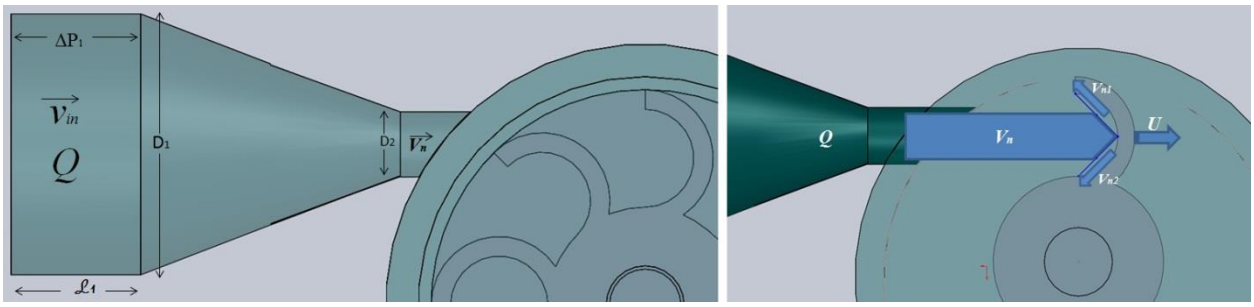

Figure 2.2 Jet velocity: From nozzle the first blade is impacted.

Bernoulli's equation [69], [70], is defined as:

$$p_{in} + \frac{\rho v_{in}^2}{2} + \rho g h_1 = p_n + \frac{\rho v_n^2}{2} + \rho g h_2 \qquad 2.9$$

where

ρ = fluid density (kg/m^3);

g = acceleration due to gravity on Earth (m/s^2);

h = height from an arbitrary point in the direction of gravity (m).

pin = Inlet pressure (N/m^2, Pa).

pn = Nozzle pressure (N/m^2, Pa).

v_{in} = mean inlet velocity (m/s).

v_n = mean nozzle velocity (m/s).

If $h_1=h_2$, then the equation is reduced to:

$$\frac{\rho}{2}(v_n^2 - v_{in}^2) = p_{in} - p_n \quad 2.10$$

on the other hand, the potential power or power extracted [69], [70], [73] from the turbine nozzle (P_n) is

$$P_n = \rho g Q h \quad 2.11$$

but,

$$v_n = \sqrt{2gh} \quad 2.12$$

to find an expression to power (P_n), in function of known and defined variables, combine $Q, P_n,$ and $v_n$equations:

$$P_n = \frac{\rho A_n v_n^3}{2} \quad 2.13$$

The velocity triangle shown in Fig. 2.3 is typically used to explain the interaction between the fluid and the blades in a turbine, and determines the components of velocities and the forces acting on the rotor. The rotor is moved by the action of forces from the nozzle jet stream, which impacts the blades. The kinetic energy is transformed to mechanical energy, producing a continuous spin of the rotor. The mass of the liquid striking the blades per second [78]–[81] is given by

$$\dot{m} = \rho A_n V_n \quad 2.14$$

where A_n is the transversal area of the nozzle, V_n is the velocity of the fluid from nozzle to blades, and ρ is the density of the liquid. The product of mass of the fluid striking per second and the component of velocity impacting the blades in tangential direction (V_{w_i}) is known as the momentum of the fluid striking the blades [69], [73] and the general equation is given by

$$M_i = \dot{m}V_{w_i} = \rho A_n V_n V_{w_i} \qquad 2.15$$

similar momentums are produced by the fluid from the nozzle, striking the blade, and the fluid striking the outlet of each blade. The new components are V_{w_1} in the tangential direction of the blade inlet, and V_{w_2} in the tangential direction of the outlet of each blade. The velocity components can be positive or negative. If it contributes to the movement, it is positive, otherwise it will be negative.

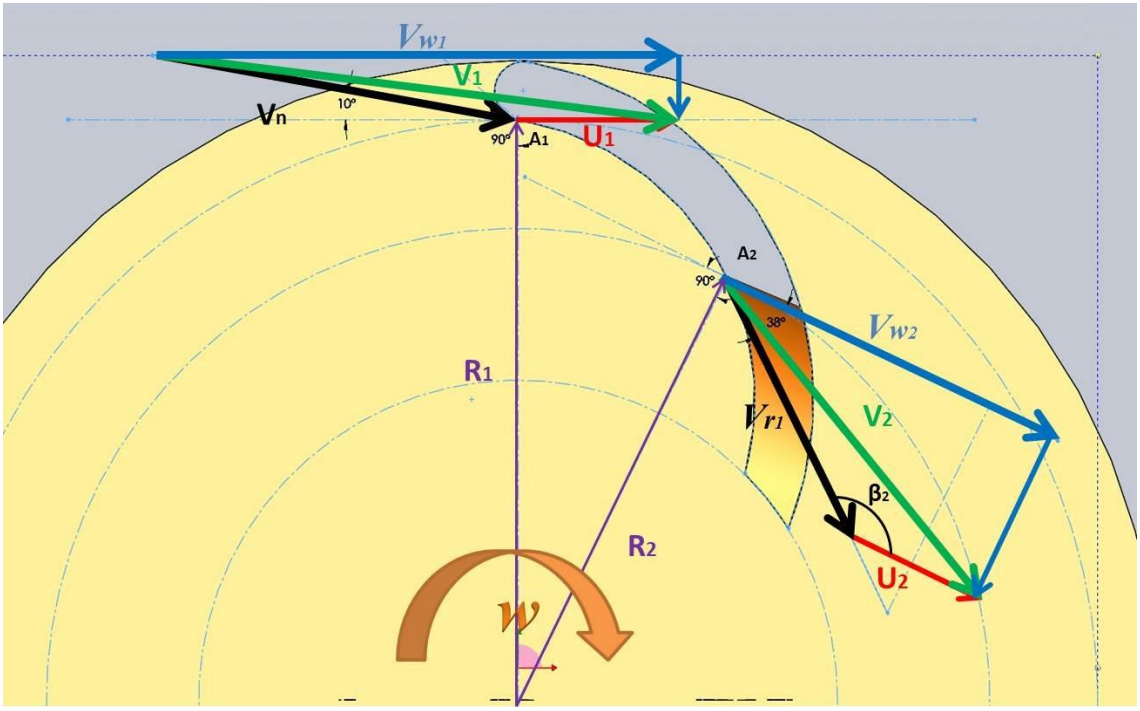

Figure 2.3 Velocity triangles.

If the momentum of the liquid at the nozzle and the momentum leaving the blade are combined as a product of radial distances, the results will be the angular momentum per second at the inlet and at the outlet of the blade.

$$M_{A_i} = \rho A_n V_n V_{w_i} R_1 \tag{2.16}$$

$$M_{A_2} = \rho A_n V_n V_{w_i} R_2 \tag{2.17}$$

The equations 2.19 and 2.20 are related in the impulse momentum theorem [69], [70], [82], which states that the rate of change of angular momentum is equal to the torque on the wheel or torque on the rotor. The equation is given by

$$T = \rho A_n V_n V_{w_1} R_1 \pm \rho A_n V_n V_{w_2} R_2$$

$$T = \rho A_n V_n \left(V_{w_1} R_1 \pm V_{w_2} R_2\right) \tag{2.18}$$

also, the torque equation could be written as,

$$T = F_t R_i \tag{2.19}$$

where F_t is the total force applied to each blade, in a direction tangential to the rotor, and R_i is the distance or radius from which the forces are applied, measured from rotor axis of rotation.

Power from the turbine (P_r) is a function that relates torque and angular velocity, and is expressed in the Euler turbomachine equation [47], [69], [70]. The power delivered to the fluid is thus,

$$P_r = T\omega \tag{2.20}$$

The angular velocity ω and torque T are variables that characterize the rotor behavior, which were defined in equations 2.18 and 2.21,

$$\omega = \frac{U_i}{R_i} \tag{2.21}$$

the U_i variables are the blade tangential velocities, measured in different points with radius R_i measured from the axis of rotation to each defined point on the blade. Finally, the power from the rotor is a relationship between rotor torque (T) and angular velocity(ω). The rotor torque is in direct relation with the forces impacting the blades, especially the blades located between the nozzle output and the turbine output zone as shown in Figure 2.4.

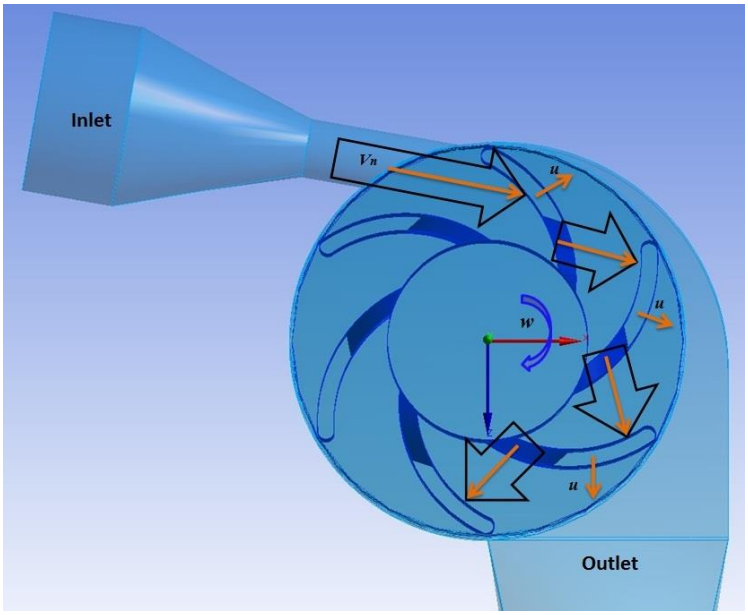

Figure 2.4 Blades located between nozzle and the turbine output

Finally, all equations are related in one expression known as efficiency of the system $(\boldsymbol{\eta})$ [69], [70], [77], which reflects the system's behavior, showing the percent of losses into the system, when the potential energy is converted to mechanical energy. The efficiency is calculated with the following relation,

$$Efficiency\ (\eta) = \frac{P_r}{P_n} \qquad 2.22$$

2.3 Equations Describing Electromagnetic Field

There are constitutive relations in electromagnetic systems which describe how two or more physical parameters are related, depending on the medium's properties

involved in the process. The relationship between electric field intensity (E) and the conductive current due to the movements of free charges (J) is given by the microscopic form of the Ohm's law, $J = \sigma E$ and $D = \varepsilon E$, where σ and ε are electric conductivity and dielectric permittivity; also, the relationship between the magnetic induction or magnetic flux density (B), the magnetic field strength (H), and the magnetic polarization (M) are given by $B = \mu H$ and $M = \chi H$, where μ and χ are the magnetic permeability and magnetic susceptibility [13], [14], [83], [84]. Assuming, $\sigma, \varepsilon, \mu, \text{and } \chi$ describe the electromagnetic properties of a material, then an electromagnetic phenomena can be described by four relationships known as Maxwell's equations [13], [14], [84], which describe how objects can be influenced by the propagation of electric and magnetic fields and how the system response could be in accordance with that kind of electromagnetic input. The simpler form preferred by authors in books [13], [14] and papers [12], [85], [86] are written as,

$$\nabla \times \bar{H} = \bar{J} + \frac{\partial D}{\partial t} \qquad 2.23$$

this equation is known as Ampere's law, and

$$\nabla \times \bar{E} = -\frac{\partial B}{\partial t} \qquad 2.24$$

is known as Faraday's law. Now, using a form of the Gaussian theorem and the relationship $D = \varepsilon E$ [87]–[89], the next two equations are derived. The magnetic Gauss's law states that if the magnetic source is contained in a closed surface, the net magnetic flux crossing through this surface is zero,

$$\nabla \cdot \bar{B} = 0 \qquad 2.25$$

the relationship between magnetic field intensity H and magnetic field density B can be written as

$$B = \mu H = (\mu_r \mu_0) H \quad 2.26$$

where μ_r is the relative permeability of the medium (unit less) and μ0 is the magnetic permeability in vacuum ($\mu_0 = 4\pi \times 10^{-7}\ henry/m$) [87]–[89].

Finally, the magnetic Gauss's law may be derived from Faraday's and Ampere's laws going from open surface to become a closed surface. This Maxwell equation is defined in terms of electric flux density and electric charge density, to state how the electric field acts around electric charges.

$$\nabla \cdot \bar{D} = \rho \quad 2.27$$

The total magnetic flux density B inside the magnetic material and the presence of an external magnetic field H, are related through magnetization M, and can be written as

$$\nabla \times \bar{B} = \mu_0 (\bar{H} + \bar{M}) \quad 2.28$$

Equations on section 2.3 are used to define any electromagnetic system, but in this dissertation I only use the equations involved in the conversion of kinetic energy to electricity through an electromagnetic induction and starting with Faraday's law. In 1831, Michel Faraday discovered the phenomenon known as electromagnetic induction. His experiments demonstrated that an electric current is induced, in a wire in loop shape, by changing the magnetic field. Faraday's law states that an electromotive force (emf) is generated, if for any reason, the magnetic flux changes with the time. The average of emf, induced in a coil of N turns is expressed in the following equation:

$$\varepsilon = -N\left(\frac{\emptyset - \emptyset_0}{t - t_0}\right) = -N\frac{\Delta\emptyset}{\Delta t} = -\omega\frac{\Delta\emptyset}{\Delta\theta} \quad 2.29$$

where N is the number of turns on each coil, ω is the angular velocity, and $\emptyset$ is the magnetic flux. The magnetic flux is the total flux through a surface. $\emptyset$ is found by integrating the flux density over this area

$$\emptyset = \int BdA \tag{2.30}$$

if the flux density is constant through this area, the above equation will be expressed as,

$$\emptyset = \vec{B}.\vec{A} = BA \times cos\theta \tag{2.31}$$

where θ is the angle between $\vec{B}$ and the normal vector from a transversal coil area $\vec{A}$, so if the spatially uniform magnetic field $\vec{B}$ is used, this equation will be written as

$$\emptyset = -BR_s\alpha_t l_t \tag{2.32}$$

where R_s is the radius of the stator surface, α_t is the coil arc, expressed in radians, and l_t is the effective axial length of each coil. The combination of flux density and magnetic field produce the induced voltage equation which can be written as

$$\varepsilon = -N\left[\frac{d}{dt}(BAcos\theta)\right] = -N\left[\left(\frac{dB}{dt}\right)Acos\theta + B\left(\frac{dA}{dt}\right)Cos\theta - BAsin\theta\left(\frac{d\theta}{dt}\right)\right] \tag{2.33}$$

As is stated in Farady's law [90], [91], the three components of the induced voltage equation determine that an emf can be induced, by modifying at least one of the three parameters involved in this expression, the magnetic field, the coil transversal area, or the angle between $\vec{A}$ and $\vec{B}$. In this research work, only the case when the magnetic field is rotated around the coils is considered, resulting in the following equation,

$$\varepsilon = -N\left[\frac{d}{dt}(BAcos\theta)\right] = -N\left[\left(\frac{dB}{dt}\right)Acos\theta\right] = -N\left[\left(\frac{dB}{dt}\right)R_s\alpha_t l_t\right] \tag{2.34}$$

this equation represents the variation of the electromagnetic field into the coils, which induces currents into coils and generates emf (voltage) in the coils terminals.

Faraday's law of induction is a basic law of electromagnetism, which supposes that a magnetic field will create an electric current, relating to the operating principles of generators, electrical motors and transformers; also, Lenz's law reaffirms the applicability of Faraday's law, which states that the induced emf in the coil, results from a changing magnetic flux, and has a polarity that leads to a induced current, which in turn tends to oppose the change in magnetic flux that induces such currents.

The interaction between PM's and the stator coil slots and the effects produced by electromagnetic forces will be presented in the next chapter, but the analysis of some effects which could unbalance the system or generate cogging torques will be presented as future works that will complement this theoretical analysis.

2.4 Permanent Magnet Machines

The development of permanent magnet (PM) machines have grown significantly in the last ten years [92]. This is associated with the development of power electronics, and the high demand in applications such as mixers, pumps, and micro motors/generators, used in medical equipment, domestic machines and industrial and military devices. The International Union of Pure and Applied Chemistry (IUPAC) defines a group of seventeen chemical elements in the periodic table as rare earth elements or rare earth metals, scandium (Sc), yttrium (Y) and the lanthanides — lanthanum (La), cerium (Ce), praseodymium (Pr), neodymium (Nd), promethium (Pm), samarium (Sm), europium (Eu), gadolinium (Gd), terbium (Tb), dysprosium (Dy), holmium (Ho), erbium (Er), thulium (Tm), ytterbium (Yb), and lutetium (Lu). These

elements mixed with other metals can produce new materials or alloys, with superior magnetic characteristics, increasing melting point and strength properties, which convert them into a new alternative to improve old systems and to make new devices and systems with high technological demand.

Taken from DOI, U.S. Geological Survey, Circular 930-N; Table 2.1 shows rare earth materials and applications. Currently, rare earths materials such as neodymium (Nd) and samarium (Sm) are the principal components of alloys to create modern magnetic applications. Neodymium-iron-boron magnets (NdFeB) are the most common type of magnets commercially available because they have high intensity at a very low volumes, which allows them to be used in the miniaturization of electronic devices and can be manufactured in a wide range of shapes, sizes, and grades [93]. These kinds of magnets are made from an alloy of neodymium, iron and boron and are being used in mini and nano scale applications. Table 2.2 from Minowa 2008 [94], shows some applications where PM's are being used.

A PM machine is a kind of electro-mechanical device that converts electrical energy to mechanical energy or vice versa, using the magnetic, electric and mechanical properties of materials and devices involved in the system to transform the energy (physical change) from one form to another. Many designs of PM machines have been developed according with the applications, where orientation, shape, number of poles, and size were the more important parameters taken into account. Configurations of PM's and coils model designs are shown in Figures 2.5 and 2.6.

Table 2.1 Major uses of individual rare-earth elements. Credit: U. S. Geological Survey U. S. Geological Survey/Table by USGS/Ft. CO et al. [95]

[Simplified from Pincock, Allen and Holt, Inc., 1988]

Industry	Mixed REE	Rare-earth element														
		La	Ce	Pr	Nd	Pm	Sm	Eu	Gd	Tb	Dy	Ho	Er	Tm	Yb	Lu	Y
Metallurgy																	
Ferrous	X	X	X														X
Nonferrous	X	X	X	X	X			X									X
Magnets	X	X	X	X	X		X		X		X						X
Ceramic	X	X	X	X									X				X
Electronic	X	X	X	X	X		X	X	X	X	X	X	X	X	X		X
Chemical (metallurgical catalysts)	X	X	X		X		X		X		X				X		X
Catalysts	X	X	X		X		X		X						X		
Optical (including glasses)	X	X	X	X	X	X	X	X	X	X		X	X	X			X
Medical							X	X	X	X				X			X
Pharmaceuticals		X	X		X				X								
Nuclear																	
Fuel			X														
Control and shielding			X				X	X	X		X	X					X
Miscellaneous																	
Farming	X																
Hydrogen storage		X	X	X	X												
Cryogenics		X															
Batteries		X			X												X

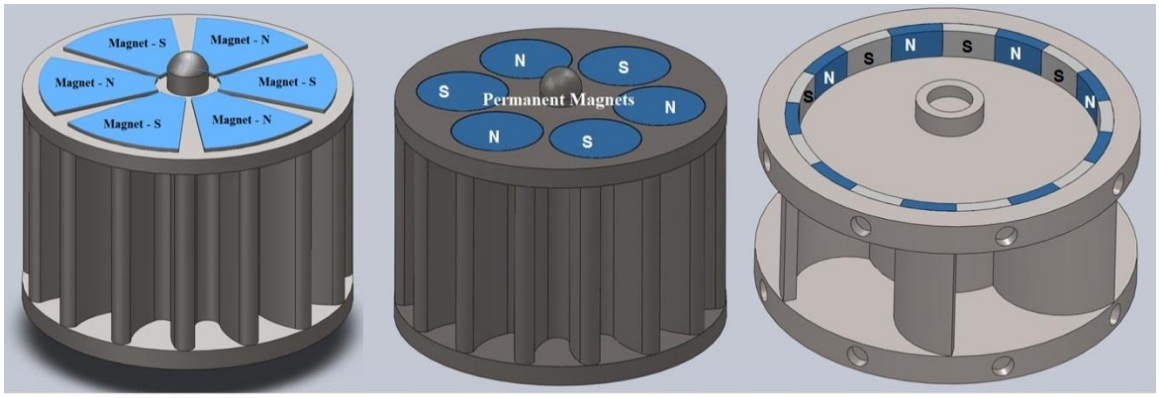

Figure 2.5 PM's shapes and orientation. Axial orientations are shown in (a) and (b), radial orientation is shown in (c).

Table 2.2 Products utilizing Nd magnets. From Minowa et al. [94]

Field	Products
Computer	VCM for HDD
Domestic	Air conditioner, refrigerator, washing machine, cleaner, digital camera, electric shaver
Audiovisual	Mobile phone, speaker, DVD, CD, mobile music player
Industrial	Elevator, industrial robot, injection molding machine, NC processing machine, linear motor
Automobile	Driving motor for HEV/fuel cell/electric power steering system, car sensor
others	MRI, motors for trains, wind power generators, electric bicycles

HDD, hard disk drive; HEV, hybrid electric vehicle; MRI, magnetic resonance imaging; NC, numerical control; VCM, voice coil motor.

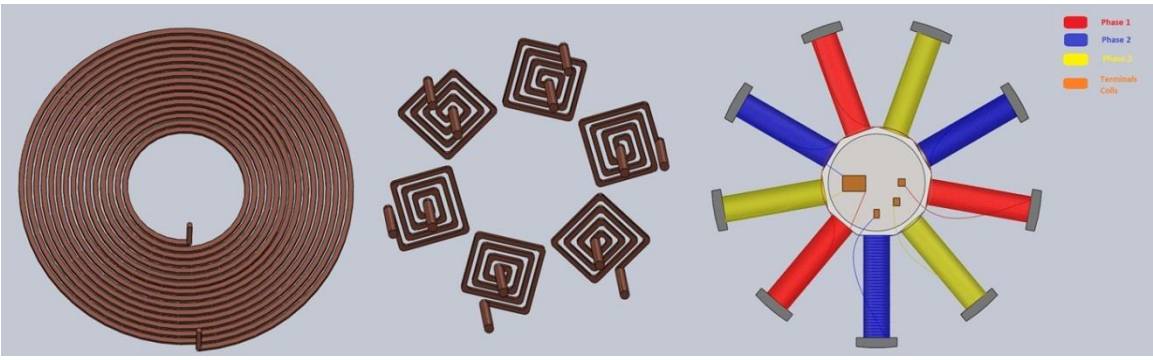

Figure 2.6 Coils shapes used in PM machines.

2.5 Permanent Magnets (PM) Brushless Machines

PM's brushless machines are electromechanical systems which can be operated as generators or motors. There are different topologies of PM brushless machines [90], [92], [96], [97], but these can be grouped in two general types: radial flux permanent magnets (RFPM) and axial flux permanent magnets (AFPM), which in turn can be classified into slotted or slotless, and internal or external rotor. Although various rotor and stator topologies may be employed to develop motor and generator machines, the most common RFPM and AFPM uses configurations of permanent magnets attached on the rotor, and the coil or armature winding, mounted on the stator. The magnetic distribution and flux flow direction are the principal differences of AFPM and RFPM machines. The magnetic field in RFPM machines flows radially between rotor and stator, while the magnetic field in AFPM flows axially in the direction parallel to the vertical axis of the rotor. Figure 2.7 shows a RFPM machine schematic.

Permanent-magnet brushless turbine generators are machines (PMBLM) that produce electricity through variation magnetic field created by moving PM's, which induce currents within stator windings. The core benefit of a PMBLM, is that it does not

require any additional or external excitation current. Table 2.3 shows some advantages and disadvantages of PM brushless machines.

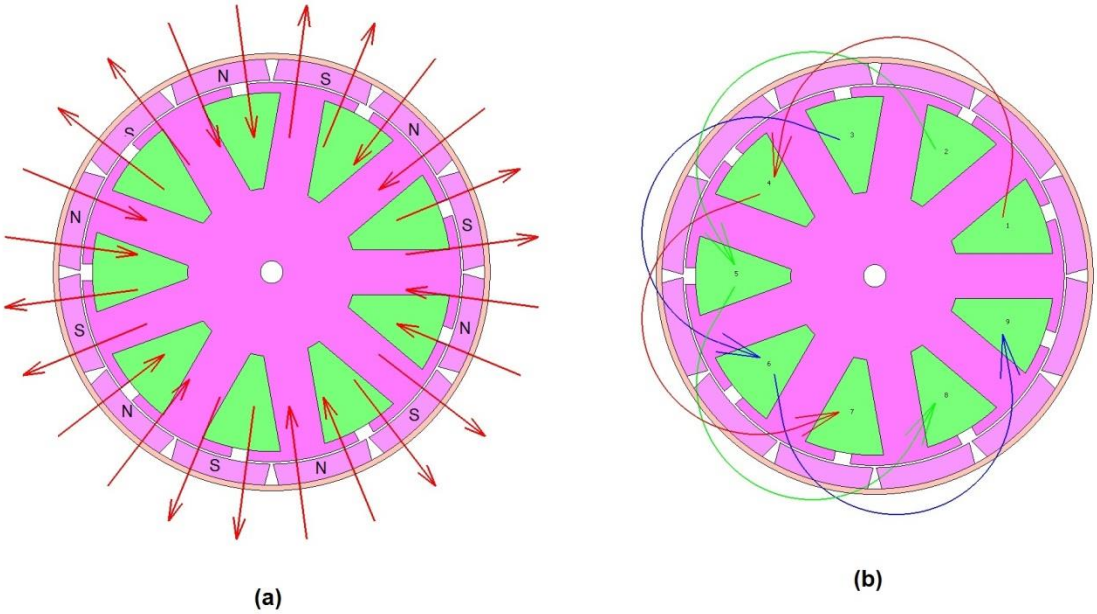

Figure 2.7 Permanent magnet machine. (a) Magnetic field in radial, (b) 9 coils in 3-phase configuration.

Table 2.3 Advantages and disadvantages of brushless machine type [90]

	Advantages	Disadvantages
Brushless Permanent magnet Machine	• Smaller and lighter designs can be developed. • High power density (factor) • Easily implemented, reduced maintenance cost and operating costs for some types of machines. • Minimal energy losses in the rotor • Easily automated • Good speed vs. torque. characteristics. Large air-gap length	• The price of magnets used defines the final cost • The system could suffer demagnetization of permanent magnets by excesses of temperatures and other physical conditions.

CHAPTER 3: CAD-DESIGNS AND MATHEMATICAL MODELS

This chapter presents the geometries, CAD designs, and the results of theoretical calculations involved in the development of the miniature generator system. The chapter is divided into three sections and describes the geometries used and theoretical calculations which support the computer aided-designs (CAD) of all parts of the turbine and the magnetic generator system. The first part is centered in the turbine system, the second in the motor generator system, and the third is the integration of both in a closed system.

3.1 Turbine System Final Design

In the development of this dissertation, many CAD design models were simulated, analyzed, and some prototypes were built and tested. The critical parameters observed in each model included: the mechanical and electrical power, efficiency, size, shape, and easy of fabrication. Also the available resources and university facilities were another fundamental point, because these determined the final cost and the possibility to develop the models at USF laboratories. This long process was used to search the best model bearing in mind future applications. The final model was simulated and analyzed in transient and steady states and the results are shown in chapter 4. The turbine is divided in two main parts: rotor and holder or casing. The design model of both turbine parts is detailed in the following sections of this chapter.

3.1.1 Rotor Design

The Micro generator includes a new model of impulse turbine with immersed rotor, which additionally uses reaction characteristics to contribute to the rotor spin. The rotor structure is divided into three parts: a cylindrical hub, two support discs on the top and bottom of the rotor, and notched blades arranged concentrically around the cylindrical hub supported by the two rotor support discs. The blades have curved forms to improve the capabilities of the design. The intersection point between the reference line and the radius of the internal circle R3, plus the blade thickness, defines the shape and curvature of each blade. Figure 3.1 shows the geometry used in the blade design, where the reference line is 45^{o} degrees, the radius of the inner circle is half of the total turbine radius (R_3 = 2.15 mm), the rotor thickness is 10% of the total turbine radius, the internal blade radius R=1.9 mm, and the internal blade arc is 90^{o} degrees, measured between intersection point denoted as A (intersection point of the vertical axis and the circle of radius R_2) and intersection point denoted as B (intersection point of reference line and the circle of radius R_3).

The rotor design, Figure 3.3, utilizes a semicircular notch on the internal proximal edge of the blades. The notches are centrally located about the tangential axis of the turbine. The radius of the notches arc is equal to or less than half of the radius of a blade. Notch geometry is shown in Figure 3.2. The internally notched blades permit a continuous circulation of fluid inside the rotor chamber, which decreases the possibility of clogging, fouling, or stagnation of the flow. As part of the reaction benefits, the notch also assures more interaction between the fluid and the blades because at the time of jet stream impact to the blade, the notch redirects the fluid and more than one blade is

impacted increasing the impulse force and the angular velocity of the blades. When the blades are initially impacted by the liquid, the direction of the liquid is changed, but the notched blades are able to redirect around 40% of the fluid to the outer surface of the next blade of the rotor chamber, adding more force that contributes to the continuous spin of the rotor. Therefore, the notch not only contributes toward increasing rotation, but towards minimizing the vortices between blades, thus, guaranteeing the proper rotation of the fluid inside of the rotor chamber and between blades.

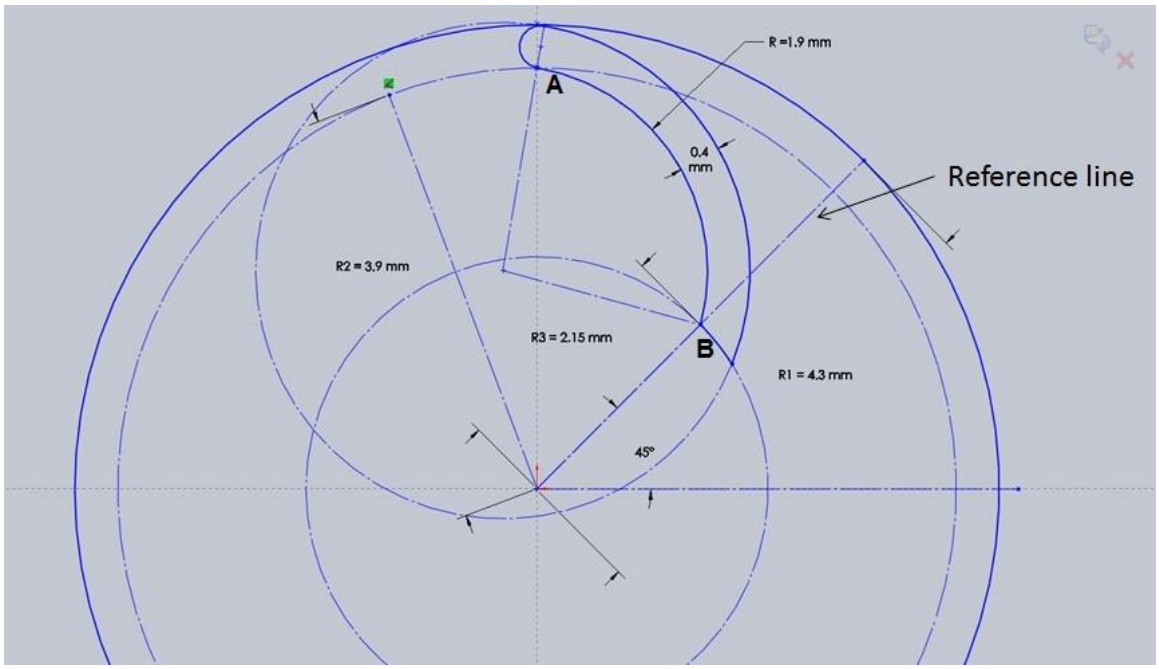

Figure 3.1 Rotor geometry.

As is shown in Fig. 3.3, the rotor consists of a circular solid disc with 6 blades, also called “buckets”, and the top and bottom of the blades are supported in a circular disc to assure blade stability, and to canalize and redirect the fluid flow to the central hub or the internal notch of each blade. Complementally, the top and bottom of the rotor have a special design, which joins the hub and the blades in a unique piece, making the

blade stronger and increasing its resistance. Also, the top and bottom design helps to support the assembling of the spindle machine, which finally will convert the mechanical energy to electric energy. The final rotor design viewed in different positions is shown in Fig. 3.4.

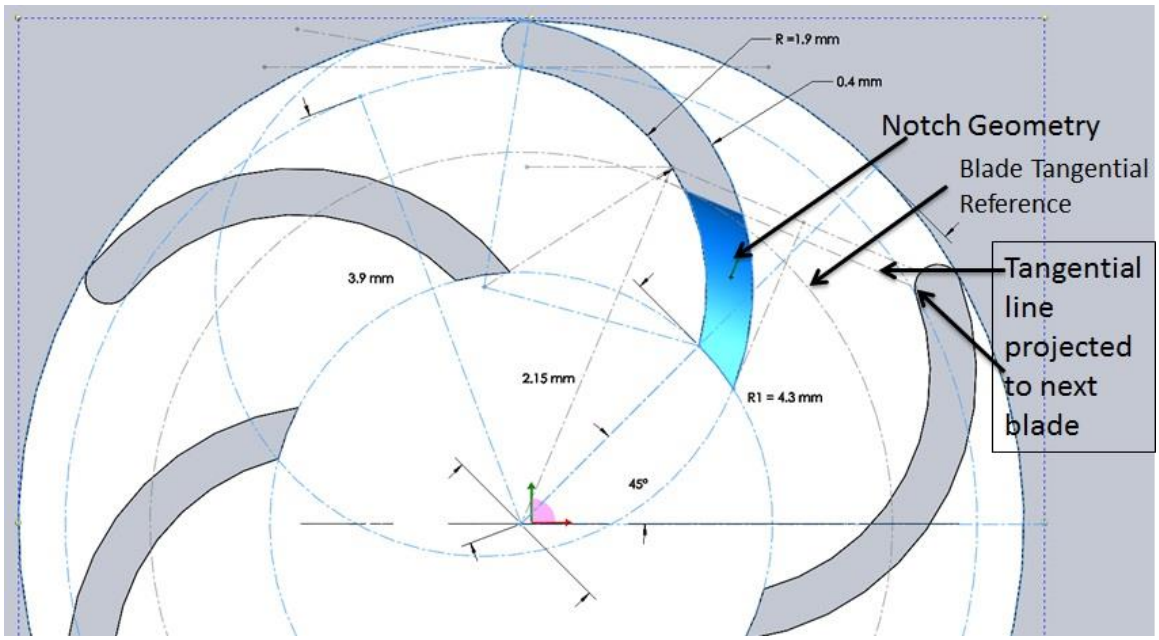

Figure 3.2 Notch geometry.

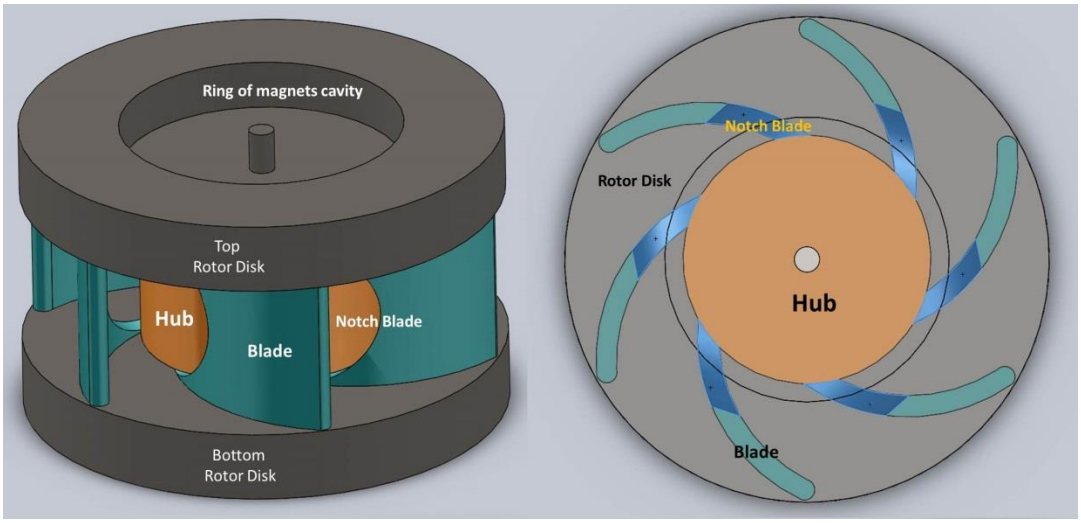

Figure 3.3 Rotor isometric and top plane section view. Isometric - left side, and rotor top plane section view – right side.

As is shown in Fig. 3.3, the rotor consists of a circular solid disc with 6 blades, also called “buckets”, and the top and bottom of the blades are supported in a circular disc to assure blade stability, and to canalize and redirect the fluid flow to the central hub or the internal notch of each blade. Complementally, the top and bottom of the rotor have a special design, which joins the hub and the blades in a unique piece, making the blade stronger and increasing its resistance. Also, the top and bottom design helps to support the assembling of the spindle machine, which finally will convert the mechanical energy to electric energy. The final rotor design viewed in different positions is shown in Fig. 3.4.

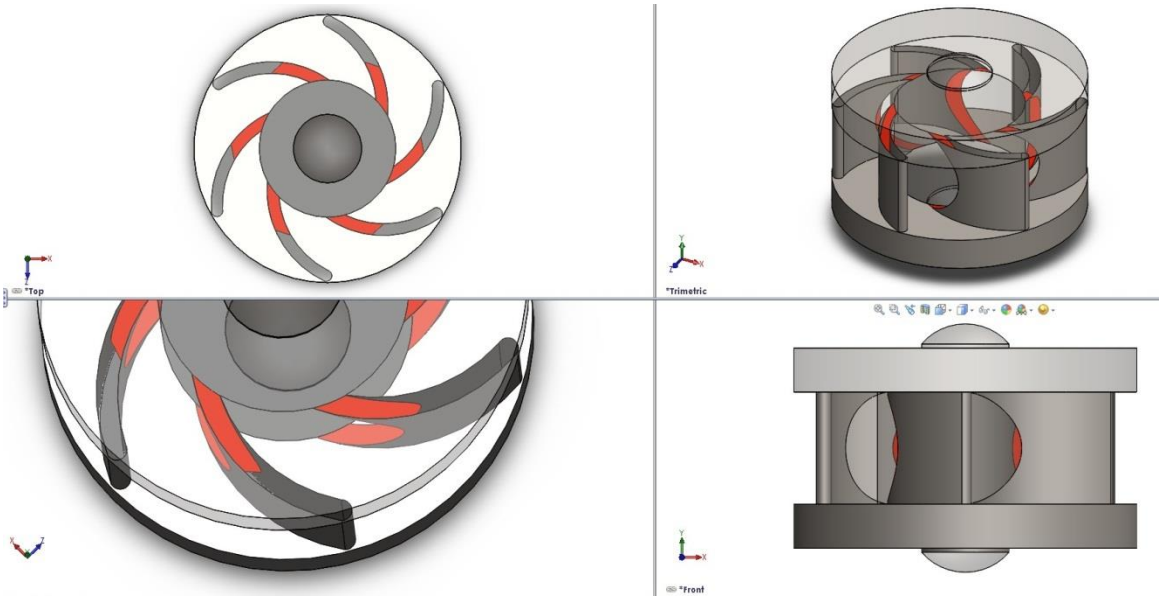

Figure 3.4 Rotor CAD design.

3.1.2 Holder Design

The holder or casing is a new design which is the final product of three years of research work. The CAD designs, simulations, prototypes and testing of pieces, helped

find the best model, and were done according to potential applications as well as to satisfy the basic principles of stability, compatibility, adaptability, and simple assembly. The holder is divided in three sections: Inlet-Nozzle, rotor chamber, and outlet. The input and output of the turbine were designed using a standard circular shape, with initial inlet and final output diameters of 4 mm, which is an ideal size to connect the micro turbine with microfluidic systems such as the circulatory system, micro pumps, mixers and refrigeration systems found in medical equipment, automotive systems, and home appliances.

Figure 3.5 Inlet turbine geometry.

The Inlet-Nozzle section, Figure 3.5, shows a gradual contraction between the input and the nozzle, where a conical section is formed with sharp discontinuities at the intersections. The inlet and nozzle dimensions used are a response to the laminar behavior requirement, especially in the blood system. The nozzle geometry has 10^{o} degrees of inclination with respect to the horizontal axis, to concentrate the jet on the maximum area of the first blade and optimize the impact. Also, this inclination contributes to the discharge through the notch and reduces the vortices in the central area of the rotor. The inlet was designed into a gradual contraction pipe or funnel shape

to create a venturi effect with the fluid flow, increasing the output velocity of the fluid at the nozzle and focusing the jet on the blades.

The rotor chamber and the outlet section have new and special geometries that permit free flow circulation to the output. Figure 3.6 shows the casing CAD design. The rotor chamber was designed with a curvature, which combines parabolas and circular geometries, to ease the flow discharge, and direct the impact of the fluid on more than one blade, and to increase the pressure on the output area of the turbine. The outlet section is designed to reestablish the inlet pressure which was modified when the fluid crossed the inlet conical section to later to be introduced through the nozzle to the rotor chamber.

In addition, the curved shape of the walls surrounding the rotor chamber contributes to the free flow of the fluid, avoiding any type of accumulation or stenosis, thus reducing stress on walls and assuring a good fluid displacement to the outlet turbine. Finally, and looking to have the best adaptability, the inlet and outlet of the turbine were designed as circular pipes given that it is the most common shape used to transport and connect microfluidic systems.

In summary, Figure 3.7 shows all the characteristics of the turbine casing, where inlet, rotor chamber, and outlet were defined according to biomedical and circulatory system specifications. The rotor chamber was designed to keep the turbine rotor aligned in the center and frictionless and to keep a variable gap between rotor and enclosing walls. The gap contributes to the circulation and redirects the fluid to the blades; also, the gap design avoids the friction when the rotor is in motion. The outlet

chamber is a free zone to discharge the fluid from rotor chamber with a conical shape and circular end.

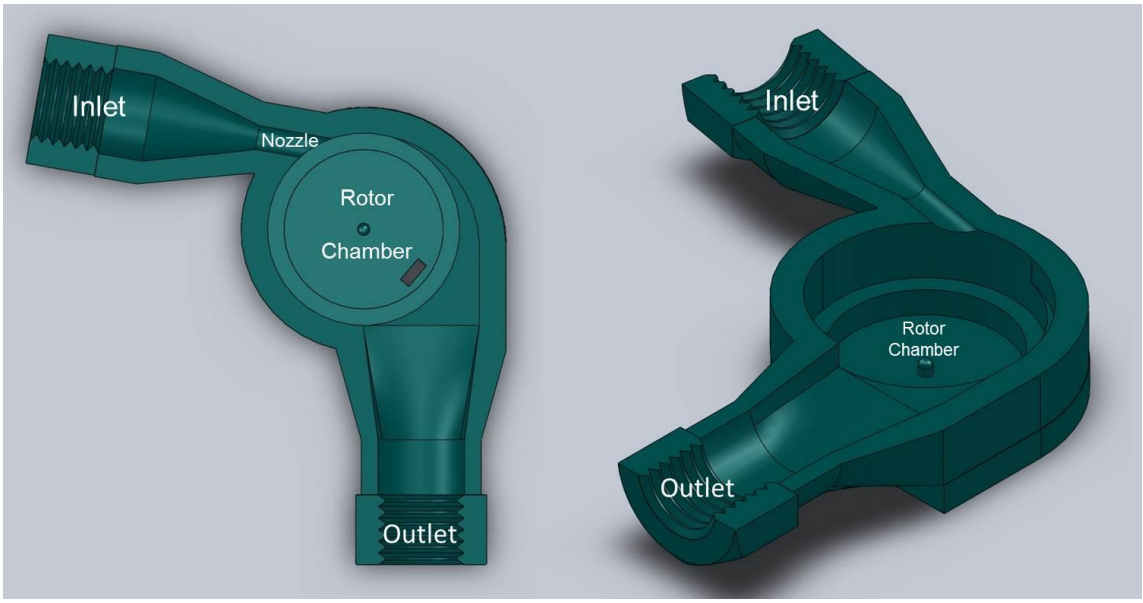

Figure 3.6 Turbine casing design.

3.1.3 Turbine Mathematical Model

The miniature notch turbine system is a new turbine model, especially designed to work with microfluids in immersed conditions. Given its novelty, a new mathematical model was developed to explain the physical behavior and the interrelation between parameters such as linear and tangential velocities, volume flow rate, forces applied on blades, and the required mechanical power, depending on the kind of fluid used to move the rotor. In the turbine mathematical model, the mass of fluid per second, entering from nozzle to the rotor chamber, is used to find the momentum of the liquid when the blades are pushed, and establishes the relationship with the forces striking the blades, torque and mechanical power generated by the system.

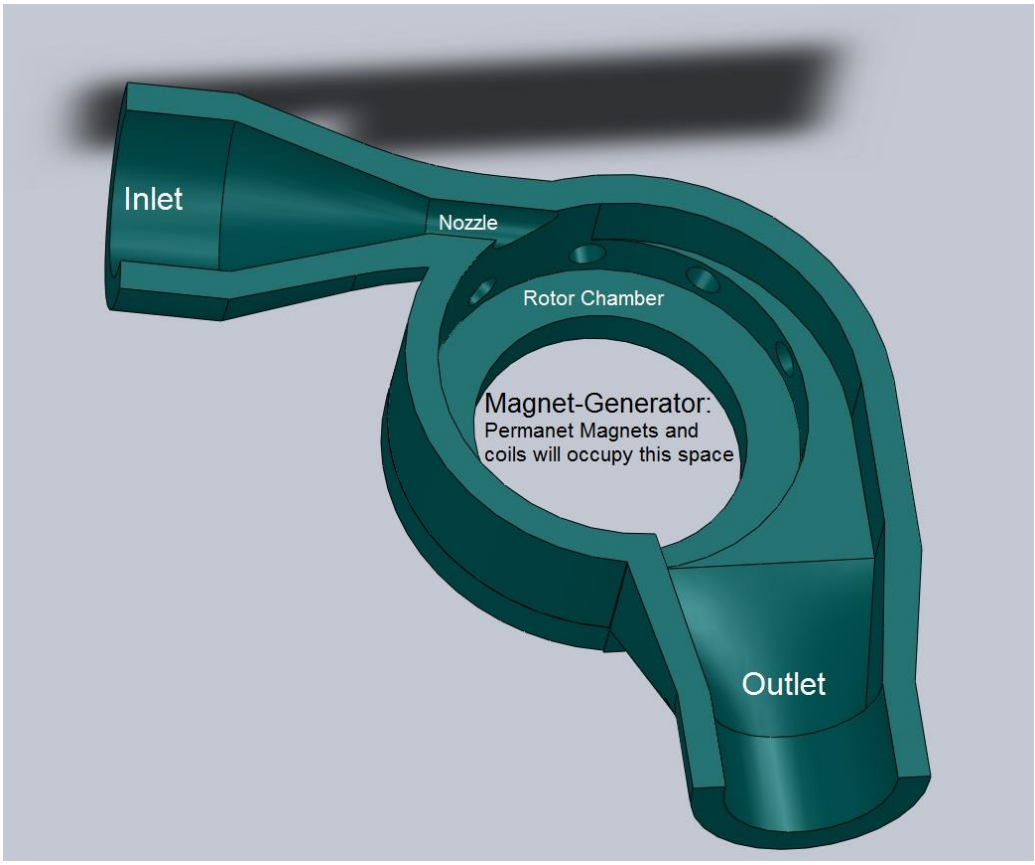

Figure 3.7 Turbine casing design horizontal section view.

A vector representation of velocities and flow direction is shown in Figure 3.8, where red curves represent the velocity trajectories of the fluid applied from nozzle. Purple curves represent the permanent internal flow fluid circulation, and blue arrows are the forces produced by the injected flow fluid, which finally create the torque to keep the rotor in constant speed. Also, to concentrate the analysis and develop the mathematical model, three principal points, central, external, and internal, were defined on each blade.

To know the minimum and maximum values of volume flow rate required to satisfy the mechanical power and angular velocities of this turbine, an analysis involving torques, forces, areas, and linear velocities affecting the blades was developed. Starting with the velocity and fluid flow behavior to the first blade, Figure 3.9, where the total

velocity is represented as the sum of angular velocity ($\boldsymbol{U_i}$) on rotor and the lineal velocity of flow fluid entering from nozzle ($\boldsymbol{V_n}$). However, the analysis needed to know the real impact of the fluid entering on each of blade is centered on the velocity vector, which is a subtraction between angular velocity on rotor and the lineal velocity of flow fluid entering from nozzle. Figure 3.9 shows the first blade vector analysis, which represents the components of velocities of the working fluid in a turbomachine. This analysis produced as a result, the equation that connects the desired rotor behavior (speed and torque) with the inlet volume flow rate, velocity, and forces of the fluid flow pushing the blades.

According to the shapes and geometries defined for this novel turbine, two velocity triangles on two points (internal A_2 and external A_1 points) of the first blade are defined, but a blade by blade analysis is developed. This is followed by the mechanical power and the efficiency equations of the turbine. The velocity triangles used in this analysis explain the flow direction and state the principal points of pressure, through which torque is applied to spin the rotor.

Through the vector analysis of velocities (velocity triangles), on two points of the first blade, the equations which explain the behavior of the notched blade turbine as an impulse turbine are defined. In Figure 3.9 V_{w_1} and V_{w_2} are the tangential velocities at A_1 and A_2 , and V_n is the jet velocity at the output of the nozzle. In addition, an angle α_1 is formed between the nozzle and the horizontal plane tangent to the rotor radius. Also, the horizontal plane and the tangential line in A2, create an angle α_2, just into the notch of the first blade, in the direction of the second blade.

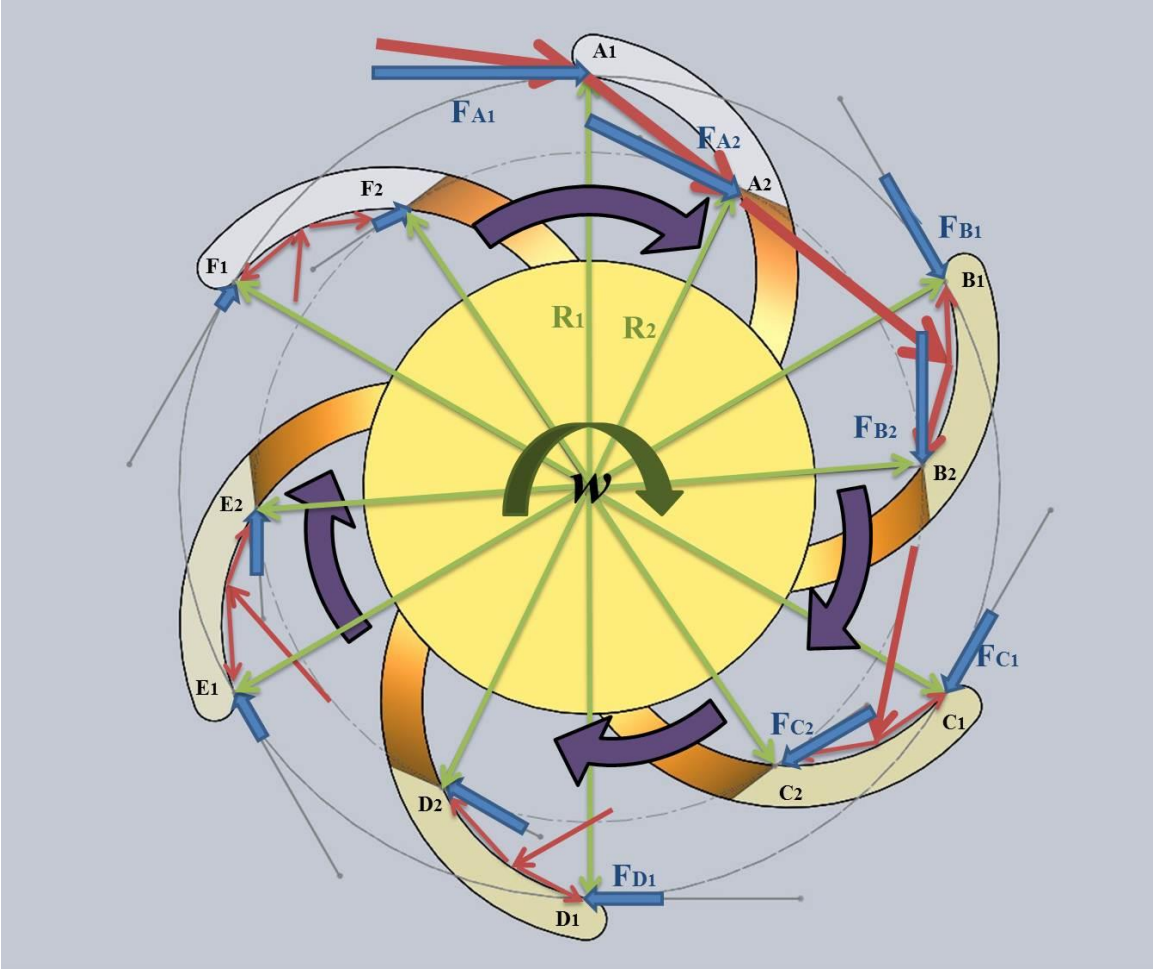

Figure 3.8 Physical variables affecting the rotor.

The system on the first blade is analyzed as an impulse turbine and the equations on the first blade are developed at two positions, A_1 and A_2 resulting in the tangential velocities V_{w_1} and V_{w_2}, as shown in Figure 3.9. In both cases, the results of the tangential velocities are functions of the nozzle velocity and the angles involved in the input and output of the fluid on the blade. Also, the flow fluid leaving the first blade has a velocity V_A.

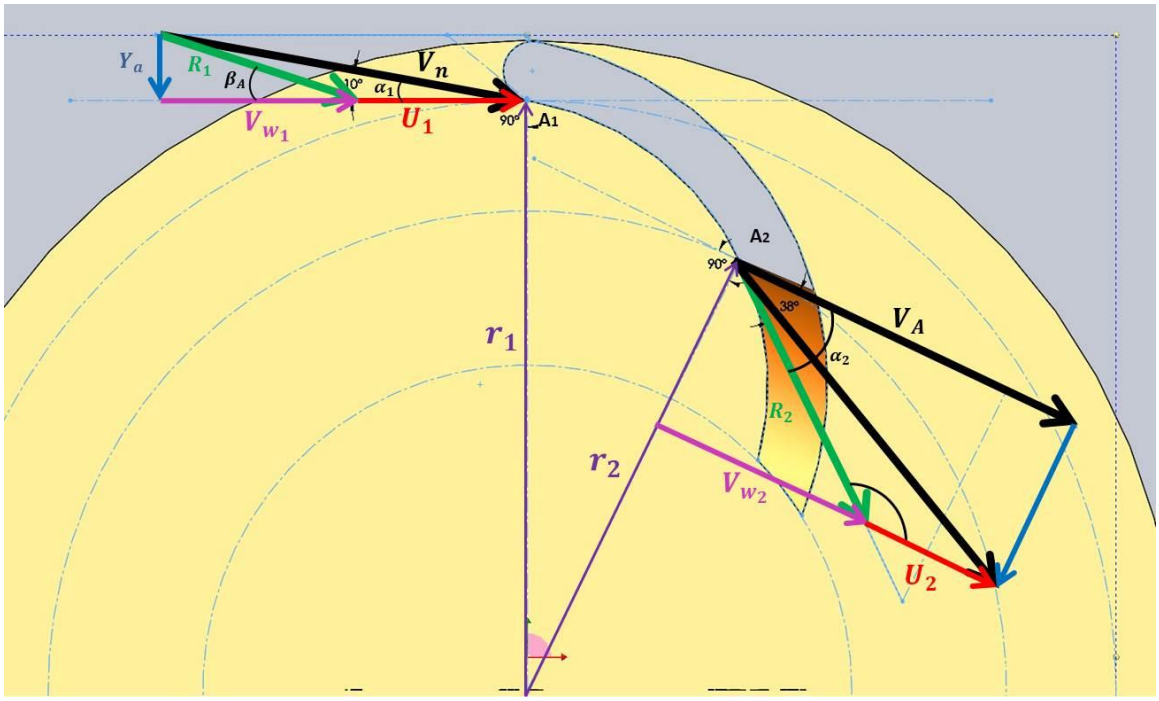

Figure 3.9 Velocity triangle first blade.

The equations 3.1, 3.2 and 3.3 are the velocity triangle analysis on the first blade, where V_{w_1} is the tangential inlet velocity, V_{w_2} and is the tangential outlet velocity (notch velocity), and V_A is the fluid velocity crossing the notch of the first blade,

$$V_{w_1} = V_n \cos \alpha_1 - U_1 \quad 3.1$$

$$V_{w_2} = (V_N \cos \alpha_1 - U_1) \cos \propto_2 \quad 3.2$$

$$V_A = V_{w_2} + U_2 = (V_N \cos \alpha_1 - U_1) \cos \propto_2 + U_2 \quad 3.3$$

The model of forces on the first blade was found using the geometry shown in Figures 3.8, and 3.9, but applying the momentum balance analysis combined with the velocity triangles. Also, the torque equation on first blade was found as the product of these forces and the radial distances. The equations 3.4, 3.5 and 3.6 develop the analysis of forces and torques on first blade,

$$F_A = \rho Q\left(V_{w_1} + V_{w_2}\right) = (V_N \cos\alpha_1 - U_1)(1 + \cos\propto_2) \quad 3.4$$

$$T_A = \rho Q\left(V_{w_1} r_1 + V_{w_2} r_2\right) = \rho Q[V_N \cos\alpha_1 (r_1 + r_2 \cos\propto_2) - U_1(r_1 + r_2 \cos\propto_2)]$$

$$T_A = \rho Q[(V_N \cos\alpha_1 - U_1)(r_1 + r_2 \cos\propto_2)] \quad 3.5$$

$$T_A = \rho Q(V_N A\cos\alpha_1 - U_1 A) \quad 3.6$$

where

$$A = (r_1 + r_2 \cos\propto_2) \quad 3.7$$

The analysis to find the equations on the second blade starts with the flow fluid from the first blade after passing by the notch, and goes until it totally leaves the second blade, but includes the central impact on second blade. As Figure 3.10 shows, the velocity V_A from the notch area of the first blade enters to the second blade with an inclination angle α_3, measured between the central point of the second blade, in the tangential direction to the rotor.

V_A is the inlet velocity at the second blade, but has an inclination angle $\propto_3$ casing measured between the flow fluid direction and the center blade on the tangential line of this point. Figure 3.10, shows the geometry, while the equations for the second blade on the B_1, B_2, and the central point B_m are described in equations 3.8 to 3.20

$$V_A = V_{w_2} + U_2 = (V_N \cos\alpha_1 - U_1)\cos\propto_2 + U_2 \quad 3.8$$

where tangential inlet velocity on second blade, denoted as V_{M_B} is written as,

$$V_{M_B} = V_A \cos\alpha_3 = \left(V_{w_2} + U_2\right)\cos\alpha_3 = [(V_N \cos\alpha_1 - U_1)\cos\propto_2 + U_2]\cos\alpha_3$$

$$V_{M_B} = \left[(V_N \cos\alpha_1 - U_1)\cos\propto_2 + U_1\frac{r_2}{r_1}\right]\cos\alpha_3$$

$$V_{M_B} = V_N \cos\alpha_1 \cos\propto_2 \cos\alpha_3 - U_1\left(\cos\propto_2 - \frac{r_2}{r_1}\right)\cos\alpha_3 \quad 3.9$$

$$V_{M_B} = V_N B cos\,\alpha_1 - U_1 C \qquad 3.10$$

where

$$B = cos \propto_2 cos\,\alpha_3 \qquad 3.11$$

$$C = \left(B - \frac{r_2}{r_1} cos\,\alpha_3\right) \qquad 3.12$$

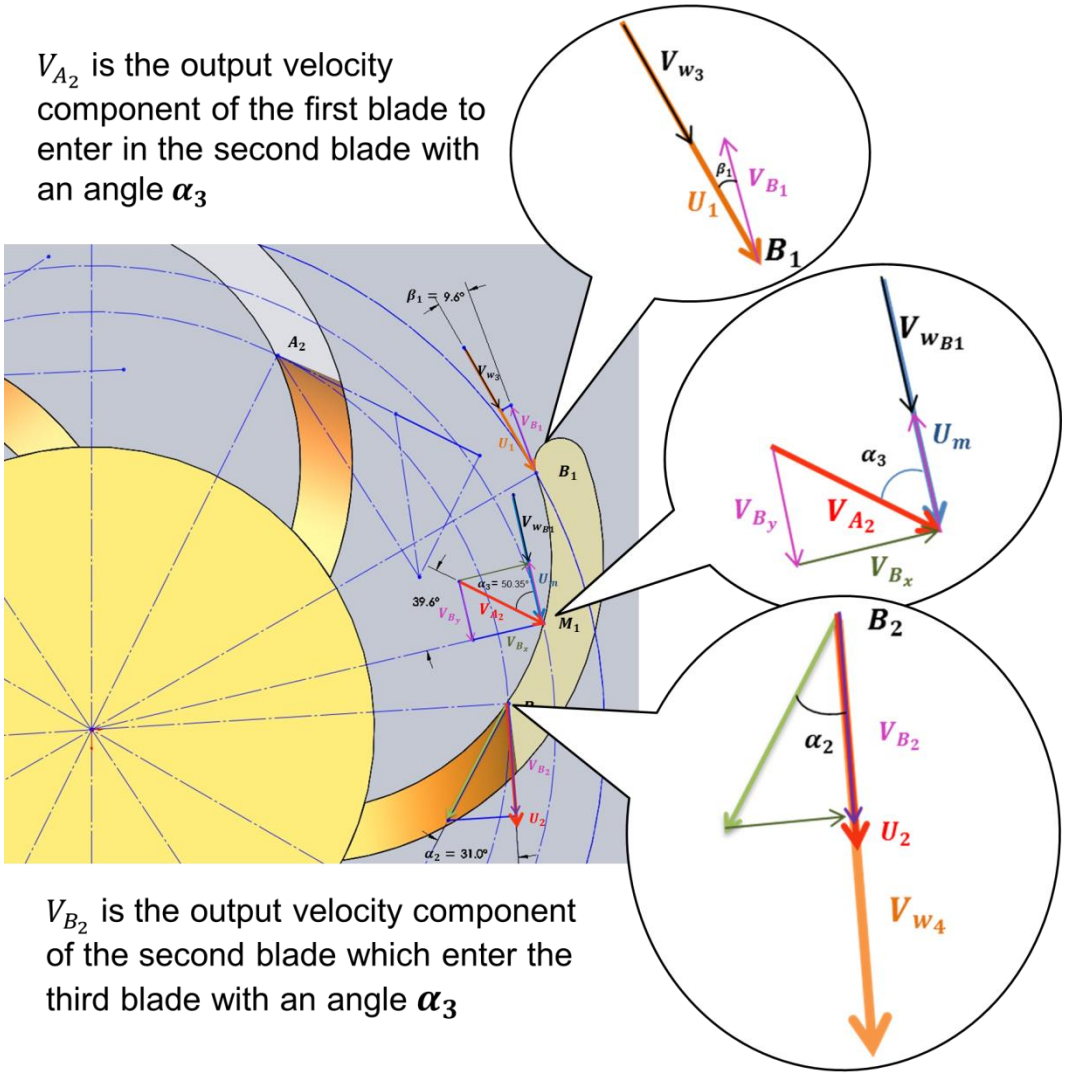

Figure 3.10 Second blade analysis.

Flow fluid velocity from the first blade impacts the second blade on center place, then the fluid flow is divided into two components after pushing the second blade, the

first velocity component is directed to the external edge B_1, and the second component is directed to the internal edge B_2 or notch. The velocities results on B_1 and B_2 have a tangential direction in the same line of the rotor tangential velocity on these points. The component on B_1 is opposite of that of tangential velocity U_1, while the component on B_2 has the same direction as the tangential velocity on this point U_2.

$$\mathrm{V}_{B_1} = U_1 - \left(V_{M_B} - U_M\right) cos\, \beta_1 \tag{3.13}$$

$$V_{B_2} = U_2 + \left(V_{M_B} - U_M\right) cos \propto_2 \tag{3.14}$$

$$\Delta V_{B_1} = V_{M_B} - V_{B_1}$$

$$\Delta V_{B_1} = V_{M_B}(1 + cos\, \beta_1) - U_1 \left(1 + \frac{r_m}{r_1} cos\, \beta_1\right) \tag{3.15}$$

$$\Delta V_{B_2} = V_{M_B} - V_{B_2}$$

$$\Delta V_{B_2} = V_{M_B}(1 - cos \propto_2) - U_1 \left(\frac{r_2}{r_1} - \frac{r_m}{r_1} cos \propto_2\right) \tag{3.16}$$

the force on second blade is represented by

$$F_B = \rho Q\left(\Delta V_{B_1} + \Delta V_{B_2}\right)$$

$$F_B = \rho Q\left(V_{M_B}[(1 + cos\, \beta_1) + (1 - cos \propto_2)]\right) - U_1 \left[\left(1 + \frac{r_M}{r_1} cos\, \beta_1\right) + \left(\frac{r_2}{r_1} - \frac{r_m}{r_1} cos \propto_2\right)\right] \tag{3.17}$$

By using the above equations plus the mass flow rate $(\dot{m} = \rho Q)$ then the torque on second blade is found

$$T_B = \rho Q\left(\Delta V_{B_1} r_1 + \Delta V_{B_2} r_2\right)$$

$$T_B = \rho Q \left[V_{M_B}\left(r_1(1 + cos\, \beta_1) + r_2(1 - cos \propto_2)\right) - U_1 \left(r_1 \left(1 + \frac{r_M}{r_1} cos\, \beta_1\right) + r_2 \left(\frac{r_2}{r_1} - \frac{r_m}{r_1} cos \propto_2\right)\right)\right]$$

to simplify the torque equations two constants D and E are defined,

$$D = r_1(1 + cos\, \beta_1) + r_2(1 - cos \propto_2) \tag{3.18}$$

$$E = r_1 \left(1 + \frac{r_M}{r_1} cos\, \beta_1\right) + r_2 \left(\frac{r_2}{r_1} - \frac{r_m}{r_1} cos \propto_2\right) \tag{3.19}$$

then torque on second blade is rewritten as

$$T_B = \rho Q\left(V_{M_B} D - U_1 E\right) = \rho Q[V_N BD\cos\alpha_1 - U_1 CD - U_1 E]$$

$$T_B = \rho Q[V_N BD\cos\alpha_1 - U_1(CD + E)] \qquad 3.20$$

The analysis to find the equations in the next blades, third to sixth, use the same physical principles and the same geometry as the first and second blades, which starts with the fluid flow from the previous blade, passing through the notch in direction of the next blade at the central point of the blade. As shown in Figures 3.8, 3.9, and 3.10, there are components of velocity from the notch areas by each blade which enter to the next blade with an inclination angle β_1, measured between the central point of the blade and in the rotor radial direction. The components of velocity have the same angle on entry and exit on each blade, but the magnitudes of these vectors are different, having the maximum value in the first blade and a minimum in the sixth blade. The equations 3.21 to 3.28 are the analysis on third blade. The triangle of velocity is written as,

$$V_{M_C} = V_{B_2}\cos\alpha_3 = \left(U_2 + \left(V_{M_B} - U_M\right)\cos\propto_2\right)\cos\alpha_3$$

$$V_{M_C} = (U_2 + (V_N B\cos\alpha_1 - U_1 C - U_M)\cos\propto_2)\cos\alpha_3$$

$$V_{M_C} = \left(V_N B\cos\alpha_1\cos\propto_2\cos\alpha_3 + U_1\frac{r_2}{r_1}\cos\propto_3 - U_1 C\cos\propto_2\cos\alpha_3 - U_1\frac{r_m}{r_1}\cos\propto_2\cos\alpha_3\right)$$

$$V_{M_C} = \left[V_N B^2\cos\propto_1 + U_1\left(\frac{r_2}{r_1}\cos\propto_3 - BC - B\frac{r_m}{r_1}\right)\right] \qquad 3.21$$

$$V_{C_1} = U_1 - \left(V_{M_C} - U_M\right)\cos\beta_1 \qquad 3.22$$

$$V_{C_2} = U_2 + \left(V_{M_C} - U_M\right)\cos\propto_2 \qquad 3.23$$

$$\Delta V_{C_1} = V_{M_C} - V_{C_1}$$

$$\Delta V_{C_1} = V_{M_C}(1 + \cos\beta_1) - U_1\left(1 + \frac{r_m}{r_1}\cos\beta_1\right) \qquad 3.24$$

$$\Delta V_{C_2} = V_{M_C} - V_{C_2}$$

$$\Delta V_{C_2} = V_{M_C}(1 - cos \propto_2) - U_1 \left(\frac{r_2}{r_1} - \frac{r_m}{r_1} cos \propto_2\right) \quad 3.25$$

while the equation describing the forces on third blade as written as,

$$F_C = \rho Q\left(\Delta V_{C_1} + \Delta V_{C_2}\right)$$

$$F_C = \rho Q\left(V_{M_C}[(1 + cos\,\beta_1) + (1 - cos \propto_2)]\right) - U_1 \left[\left(1 + \frac{r_M}{r_1} cos\,\beta_1\right) + \left(\frac{r_2}{r_1} - \frac{r_m}{r_1} cos \propto_2\right)\right] \quad 3.26$$

the total torque on third blade is written as,

$$T_C = \rho Q\left(\Delta V_{C_1} r_1 + \Delta V_{C_2} r_2\right)$$

$$T_C = \rho Q \left[V_{M_C}\left(r_1(1 + cos\,\beta_1) + r_2(1 - cos \propto_2)\right) - U_1 \left(r_1\left(1 + \frac{r_M}{r_1} cos\,\beta_1\right) + r_2\left(\frac{r_2}{r_1} - \frac{r_m}{r_1} cos \propto_2\right)\right)\right] \quad 3.27$$

if equations 3.18 and 3.19 are substituted in equation 3.27, then torque on third blade is rewritten as

$$T_C = \rho Q\left(V_{M_C} D - U_1 E\right)$$

$$T_C = \rho Q \left[V_N(B^2 D\, cos \propto_1) + U_1 \left(\frac{r_2}{r_1} D\, cos \propto_3 - CBD - B\frac{r_m}{r_1} D - E\right)\right] \quad 3.28$$

The equations 3.29 to 3.36 are the analysis on fourth blade. The triangle of velocity is written as,

$$V_{M_D} = V_{C_2} cos\,\alpha_3 = \left(U_2 + \left(V_{M_C} - U_M\right) cos \propto_2\right) cos\,\alpha_3$$

$$V_{M_D} = \left(U_2 + \left(V_N B^2\, cos \propto_1 + U_1 \left(\frac{r_2}{r_1} cos \propto_3 - CB - B\frac{r_m}{r_1}\right) - U_M\right) cos \propto_2\right) cos\,\alpha_3$$

$$V_{M_D} = \left(V_N B^3\, cos \propto_1 + U_1 \frac{r_2}{r_1} cos \propto_3 + U_1 B \frac{r_2}{r_1} cos \propto_3 - U_1 CB^2 - U_1 \frac{r_m}{r_1} B^2 - U_1 \frac{r_m}{r_1} B\right)$$

$$V_{M_D} = \left[V_N B^3\, cos \propto_1 + U_1 \left(\frac{r_2}{r_1} cos \propto_3 + B\frac{r_2}{r_1} cos \propto_3 - CB^2 - B^2 \frac{r_m}{r_1} - B\frac{r_m}{r_1}\right)\right] \quad 3.29$$

$$V_{D_1} = U_1 - \left(V_{M_D} - U_M\right) cos\,\beta_1 \quad 3.30$$

$$V_{D_2} = U_2 + \left(V_{M_D} - U_M\right) cos \propto_2 \quad 3.31$$

$$\Delta V_{D_1} = V_{M_D} - V_{D_1}$$

$$\Delta V_{D_1} = V_{M_D}(1 + cos\,\beta_1) - U_1\left(1 + \frac{r_m}{r_1} cos\,\beta_1\right) \quad 3.32$$

$$\Delta V_{D_2} = V_{M_D} - V_{D_2}$$

$$\Delta V_{D_2} = V_{M_D}(1 - cos\,\propto_2) - U_1\left(\frac{r_2}{r_1} - \frac{r_m}{r_1} cos\,\propto_2\right) \quad 3.33$$

while the equation describing the forces on fourth blade as written as,

$$F_D = \rho Q\left(\Delta V_{D_1} + \Delta V_{D_2}\right)$$

$$F_D = \rho Q\left(V_{M_D}[(1 + cos\,\beta_1) + (1 - cos\,\propto_2)]\right) - U_1\left[\left(1 + \frac{r_M}{r_1} cos\,\beta_1\right) + \left(\frac{r_2}{r_1} - \frac{r_m}{r_1} cos\,\propto_2\right)\right] \quad 3.34$$

and the torque on the fourth blade is written as

$$T_D = \rho Q\left(\Delta V_{D_1} r_1 + \Delta V_{D_2} r_2\right)$$

$$T_D = \rho Q\left[V_{M_D}\left(r_1(1 + cos\,\beta_1) + r_2(1 - cos\,\propto_2)\right) - U_1\left(r_1\left(1 + \frac{r_M}{r_1} cos\,\beta_1\right) + r_2\left(\frac{r_2}{r_1} - \frac{r_m}{r_1} cos\,\propto_2\right)\right)\right] \quad 3.35$$

if equations 3.18 and 3.19 are substituted in equation 3.35, then torque on fourth blade is rewritten as

$$T_D = \rho Q\left(V_{M_D} D - U_1 E\right)$$

$$T_D = \rho Q\left[D\left(V_N B^3\, cos\,\propto_1 + U_1\left(\frac{r_2}{r_1} cos\,\propto_3 + B\frac{r_2}{r_1} cos\,\propto_3 - CB^2 - B^2\frac{r_m}{r_1} - B\frac{r_m}{r_1}\right)\right) - U_1 E\right]$$

$$T_D = \rho Q\left[V_N B^3 D\, cos\,\propto_1 + U_1\left(\frac{r_2}{r_1} D cos\,\propto_3 + BD\frac{r_2}{r_1} cos\,\propto_3 - B^2 C\, D - B^2 D\frac{r_m}{r_1} - BD\frac{r_m}{r_1} - E\right)\right] \quad 3.36$$

The equations 3.37 to 3.44 are the analysis on fifth blade. The triangle of velocity is written as,

$$V_{M_E} = V_{D_2} cos\,\alpha_3 = \left(U_2 + \left(V_{M_D} - U_M\right) cos\,\propto_2\right) cos\,\alpha_3$$

$$V_{M_E} = \left(U_2 + \left(V_N B^3\, cos\,\propto_1 + U_1\left(\frac{r_2}{r_1} cos\,\propto_3 + B\frac{r_2}{r_1} cos\,\propto_3 - CB^2 - B^2\frac{r_m}{r_1} - B\frac{r_m}{r_1}\right) - U_M\right) cos\,\propto_2\right) cos\,\alpha_3$$

$$V_{M_E} = \left(V_N B^4\, cos\,\propto_1 + U_1\frac{r_2}{r_1} cos\,\propto_3 + U_1 B\frac{r_2}{r_1} cos\,\propto_3 + U_1 B^2\frac{r_2}{r_1} cos\,\propto_3 - U_1 CB^3 - B^3 U_1\frac{r_m}{r_1} - B^2 U_1\frac{r_m}{r_1} - U_1\frac{r_m}{r_1} B\right)$$

$$V_{M_E} = \left[V_N B^4\, cos\,\propto_1 + U_1\left(\frac{r_2}{r_1} cos\,\propto_3 + B\frac{r_2}{r_1} cos\,\propto_3 + B^2\frac{r_2}{r_1} cos\,\propto_3 - CB^3 - B^3\frac{r_m}{r_1} - B^2\frac{r_m}{r_1} - \frac{r_m}{r_1} B\right)\right] \quad 3.37$$

$$V_{E_1} = U_1 - \left(V_{M_E} - U_M\right) cos\,\beta_1 \quad 3.38$$

$$V_{E_2} = U_2 + \left(V_{M_E} - U_M\right) cos \propto_2 \quad 3.39$$

$$\Delta V_{E_1} = V_{M_D} - V_{D_1}$$

$$\Delta V_{E_1} = V_{M_E}(1 + cos\,\beta_1) - U_1\left(1 + \frac{r_m}{r_1} cos\,\beta_1\right) \quad 3.40$$

$$\Delta V_{E_2} = V_{M_E} - V_{E_2}$$

$$\Delta V_{E_2} = V_{M_E}(1 - cos \propto_2) - U_1\left(\frac{r_2}{r_1} - \frac{r_m}{r_1} cos \propto_2\right) \quad 3.41$$

while the equation describing the forces on fifth blade as written as,

$$F_E = \rho Q\left(\Delta V_{D_1} + \Delta V_{D_2}\right)$$

$$F_E = \rho Q\left(V_{M_E}[(1 + cos\,\beta_1) + (1 - cos \propto_2)]\right) - U_1\left[\left(1 + \frac{r_M}{r_1} cos\,\beta_1\right) + \left(\frac{r_2}{r_1} - \frac{r_m}{r_1} cos \propto_2\right)\right] \quad 3.42$$

and the torque on fifth blade is written as

$$T_E = \rho Q\left(\Delta V_{E_1} r_1 + \Delta V_{E_2} r_2\right)$$

$$T_E = \rho Q\left[V_{M_E}\left(r_1(1 + cos\,\beta_1) + r_2(1 - cos \propto_2)\right) - U_1\left(r_1\left(1 + \frac{r_M}{r_1} cos\,\beta_1\right) + r_2\left(\frac{r_2}{r_1} - \frac{r_m}{r_1} cos \propto_2\right)\right)\right] \quad 3.43$$

if equations 3.18 and 3.19 are substituted in equation 3.43, then torque on fifth blade is rewritten as

$$T_E = \rho Q\left(V_{M_E} D - U_1 E\right)$$

$$T_E = \rho Q\left[D\left(V_N B^4 cos \propto_1 + U_1\left(\frac{r_2}{r_1} cos \propto_3 + B\frac{r_2}{r_1} cos \propto_3 + B^2\frac{r_2}{r_1} cos \propto_3 - CB^3 - B^3\frac{r_m}{r_1} - B^2\frac{r_m}{r_1} - \frac{r_m}{r_1} B\right)\right) - U_1 E\right]$$

$$T_E = \rho Q\left[V_N B^4 D\, cos \propto_1 + U_1\left(\frac{r_2}{r_1} D\, cos \propto_3 + BD\frac{r_2}{r_1} cos \propto_3 + B^2 D\frac{r_2}{r_1} cos \propto_3 - B^3 CD - B^3 D\frac{r_m}{r_1} - B^2 D\frac{r_m}{r_1} - \frac{r_m}{r_1} BD - E\right)\right] \quad 3.44$$

The equations 3.45 to 3.51 are the analysis on sixth blade. The triangle of velocity is written as,

$$V_{M_F} = V_{E_2} cos\,\alpha_3 = \left(U_2 + \left(V_{M_E} - U_M\right) cos \propto_2\right) cos\,\alpha_3$$

$$V_{M_F} = \left(U_2 + \left(V_N B^4 cos \propto_1 + U_1\left(\frac{r_2}{r_1} cos \propto_3 + B\frac{r_2}{r_1} cos \propto_3 + B^2\frac{r_2}{r_1} cos \propto_3 - CB^3 - B^3\frac{r_m}{r_1} - B^2\frac{r_m}{r_1} - \frac{r_m}{r_1} B\right) - U_M\right) cos \propto_2\right) cos\,\alpha_3$$

$$V_{M_F} = \left(V_N B^5 \cos \propto_1 + U_1 \frac{r_2}{r_1} \cos \propto_3 + U_1 B \frac{r_2}{r_1} \cos \propto_3 + U_1 B^2 \frac{r_2}{r_1} \cos \propto_3 + U_1 B^3 \frac{r_2}{r_1} \cos \propto_3 - U_1 C B^4 - B^4 U_1 \frac{r_m}{r_1} - B^3 U_1 \frac{r_m}{r_1} - B^2 U_1 \frac{r_m}{r_1} - U_1 \frac{r_m}{r_1} B\right)$$

$$V_{M_F} = \left[V_N B^5 \cos \propto_1 + U_1 \left(\frac{r_2}{r_1} \cos \propto_3 + B \frac{r_2}{r_1} \cos \propto_3 + B^2 \frac{r_2}{r_1} \cos \propto_3 + B^3 \frac{r_2}{r_1} \cos \propto_3 - C B^4 - B^4 \frac{r_m}{r_1} B^3 \frac{r_m}{r_1} - B^2 \frac{r_m}{r_1} - \frac{r_m}{r_1} B\right)\right] \quad 3.45$$

$$V_{F_1} = U_1 - \left(V_{M_F} - U_M\right) \cos \beta_1 \quad 3.46$$

$$V_{F_2} = U_2 + \left(V_{M_F} - U_M\right) \cos \propto_2 \quad 3.47$$

$$\Delta V_{F_1} = V_{M_F} - V_{F_1}$$

$$\Delta V_{F_1} = V_{M_F}(1 + \cos \beta_1) - U_1 \left(1 + \frac{r_m}{r_1} \cos \beta_1\right) \quad 3.48$$

$$\Delta V_{F_2} = V_{M_F} - V_{F_2}$$

$$\Delta V_{F_2} = V_{M_F}(1 - \cos \propto_2) - U_1 \left(\frac{r_2}{r_1} - \frac{r_m}{r_1} \cos \propto_2\right) \quad 3.49$$

while the equation describing the forces on sixth blade as written as,

$$F_F = \rho Q\left(\Delta V_{D_1} + \Delta V_{D_2}\right)$$

$$F_F = \rho Q\left(V_{M_F}[(1 + \cos \beta_1) + (1 - \cos \propto_2)]\right) - U_1 \left[\left(1 + \frac{r_M}{r_1} \cos \beta_1\right) + \left(\frac{r_2}{r_1} - \frac{r_m}{r_1} \cos \propto_2\right)\right]$$

and the torque on sixth blade

$$T_F = \rho Q\left(\Delta V_{F_1} r_1 + \Delta V_{F_2} r_2\right)$$

$$T_F = \rho Q \left[V_{M_F}\left(r_1(1 + \cos \beta_1) + r_2(1 - \cos \propto_2)\right) - U_1 \left(r_1 \left(1 + \frac{r_M}{r_1} \cos \beta_1\right) + r_2 \left(\frac{r_2}{r_1} - \frac{r_m}{r_1} \cos \propto_2\right)\right)\right] \quad 3.50$$

if equations 3.18 and 3.19 are substituted in equation 3.50, then torque on sixth blade is rewritten as,

$$T_F = \rho Q\left(V_{M_F} D - U_1 E\right)$$

$$T_F = \rho Q \left[D \left(V_N B^5 \cos \propto_1 + U_1 \left(\frac{r_2}{r_1} \cos \propto_3 + B \frac{r_2}{r_1} \cos \propto_3 + B^2 \frac{r_2}{r_1} \cos \propto_3 + B^3 \frac{r_2}{r_1} \cos \propto_3 \right.\right.\right.$$

$$\left.\left.\left. - C B^4 - B^4 \frac{r_m}{r_1} - B^3 \frac{r_m}{r_1} - B^2 \frac{r_m}{r_1} - \frac{r_m}{r_1} B\right)\right) - U_1 E\right]$$

The rotor mechanical power is calculated as the product of torque multiplied by the angular velocity [98]–[102], but total torque is found as the sum of the total torque on each blade, and torque can be rewritten as,

a. first blade,

$$T_A = \rho Q (V_N A cos\, \alpha_1 - U_1 A) \quad 3.51$$

b. second blade,

$$T_B = \rho Q \left(V_{M_B} D - U_1 E\right) \quad 3.52$$

c. third blade,

$$T_C = \rho Q \left(V_{M_C} D - U_1 E\right) \quad 3.53$$

d. fourth blade,

$$T_D = \rho Q \left(V_{M_D} D - U_1 E\right) \quad 3.54$$

e. fifth blade,

$$T_E = \rho Q \left(V_{M_E} D - U_1 E\right) \quad 3.55$$

f. sixth blade,

$$T_F = \rho Q \left(V_{M_F} D - U_1 E\right) \quad 3.56$$

g. turbine total,

$$T_T = \rho Q \left(V_N A cos\, \alpha_1 + D\left(V_{M_B} + V_{M_C} + V_{M_D} + V_{M_E} + V_{M_F}\right) - U_1 (5E + A)\right) \quad 3.57$$

where tangential inlet velocities on each blade are written as,

$$V_{M_A} = V_N cos\, \alpha_1 - U_1 \quad 3.58$$

$$V_{M_B} = V_N B cos\, \alpha_1 - U_1 C \quad 3.59$$

$$V_{M_C} = \left[V_N B^2 \, cos \propto_1 + U_1 \left(\frac{r_2}{r_1} cos \propto_3 - BC - B\frac{r_m}{r_1}\right)\right] \quad 3.60$$

$$V_{M_D} = \left[V_N B^3 \, cos \propto_1 + U_1 \left(\frac{r_2}{r_1} cos \propto_3 + B\frac{r_2}{r_1} cos \propto_3 - CB^2 - B^2\frac{r_m}{r_1} - B\frac{r_m}{r_1}\right)\right] \quad 3.61$$

$$V_{M_E} = \left[V_N B^4 \cos \propto_1 + U_1 \left(\frac{r_2}{r_1} cos \propto_3 + B \frac{r_2}{r_1} cos \propto_3 + B^2 \frac{r_2}{r_1} cos \propto_3 - CB^3 - B^3 \frac{r_m}{r_1} - B^2 \frac{r_m}{r_1} - \frac{r_m}{r_1} B\right)\right] \quad 3.62$$

$$V_{M_F} = \left[V_N B^5 \cos \propto_1 + U_1 \left(\frac{r_2}{r_1} cos \propto_3 + B \frac{r_2}{r_1} cos \propto_3 + B^2 \frac{r_2}{r_1} cos \propto_3 + B^3 \frac{r_2}{r_1} cos \propto_3 - CB^4 - B^4 \frac{r_m}{r_1} - B^3 \frac{r_m}{r_1} - B^2 \frac{r_m}{r_1} - \frac{r_m}{r_1} B\right)\right] \quad 3.63$$

substituting equations 3.59, 3.60, 3.61, 3.62 and equation 3.63 in equation3.57, the total torque equation, T_T is rewritten as,

$$T_T = \rho Q \left\{V_N \cos \alpha_1 [A + DB(1 + B + B^2 + B^3 + B^4)] - U_1 \left[A + 5E + D\left(\left(B \frac{r_m}{r_1} - \frac{r_2}{r_1} cos \propto_3\right)(4 + 3B + 2B^2 + B^3) + BC(1 + B + B^2 + B^3) + C\right)\right]\right\} \quad 3.64$$

As was mentioned at the beginning of this section, the objective of this mathematical analysis is to find a general equation modeling the behavior of the turbine to find the minimum and maximum values of volume flow rate required to satisfy the mechanical power and angular velocities of the model. The sum of torques on each blade or total torque, multiplied by the rotor angular velocity, produce the new mechanical power general equation of this turbine, which is a function involving tangential velocity on the rotor and the velocity from the nozzle. However, as the principles of conservation of mass and momentum relate the volume flow rate and the velocity, then the mechanical power equation developed on the rotor ($P_R = T_T \omega$), satisfied the objective.

$$P_T = T_T \omega = T_T \frac{U_1}{r_1} \quad 3.65$$

Mechanical power is a function that relates torque and angular velocity, and is expressed in the Euler turbomachine equation [47], [69], [70]. Now, substituting equation 3.64 in equation 3.65, the total mechanical power of the turbine rotor is written as,

$$P_T = \frac{\rho Q}{r_1}\left\{V_N U_1 \cos\alpha_1[A + DB(1 + B + B^2 + B^3 + B^4)] - U_1^2\left[A + 5E + D\left(\left(B\frac{r_m}{r_1} - \frac{r_2}{r_1}\cos\propto_3\right)(4 + 3B + 2B^2 + B^3) + BC(1 + B + B^2 + B^3) + C\right)\right]\right\} \quad 3.66$$

however, the maximum mechanical power developed on the rotor is found by differentiating the mechanical power equation and is found where the derivative is equal to zero.

$$\frac{dP_T}{dU_1} = 0 \quad 3.67$$

$$\frac{dP_T}{dU_1} = \frac{\rho Q}{r_1}\left\{\frac{d}{dU_1}\left(V_N U_1 \cos\alpha_1[A + DB(1 + B + B^2 + B^3 + B^4)] - U_1^2\left[A + 5E + D\left(\left(B\frac{r_m}{r_1} - \frac{r_2}{r_1}\cos\propto_3\right)(4 + 3B + 2B^2 + B^3) + BC(1 + B + B^2 + B^3) + C\right)\right]\right)\right\}$$

$$0 = V_N \cos\alpha_1[A + DB(1 + B + B^2 + B^3 + B^4)] - 2U_1\left\{A + 5E + D\left[\left(B\frac{r_m}{r_1} - \frac{r_2}{r_1}\cos\propto_3\right)(4 + 3B + 2B^2 + B^3) + BC(1 + B + B^2 + B^3) + C\right]\right\} \quad 3.68$$

finally, the relationship between inlet velocity (V_N) and rotor tangential velocity is found by using the result of the equation 3.68,

$$V_N = 2U_1\frac{\left\{A+5E+D\left[\left(B\frac{r_m}{r_1}-\frac{r_2}{r_1}\cos\propto_3\right)(4+3B+2B^2+B^3)+BC(1+B+B^2+B^3)+C\right]\right\}}{\cos\alpha_1[A+DB(1+B+B^2+B^3+B^4)]} \quad 3.69$$

if in equation 3.69, numerator and denominator are substituted by F and G, the equation 3.69 could be written as,

$$V_N = 2U_1 \frac{F}{G} \tag{3.70}$$

where F and G are defined as,

$$F = \left\{A + 5E + D\left[\left(B\frac{r_m}{r_1} - \frac{r_2}{r_1}cos \propto_3\right)(4 + 3B + 2B^2 + B^3) + BC(1 + B + B^2 + B^3) + C\right]\right\} \tag{3.71}$$

$$G = cos\alpha_1[A + DB(1 + B + B^2 + B^3 + B^4)] \tag{3.72}$$

where the maximum power is reached when

$$V_N = 5.5106U_1 \tag{3.73}$$

Table 3.1 lists all parameters and constants used in equation 3.70 to found the final relationship between V_N and U_1.

Table 3.1 Notched blade turbine dimensions.

Turbine Dimensions			Constants		
Parameter	Dimension	Units		Dimension	Equation
α_1	10	degree			
α_2	30.01	degree	$\boldsymbol{A} = (r_1 + r_2 cos \propto_2)$	0.0066	3.7
α_3	50.35	degree	$\boldsymbol{B} = cos \propto_2 cos\alpha_3$	0.8528	3.11
β_1	9.6	degree	$\boldsymbol{C} = \left(cos \propto_2 - \frac{r_2}{r_1}\right)$	0.0582	3.12
r_1	3.95	mm	$\boldsymbol{D} = r_1(1 + cos\beta_1) + r_2(1 - cos \propto_2)$	0.0082	3.18
r_2	3.1	mm	$\boldsymbol{E} = r_1\left(1 + \frac{r_M}{r_1}cos\beta_1\right) + r_2\left(\frac{r_2}{r_1} - \frac{r_m}{r_1}cos \propto_2\right)$	0.0074	3.19
r_m	3.5	mm	$\boldsymbol{F} = \left\{A + 5E + D\left[\left(B\frac{r_m}{r_1} - \frac{r_2}{r_1}cos \propto_3\right)(4 + 3B + 2B^2 + B^3) + BC(1 + B + B^2 + B^3) + C\right]\right\}$	0.0435	3.71
r_N	0.65	mm	$\boldsymbol{G} = cos\alpha_1[A + DB(1 + B + B^2 + B^3 + B^4)]$	0.0509	3.72
r_r	4	mm			
A_N	1.327 E-6	m^2			

On the other hand, the potential power or power extracted from the nozzle turbine is $P_n = \rho g Q h$, but, since $V_n = \sqrt{2gh}$ then a new equation to potential power is written as,

$$P_n = \frac{\rho Q V_n^2}{2} \tag{3.74}$$

Finally, the equations of mechanical power on the rotor and the potential power from nozzle equations are related in one expression known as hydraulic efficiency of the

system (η) [69], [70], [77], which reflects the system behavior, showing the percent of losses into the system, when the potential energy is converted to mechanical energy. Hydraulic efficiency is the ratio of the power developed by the turbine rotor (rotor power) to the power supplied at the nozzle by the fluid (fluid power). The efficiency is calculated with the following relation,

$$\eta_{max} = \frac{P_T}{P_N} = \frac{T_T \omega}{\frac{1}{2} V_N^2 \rho Q} = \frac{\frac{\rho Q}{r_1}\left(V_N U_1 G - U_1^2 F\right)}{\frac{1}{2} V_N^2 \rho Q} = \frac{2\left(2U_1 \frac{F}{G} U_1 G - U_1^2 F\right)}{r_1 \left(2U_1 \frac{F}{G}\right)^2} \quad 3.75$$

$$\eta_{max} = \frac{G^2}{2 r_1 F} = 0.7499 = 74.97\% \quad 3.76$$

3.2 Magnetic Generator System Design

To support the electromagnetic design, this research assumes perfect rotation in the radial direction and a high precision in the assembly of PM's and coils, keeping constant the gap between them, when the PM's are in rotation.

In order to understand the steps to convert kinetic energy to electricity, the analysis of electromagnetic fields are a prerequisite. The position, shape, internal distribution, and the behavior of permanent magnets and coils, are key to explain the final results of the electricity induced into the coils by the action of electromagnetic induction (EMI).

3.2.1 The Alternating Current Generator

This research hinges on the combination of two systems to harvest the conversion of mechanical energy to electrical energy. The first system (previously analyzed) is the turbine, and the second is an alternating current generator, which uses electromagnetic principles to induce alternating current into coils, when permanent

magnets are rotated around of the wires, creating on them a periodical change of magnetic flux.

PM's in a ring configuration, with alternated polarity and radial direction is combined with coils to form the PM generator. The PM's around the static central axis are rotated, and the magnetic flux from them crosses the coils to induce an electromotive force (emf). The coils are distributed in a central and stationary way, inside of the circle formed by the PM's ring, with the PM's.

3.2.2 PM Generator Mathematical Model

The designs of magnets and coils used here have the same shape and distribution as most of the commercial HDD motor designs, which use a three-phase system with 9 coils and 12 magnets, distributed in a ring around the coils, with radial alternated polarity. Also, to select the number of armature coils and the number of pair poles the equation from [103], which supports the currents micro motor designs used in commercial hard drive disk machines, was used.

$$n_{coil} = \frac{3}{4} n_p \tag{3.77}$$

where n_p is the number of permanent magnets used in the ring configuration. This work uses a 3-phase winding with S=9 slots and a ring of n_p=12 PM's, creating a permanent magnet system of (S/3)/P=3/12=1/4. In this relation, the numerator 1 in ¼ is the number of slots for each phase in each pole phase and the denominator 4 is the number of poles required for a complete pattern. However, some laws and principles must be used to find the relationship between parameters of the permanent magnet machine. For instance, Ampere's Law relates the net magnetic field along a closed loop to the electric current passing through the loop, Biot-Savart's law describes the magnetic fields

induced by a current, and Lenz's Law states the direction of the induced electromotive force (emf) resulting from a changing magnetic flux which has a polarity that leads to an induced current in the coils. Finally, as defined in the second chapter, Faraday's Law states that an emf is generated, if the magnetic flux changes for any reason A, B or $\emptyset$ change.

As mentioned before, the simplest practical generator consists of circular coils and permanent magnets rotating. The coils are stationary and the ring of permanent magnets rotates with constant angular velocity ω, and a uniform magnetic field of strength B. The flux per pole area $\emptyset$ is defined as the integral of the flux density over the pole area $A_{pm} = l\frac{P_r}{n_p}$, (where n_p is the number of poles, l is the pole height, and p_r is the ring of magnets perimeter ($p_r = 2\pi r_{PM}$), also, r_{PM} is the radius of the ring of PM's), if the flux density is considered sinusoidally distributed. The flux per pole can be calculated using the winding function method [104]–[106], which is given by:

$$\emptyset = \int_{-\pi/2}^{\pi/2} B_p\, A_{pm} cos\,\theta\, d\theta = \left(2B_p A_{pm}\right) = 2B_p l\frac{p_r}{n_p} = 2B_p l\frac{2\pi r_{PM}}{n_p} \quad 3.78$$

$$\emptyset = \frac{4\pi l r_{PM} B_p}{n_p} \quad 3.79$$

when the rotor is moving and the magnets spin around the coils at constant electrical angular velocity ω_e, the flux linked by coil is given by:

$$\lambda(t) = N\phi\, cos(\omega_e t) \quad 3.80$$

the induced voltage (emf) in the full-pitch stator coil is,

$$emf = -\frac{d\lambda}{dt} = -\left(N\, cos(\omega_e t)\frac{d\phi}{dt} - N\phi\omega_e\, sin\,\omega_e t\right) = N\phi\omega_e\, sin\,\omega_e t \quad 3.81$$

$$emf = \frac{4\pi l r_{PM} B_p}{n_p}\omega_e N\, sin\,\omega_e t$$

the mechanical angular velocity and the electrical angular velocity are related in this relationship as, $\omega_e = \frac{n_p}{2}\omega_m$ (n_p is the number of machine poles and ω_m is the mechanical angular velocity).

$$emf = \frac{4\pi l r_{PM} B_p}{n_p} \frac{n_p}{2} \omega_m N \sin\left(\frac{n_p}{2}\omega_m t\right)$$

$$emf = 2\pi l r_{PM} B_p \omega_m N \sin\left(\frac{n_p}{2}\omega_m t\right) \quad 3.82$$

the maximum value is reached when $\sin\left(\frac{n_p}{2}\omega_m t\right) = 1$, then

$$efm_{max} = 2\pi l r_{PM} B_p \omega_m N \quad 3.83$$

the maximum value of induced RMS value of speed voltage is written as,

$$E_{RMS} = \frac{\phi \omega_e N}{\sqrt{2}} = \frac{2\pi l r_{PM} B_p \omega_m N}{\sqrt{2}} \ [Volt] \quad 3.84$$

Permanent magnets machines or high power AC machines may have distributed or short-pitch windings and a winding factor must be included in the E_{RMS} equation, but in this research this factor will be included in the general losses of the system.

3.3 Complete Energy Generation System Theoretical Calculations

This section presents the integration of miniature turbine and the permanent magnet machine to constitute the notched energy generator system. The CAD designs developed and explained in sections 3.1 and 3.2, are assembled and integrated in a system to be used as an energy harvester when a fluid goes through the system.

Figure 3.11 shows the integration between rotor and PMs, Figure 3.12 shows the integration between turbine casing and coils, and 3.13 shows the CAD design of the completed energy generator system. Also, a new mathematical analysis is developed to find a general equation that establishes the relationship between the mechanical system

(turbine) and the permanent magnet generator system. The initial conditions and some predefined geometry parameters are summarized in Table 3.2.

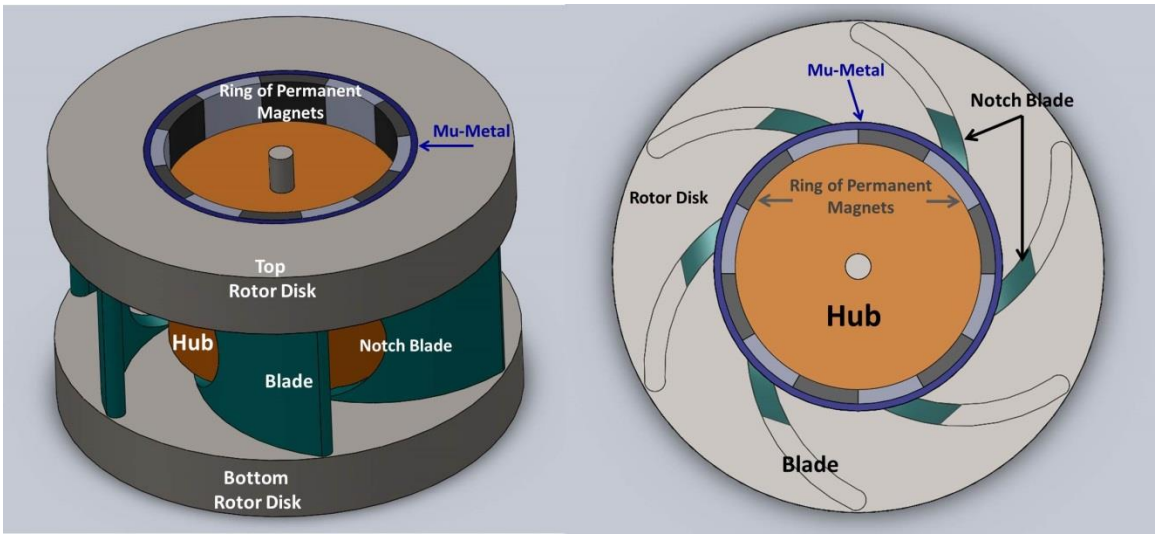

Figure 3.11 CAD integration between turbine rotor and permanent magnets.

Table 3.2 Energy generation system design dimensions.

Turbine			Permanent Magnet Machine (PMM)		
Parameter	Dimension	Units	Parameter	Dimension	Units
α_1	10	degree	n_p	12	
α_2	30.01	degree	$Slots\ (S)$	9	
α_3	50.35	degree	l	1	mm
β_1	9.6	degree	r_{PM}	2.6	mm
r_1	3.95	mm	p_r	16.34	mm
r_2	3.1	mm	N	60	$Turns$
r_m	3.5	mm	B_p	1	$Tesla$
r_N	0.65	mm	A_{pm}	1.361 E-6	m^2
r_r	4	mm	ω_m	1000-8000	RPM
A_N	1.327 E-6	m^2	Electrical Power	70-700	mW

The coil and magnet shapes were inspired by the motors used in computer hard disc drive (HDD), combined with the fundamental principles of hydro turbines. The HDD motor is a kind of brushless machine, which uses a conjunct of coils oriented in the radial direction inside a stator chamber, surrounded by a ring of frictionless permanent magnets, assembled on a rotor. In this research, the permanent magnetic configuration

is used as a magnet generator to produce current in the inductor coils, transforming the rotational motion of the turbine into electricity. Figure 3.13 shows the final position of coils and PM's on the turbine.

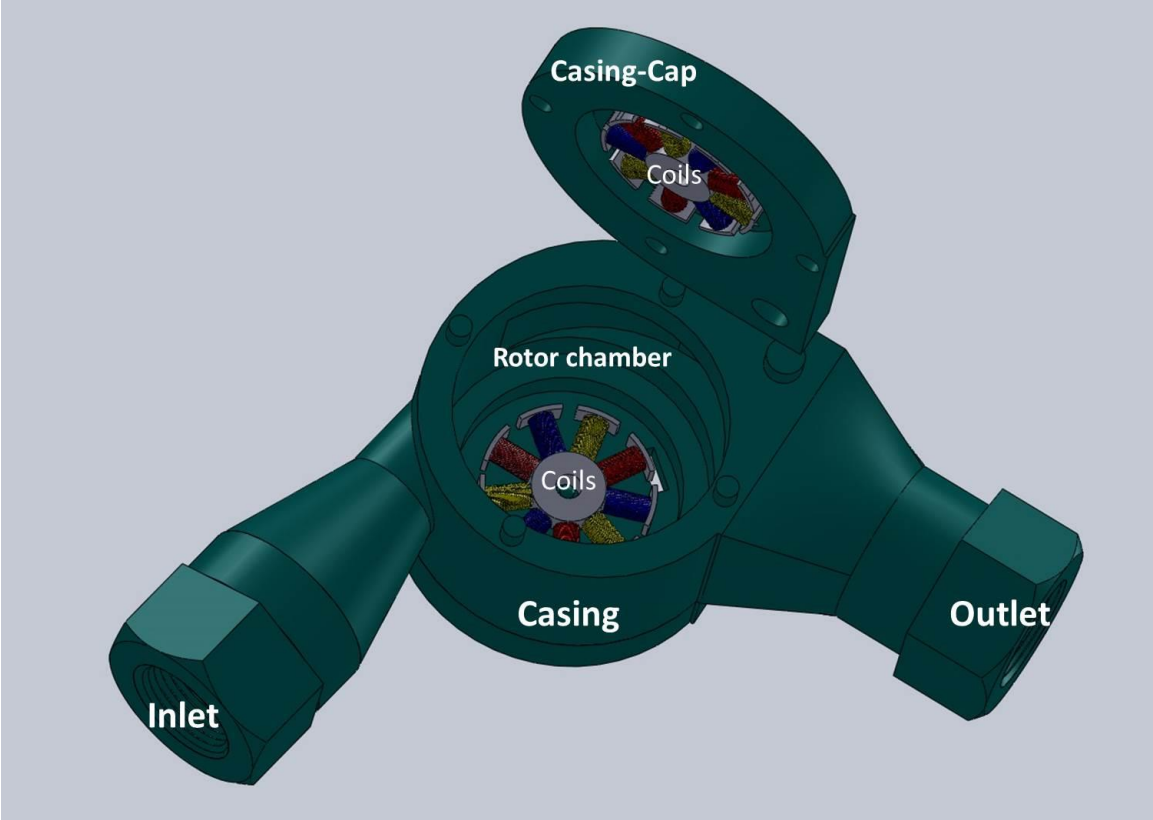

Figure 3.12 Casing and coils integration.

Nine coils configured in three phases are assembled into top and bottom of the holder exactly in the rotor chamber, to keep the coils without movement. A ring of permanent magnets is assembled on the top and bottom of the rotor, around the coils, but with a micro gap to avoid any friction when the rotor is in movement. A double combination of coils and permanent magnets assures a higher efficiency that finally translates into more energy being transformed.

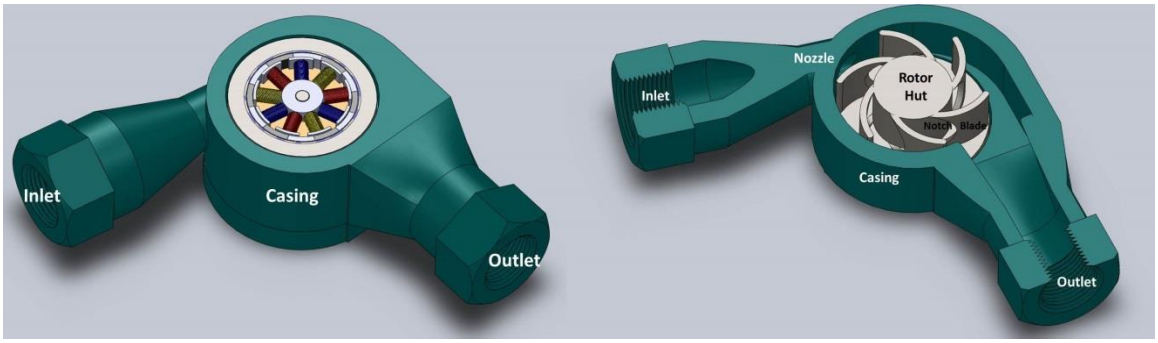

Figure 3.13 Miniature generator parts, CAD design.

The relationship between turbine and PM generator starts in the novel design of the turbine, which is integrated with the PM's and coils in a unique compact system. The final system includes the PM's and coils attached inside of the rotor and walls of the turbine without modifying the original turbine design, but using the benefits of the rotor spin to create a variable magnetic field on the fixed coils and to generate electricity. A system of three phases ($\boldsymbol{3\Phi}$) of electrical energy is the final result of the electromagnetic induction. The induction of electric currents into the coils fixed into the casing, is produced by the magnetic fields from permanent magnets (PMs), which spin when the rotor is moving. PMs assembled in alternated polarity on the rotor, and distributed in a ring configuration, produce radial lines of magnetic field which cross the coils in a perpendicular way to generate electric current, induced just when the movement of the rotor changes in position with respect to the PMs.

The mathematical models and the equations developed in the previous sections are related through the angular velocities, mechanical angular velocity (ω_m) produced on the rotor and the electrical angular velocity (ω_e) which is created on the ring of PM's. As defined in section 3.2.2, the mechanical angular velocity and the electrical angular velocity are is related as $\omega_e = \frac{n_p}{2}\omega_m$. So, if the maximum mechanical power is reached

when $V_N = 5.4528U_1$ (V_N is the fluid velocity after leave the nozzle in the rotor direction, that is known as nozzle velocity), and $U_1 = \omega_m r_1$, then a new equation emerges as a result of combining them,

$$emf = 2\pi l r_{PM} B_p \omega_m N \sin\left(\frac{n_p}{2}\omega_m t\right) = 2\pi l r_{PM} B_p \frac{U_1}{r_1} N \sin\left(\frac{n_p}{2}\omega_m t\right)$$

Substituting V_N and the constants values ($l, r_{\mathrm{PM}}, \mathrm{r}_1, \mathrm{n}_\mathrm{p}$) then the equation is rewritten as,

$$\mathrm{emf} = 2\pi \mathrm{l} r_{\mathrm{PM}} B_\mathrm{p} \frac{\mathrm{U}_1}{\mathrm{r}_1} \mathrm{N} \sin\left(\frac{\mathrm{n_p}}{2}\omega_\mathrm{m}\mathrm{t}\right)$$

$$\mathrm{emf} = \frac{2\pi \mathrm{l} r_{\mathrm{PM}} B_\mathrm{p}}{5.4528} \frac{\mathrm{V_N}}{\mathrm{r}_1} \mathrm{N} \sin\left(\frac{\mathrm{n_p}}{2}\omega_\mathrm{m}\mathrm{t}\right) \quad 3.85$$

$$\mathrm{emf} = 0.1313\, \mathrm{V_N} \sin(282.14 * \mathrm{V_N} * \mathrm{t}) \quad 3.86$$

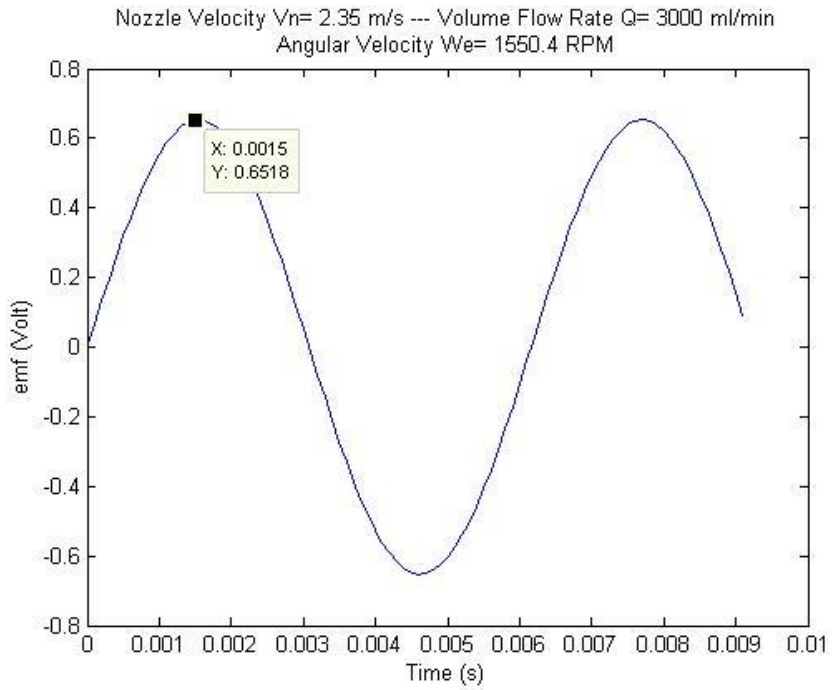

Figure 3.14 Electromotive force of the assembled system.

In Figure 3.14 is shown the emf response, when a volumetric flow rate $\mathrm{Q} = 3000\ \frac{\mathrm{ml}}{\mathrm{min}}$ goes through the system, with angular velocity $\omega_{\mathrm{e}} = 1550.4\ \mathrm{RPMs}$ and produces a mechanical power from the rotor, $\mathrm{P_r} = 102.3\ \mathrm{mW}$.

The emf equation and Figure 13.14 show the conclusion of the integration of the mathematical models developed, and complete the objective defined in the beginning of this chapter. Parameters such as volume flow rate, mechanical power on rotor, and voltage on each of the system phases will be analyzed in the next chapter, by using a scaled prototype system. Finally the behavior of the system, and the results of this chapter will be compared by the used of simulations.

3.4 Energy Analysis of Steady Flow System

In a closed system such as a turbine-generator, heat transfer $\dot{Q}$ and work transfer $\dot{W}$ can change the energy content in the system. The energy rate balance is given by the first law of thermodynamics (known as the conservation of energy principle) which is applied to a control volume (cv) with constant fluid flow, enthalpy h, velocity v, and physical height z.

3.4.1 Energy Analysis Background

The general conservation energy equation [98], [99], [107] can be written as,

$$\left(\dot{Q}_{in} - \dot{Q}_{out}\right) + \left(\dot{W}_{in} - \dot{W}_{out}\right) = \frac{dE_{sys}}{dt} \qquad 3.87$$

where $\left(\dot{Q}_{in} - \dot{Q}_{out}\right)$ is the heat transfer net rate to the system, $\left(\dot{W}_{in} - \dot{W}_{out}\right)$ is the net power input to the system, and $\frac{dE_{sys}}{dt}$ is the energy rate of change of the total system. For steady flow with one inlet and one outlet, the equation can be rewritten as,

$$\left(\dot{Q}_{in} - \dot{Q}_{out}\right) + \left(\dot{W}_{in} - \dot{W}_{out}\right) = \dot{m}_{Fluid}\left[h_{out} - h_{in} + \frac{V_{out}^2 - V_{in}^2}{2} + g(z_{out} - z_{in})\right] \qquad 3.88$$

Therefore, if the total system energy equation is divided by $\dot{m}_{Fluid}$, then the net rate of heat transfer to the system and the net power input to the system are converted in $\frac{(\dot{Q}_{in}-\dot{Q}_{out})}{\dot{m}_{Fluid}} = q_{sys}$ which is the net heat transfer to the fluid per unit mass, and $\frac{(\dot{W}_{in}-\dot{W}_{out})}{\dot{m}_{Fluid}} = w_{sys}$ which is the net shaft work input to the fluid per unit mass. Also, if the enthalpy definition ($h = u + pv = u + \frac{p}{\rho}$) is used [98], [99], [107], the total system energy equation is written as

$$w_{sys} + \frac{p_{in}}{\rho_{in}} + \frac{V_{in}^2}{2} + gz_1 = \frac{p_{out}}{\rho_{out}} + \frac{V_{out}^2}{2} + gz_{out} + u_{out} - u_{in} - q_{sys} \quad 3.89$$

equation 3.89 states that during steady flow work $(\dot{W}_{in} - \dot{W}_{out})$ and heat $(\dot{Q}_{in} - \dot{Q}_{out})$ transfer the net rate of energy to a control volume. This relationship is proportional to the difference between inlet energy and outlet energy, which is produced by the fluid flow.

3.4.2 Energy Analysis of the Notched Turbine System

The mathematical model developed for the notched turbine system assumes ideal condition parameters to produce conservation of the total mechanical energy. Therefore, if the energy is conserved, the total system energy equation is $u_{out} - u_{in} - q_{sys} = 0$. In addition, $z_1 = z_2$ because the inlet head and outlet head are equal (Head - the vertical distance) and the net shaft work input to the system (fluid per unit mass) is reduced to $w_{sys} = w_{pump} - w_{Turbine} = -w_{Turbine}$ because the system is a turbine. The previous assumptions transform the total system energy equation as follows

$$\frac{p_{in}}{\rho_{in}} + \frac{V_{in}^2}{2} = \frac{p_{out}}{\rho_{out}} + \frac{V_{out}^2}{2} + w_{Turbine} \quad 3.90$$

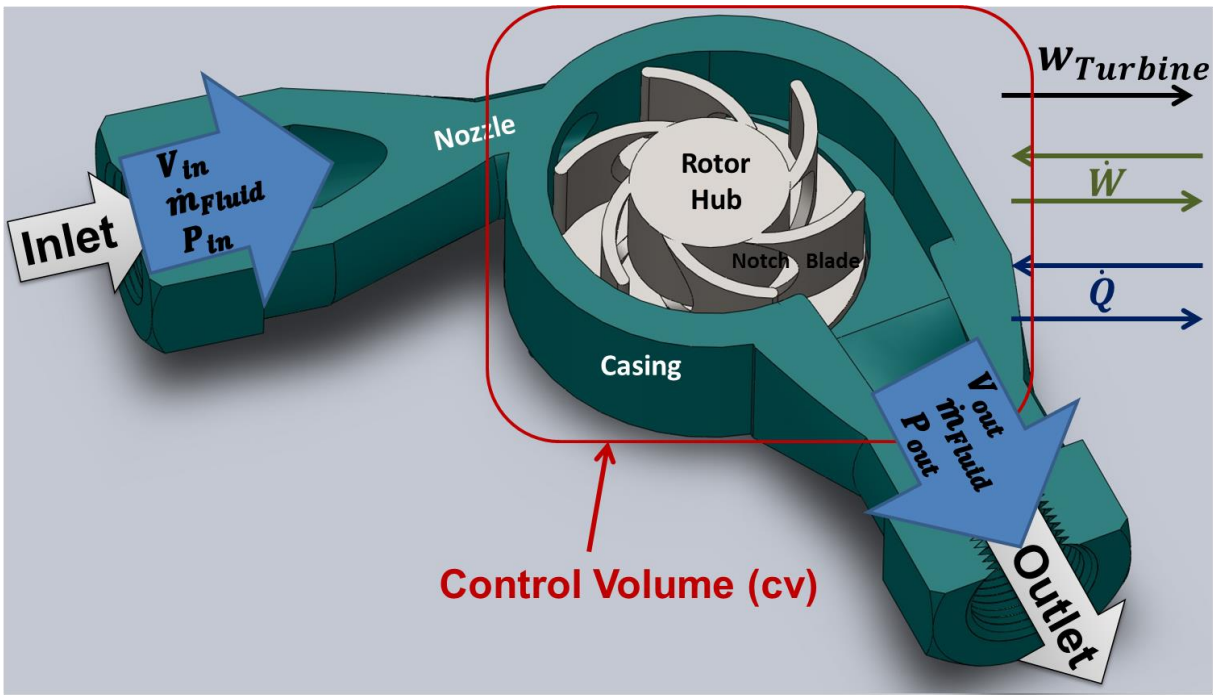

Figure 3.15 Conservation of mass principle for the notched turbine system.

Since volume flow rate is constant through the turbine, and the turbine inlet transversal area and turbine outlet transversal area are equal, then by the law of conservation of mass, we could conclude that the inlet velocity V_{in} and the outlet velocity V_{out} are also equal. Figure 3.15 shows the physical parameters used to develop the thermodynamic analysis on the notched blade turbine system. The net shaft work input equation can then be written as

$$w_{sys} = w_{Turbine} = \frac{(\dot{W}_{in} - \dot{W}_{out})}{\dot{m}_{Fluid}} = \frac{T_T \omega}{\dot{m}_{Fluid}} \qquad 3.91$$

and the total system energy equation becomes,

$$\frac{p_{in} - p_{out}}{\rho} = \frac{T_T \omega}{\dot{m}_{Fluid}} \qquad 3.92$$

Finally, four stages are developed to complete the energy analysis of the notched blade energy generation system, which includes the above results and the

mathematical model for the notched turbine-generator system developed previously in section 3.1.3.

The first stage is the summary of the torque mathematical equations, the second stage creates a relationship equation between torque and volume flow rate. The third stage combines the torque equation with the total system energy equation to obtain the relationship between inlet-outlet pressures and the volume flow rate of the notched turbine-generator system. Finally, the fourth stage is presented in a graphic that shows the relationship between the volume flow rate through the system and the inlet and outlet pressure.

- Stage 1:

  By use of the equation 3.70, nozzle velocity (V_N),

  $$V_N = 2U_1 \frac{F}{G}$$

  the equation of angular velocity (ω) which is the relationship between tangential velocity (U_1) and the volume flow rate is found to be

  $$\omega = \frac{U_1}{r_1} = \frac{V_N G}{2Fr_1} = \frac{QG}{2Fr_1 A_N} \qquad 3.93$$

  where A_N is the turbine nozzle transversal area, and F and G are constants from the notched turbine mathematical equation.

- Stage 2:

  The total torque equation expressed as a function of the volume flow rate is then written as,

  $$T_T = \rho Q U_1 F = \frac{\rho Q V_N G}{2} = \frac{\rho Q^2 G}{2A_N} \qquad 3.94$$

- Stage 3:

By substituting the angular velocity and total torque in the total system energy equation, the equation can be written as,

$$\frac{p_{in}-p_{out}}{\rho} = \frac{T_T \omega}{\dot{m}_{Fluid}} = \frac{\rho Q^3 G^2}{4Fr_1 A_N^2 \dot{m}_{Fluid}} = \frac{\rho Q^3 G^2}{4Fr_1 A_N^2 \rho Q} \quad 3.95$$

$$p_{in}-p_{out} = \frac{T_T \omega}{\dot{m}_{Fluid}} = \frac{\rho Q^3 G^2}{4Fr_1 A_N^2 \dot{m}_{Fluid}} = \frac{Q^2 G^2}{4Fr_1 A_N^2} \quad 3.96$$

where the turbine nozzle transversal area, $A_N = \pi(0.00065)^2[m^2]$, $F = 0.0435$ and $G = 0.0509$ are constants, without an associated physical dimension, from the notched turbine mathematical equation.

- Stage 4:

  Solving for p_{in}, in terms of the volume flow rate Q, establishes the dependence seen in Figure C2 below.

$$p_{in}-p_{out} = \frac{T_T \omega}{\dot{m}_{Fluid}} = \frac{Q^3 G^2}{4Fr_1 A_N^2 \dot{m}_{Fluid}} = \frac{Q^2 G^2}{4Fr_1 A_N^2} \quad 3.97$$

$$p_{in} = \frac{Q^2 G^2}{4Fr_1 A_N^2} - p_{out} \quad 3.98$$

If outlet pressure (p_{out}) is assumed as 13.333 KPa, and the volume flow rate (Q) range is between 0 and 7.5 liters/min, then the inlet pressure (p_{in}) will have the behavior shown in the next figure.

Finally, if the notched blade turbine is connected to a closed-loop system transporting 5 l/min, the ratio of pressures will be $\frac{p_2}{p_1} = \frac{13.333\ Kpa}{14.79\ Kpa} = 0.9015$, which in this case, represents a system pressure loss of around 10%.

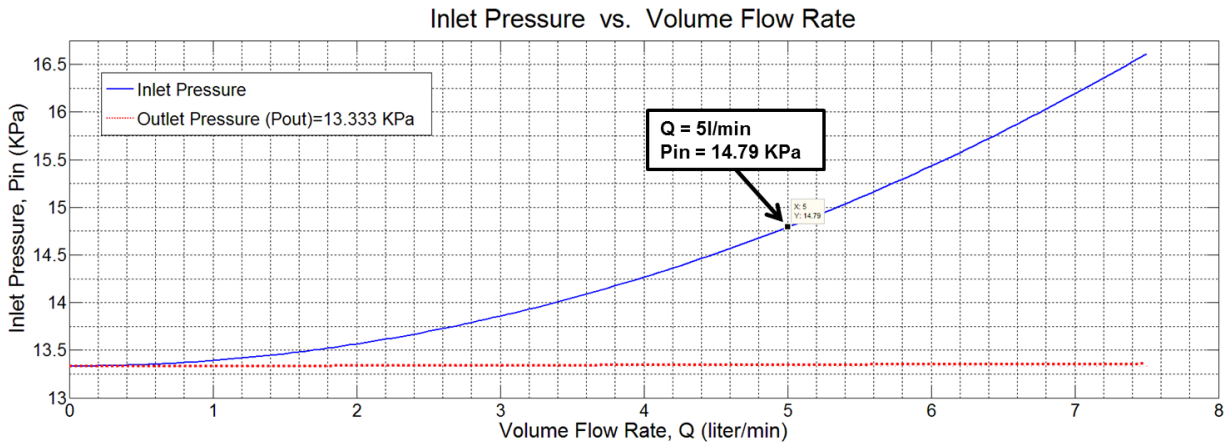

Figure 3.16 Inlet pressure vs. volume flow rate.

CHAPTER 4: ASSEMBLY, TESTING AND ANALYSIS OF RESULTS

This chapter is centered on the testing and analysis of results of three prototypes of the miniaturized power generation system. The prototypes presented in this chapter show the innovations and the most significant changes to the initial idea, with which the author began this dissertation work, which produced the final prototype as a new and patentable product. In the time line of this dissertation, six different models were assembled, but only three models were completely tested. In appendix A, all prototyped models are shown. This chapter is dedicated to explaining, comparing, and analyzing the differences between the models, through theoretical calculations, simulations and prototype testing.

The first section of this chapter is dedicated to the process of integration and assembly of three prototypes; the second section covers the lab results of these prototypes; and the final section of this chapter is a comparative analysis of the test results of the prototypes. Also, the final section shows the theoretical calculation results and simulations of the notched blade turbine-generator design and compares these results with the experimental data of the prototype.

4.1 Assembly of Prototypes

The building of the complete system was developed in three steps, which involved the integration between turbine parts and permanent magnet machine parts, to conclude with the assembling and encasing of the miniaturized notched energy generator system. To know the functionality of the assembled prototype and to develop

the final tests, the turbine inlet system was connected to a domestic water system. The measurements of volume flow rate were taken on the turbine inlet, through a volume flow rate digital meter, connected in series with the water system and a gradual flow controller. The miniaturized notched blade energy generation system connected to the domestic water system is shown in Figure 4.1a, and the connections, and meters used in the testing processes, are shown in Figure 4.1a and 4.1b.

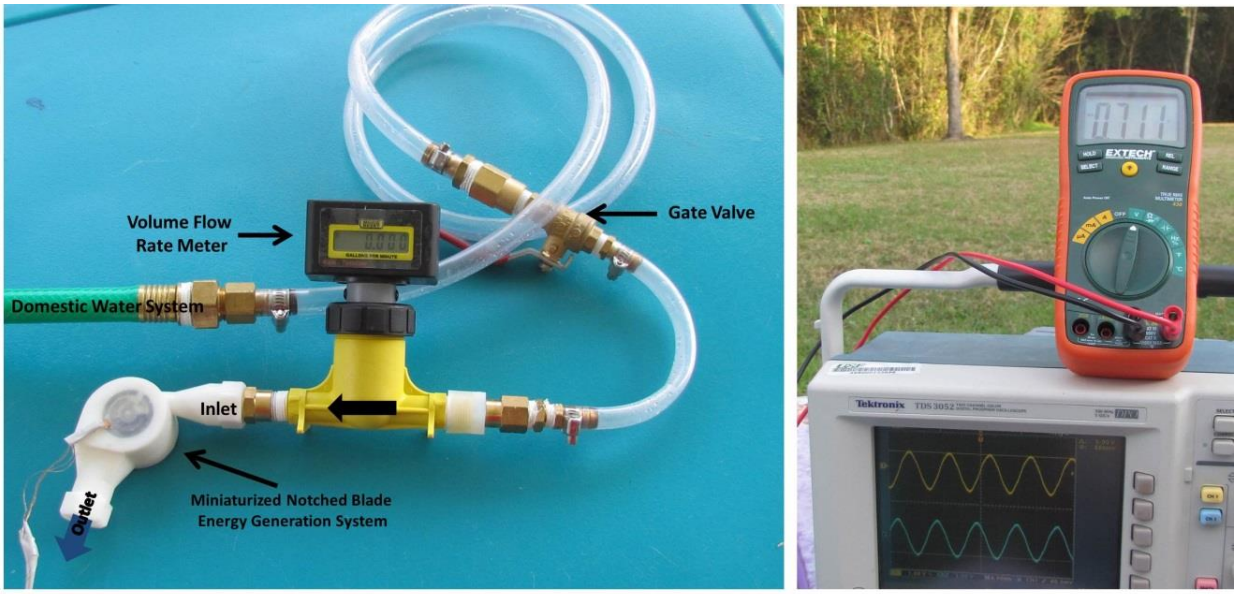

Figure 4.1 Miniaturized notched energy generator system connected to the water system.

As is shown in Figure 4.1, the measurements of induced voltage were done on the terminals of the 3-phase system through a voltmeter and an oscilloscope connected in parallel with the motor-generator terminals. The assembled prototypes are shown in Figures 4.2a, 4.2b, and 4.2c, and the test results of the three prototypes are presented in the next section.

4.1.1 Turbine

The three prototype models shown in Figure 4.2 are the last versions and summarize the final stage of this dissertation. The prototype parts of these three models are shown in Figures 4.3, 4.4 and 4.5. The model in Figure 4.3 and 4.4 have the same casing shape, but do not have all design innovations and size of the final tested model shown in Figure 4.5. A comparative analysis of shapes, sizes, and curvatures is presented in Table 4.1.

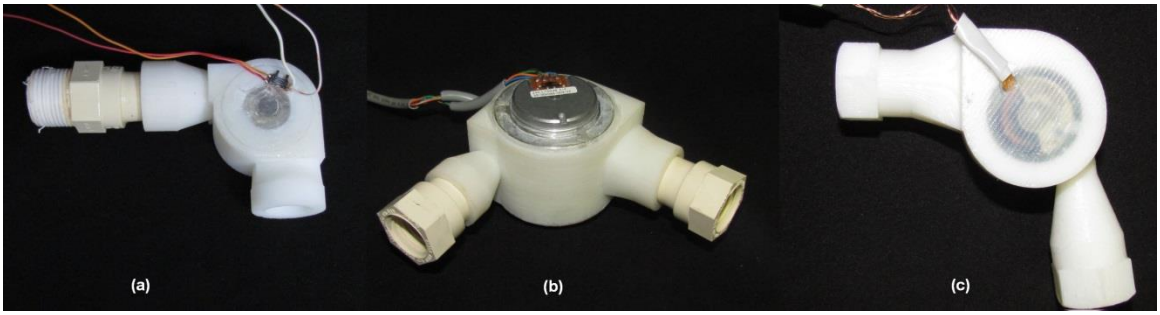

Figure 4.2 Prototype models assembled and tested: (a) not notched model, size 3.175, and 2.5-inch HDD motor; (b) not notched model, size 4, and 3.5-inch HDD motor; (c) notched model, size 3.175, and 2.5-inch HDD motor.

Table 4.1 Comparative analysis of three prototypes.

Prototype Model	Shape	Size	Geometry and curvature	Additional Characteristics
Not notched model (Figure 4.3)	8 blades	3.175X 2.5-inch HDD motor	90 degree between inlet and outlet, innovative casing design	Impulse turbine characteristics, rotor spin is require to free flow
Not notched model (Figure 4.4)	6 blades	4X 3.5-inch HDD motor	90 degree between inlet and outlet, innovative casing design	Impulse turbine characteristics, rotor spin is require to free flow
Notched model (Figure 4.5)	6 notched blades	3.175 2.5-inch HDD motor	100 degree between inlet and outlet, innovative casing design	Impulse and reaction turbine characteristics, cross-flow design, free flow

The casing shapes, of the three prototyped models are similar in geometry and distribution and only the angle of inclination of the nozzle is different. In all turbine models, the casing sections were designed to enclose the rotor and the HDD motor-

generator, for operation in micro-fluidic systems, but multiple simulations and tests resulted in the development of a new rotor model, this improving flow circulation through the new model rotor using the notched blades, without dramatically reducing the impulse effect on the first blade.

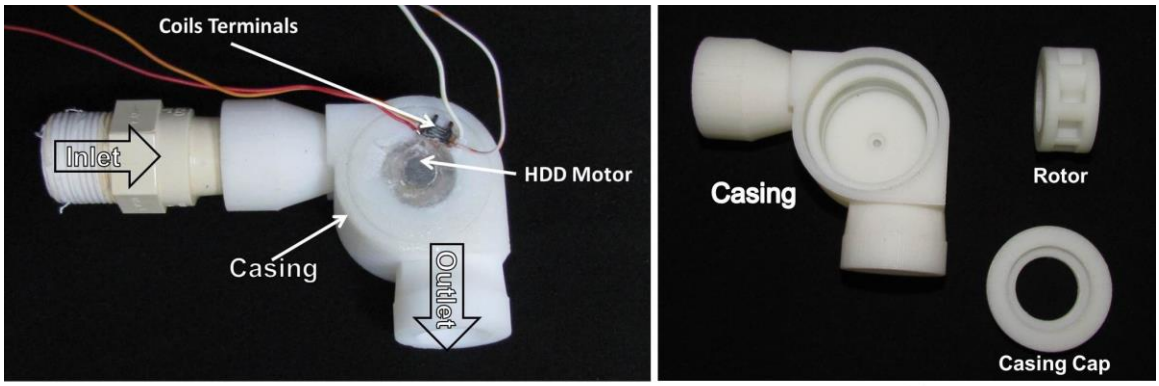

Figure 4.3 Not-notched model, scale 3.175X, 2.5 inch HDD motor.

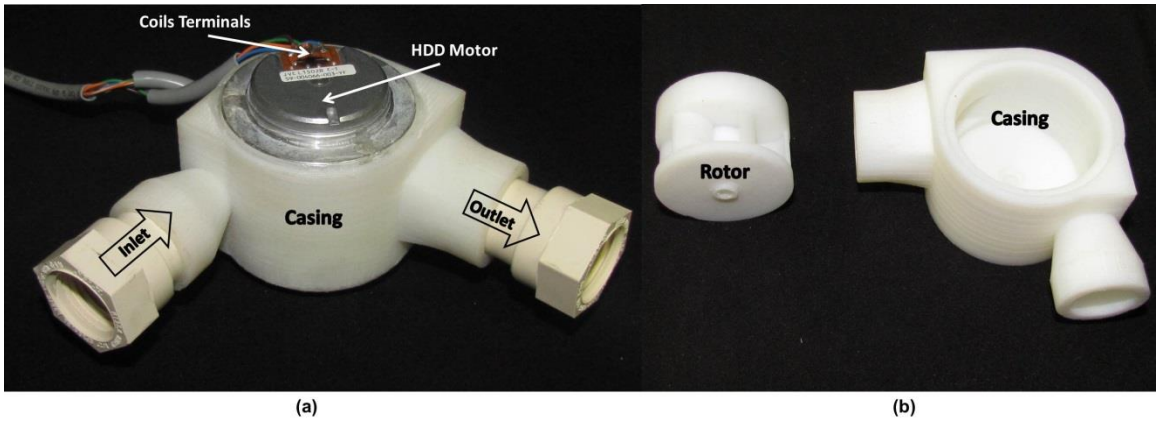

Figure 4.4 Not-notched model, scale 4X, 3.5 inch HDD motor.

The first two generation of prototypes were printed in the Virtual Manufacturing and Design Laboratory for Medical Devices (VirtualMDLab) at USF, by members of Dr. Lai-Yuen's team, and the last two generations were printed by USF's Engineering Technical Support Services (ENG TSS). Most of the prototypes developed through this

dissertation work were made using a 3D prototyping printer which uses Acrylonitrile Butadiene Styrene (ABS) plastic to build parts (Dimension sst-768), while only two sets were made using a different 3D prototyping printer which uses a proprietary powder and binder system to build the parts (3D Systems' ZPrinter-450).

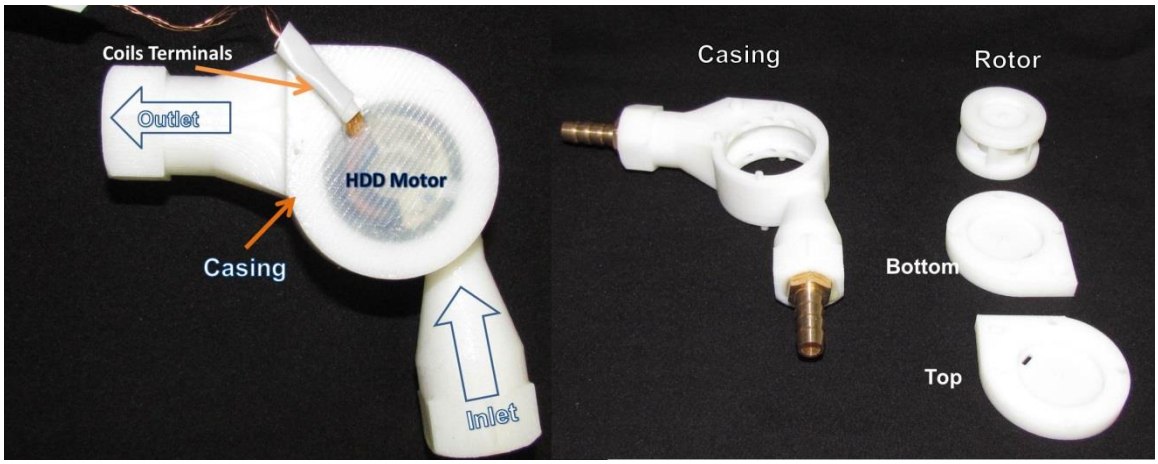

Figure 4.5 Notched model, scale 3.175X, 2.5 inch HDD motor.

The notched turbine in Figure 4.5 includes all innovations. The turbine casing has an angle of 100 degrees between the inlet and outlet sections, this inclination results in the fluid being directed more towards the distal end of each blade, which has greater surface area since the notch is located on the internal, proximal edge. The notched turbine in Figure 4.5 has casing innovations, the first is a nozzle inclination of 10 degrees with respect to the radial and tangential axes. The behavior simulations of the fluid through the turbine are shown in Figure 4.16. Also, we show the contribution of the nozzle inclination, as the discharge of the fluid through the notch, in addition to reducing the vortices between blades and on the central area of the rotor.

4.1.2 Motor Magnet Generator

There are different models of electromagnetic systems, which could be used as electromagnetic generators, but after an extensive cost benefit analysis, it was decided to use the shape and configuration of coils and permanent magnets used in typical hard disk drive (HDD) motors. These motors generally consist of a ring of permanent magnets and a winding in 9 slots, which interact to create a three-phase electric power system. Figures 4.6a and 4.6b show the shapes of coils and PMs used in this dissertation and show the exact place on the rotor and casing where they must be assembled to ensure their proper operation and functionality as a generator.

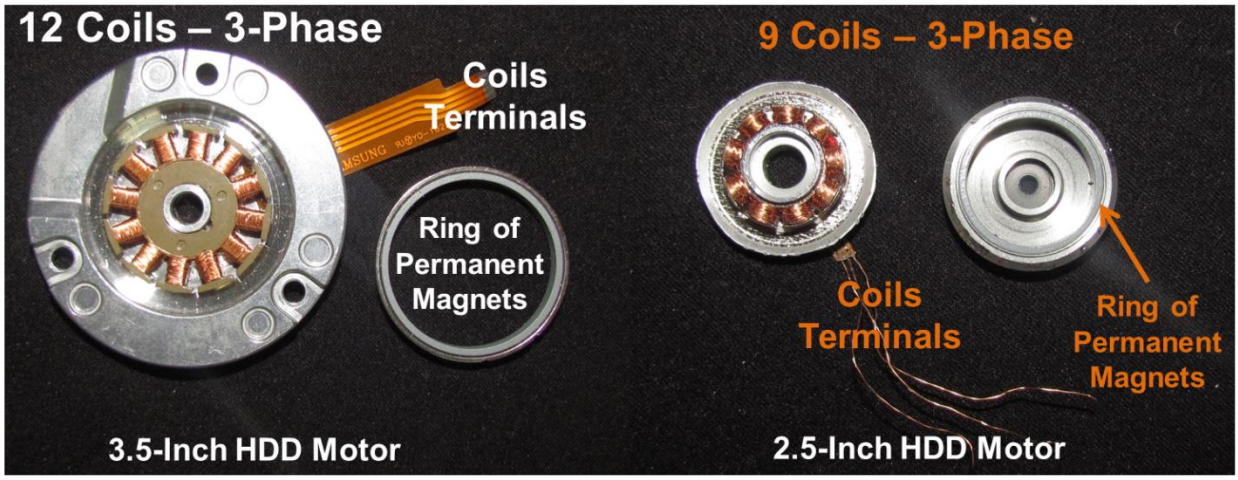

Figure 4.6 Hard drive disk motors (HDD motors).

In the assembly process of the last three prototypes 4 HDD motors were used, two of them from 3.5 inch HDD motors (3.5 inch is the physical dimensions of the drive), Figure 4.6a, and two from 2.5 inch HDD motors (2.5 inch is the physical dimensions of the drive), Figure 4.6b. These kinds of motors have the same shapes, but the sizes of all elements involved in the models are different, hence the magnetic induction

response is different. As was defined in Chapter 3, section 2, the induced voltage (emf) will be determined by the number of PMs, the surface area of each PM, the intensity and density of the magnetic field, and the rotation speed of the magnets around the coils.

In the miniaturized generator of Figures 4.3, 4.4, and 4.5, the electrical energy is generated by the rotation of the magnetic field from a ring of permanent magnets crossing the coils, as explained by Faraday's law [1–3]. A circular distribution of magnets in alternating polarity, which are attached to the notched turbine rotor, are the magnetic field source. Figure 4.7a shows the rotor and the ring of permanent magnets already assembled. Additionally, Figure 4.7b shows how the winding structure is assembled into the turbine casing and centered on the rotor axis, but it is aligned radially with the magnetic field created by the ring of permanent magnets. Figure 4.7b also shows how the coils attach to the turbine casing cap. The coils and permanent magnets shown in Figure 4.7 were extracted from a small hard disk drive (HDD) motor, and were adapted to accommodate for parts required for this specific prototype.

Table 4.2 Turbine and permanent magnets dimensions and configuration.

Turbine			Permanent Magnet Machine (PMM)		
Parameters	**Dimensions**	**Units**	**Parameters**	**Dimensions**	**Units**
α_1	10	degree	n_p	12	
α_2	30.01	degree	Slots (S)	9	
α_3	50.35	degree	l	1	mm
β_1	9.6	degree	r_{PM}	2.6	mm
r_1	3.95	mm	p_r	16.34	mm
r_2	3.1	mm	N	60	Turns
r_m	3.5	mm	B_p	1	Tesla
r_N	0.65	mm	A_{pm}	1.361 E-6	m^2
r_r	4	mm	ω_m	1000-8000	RPM
A_N	1.327 E-6	m^2	Electrical Power	70-700	mW

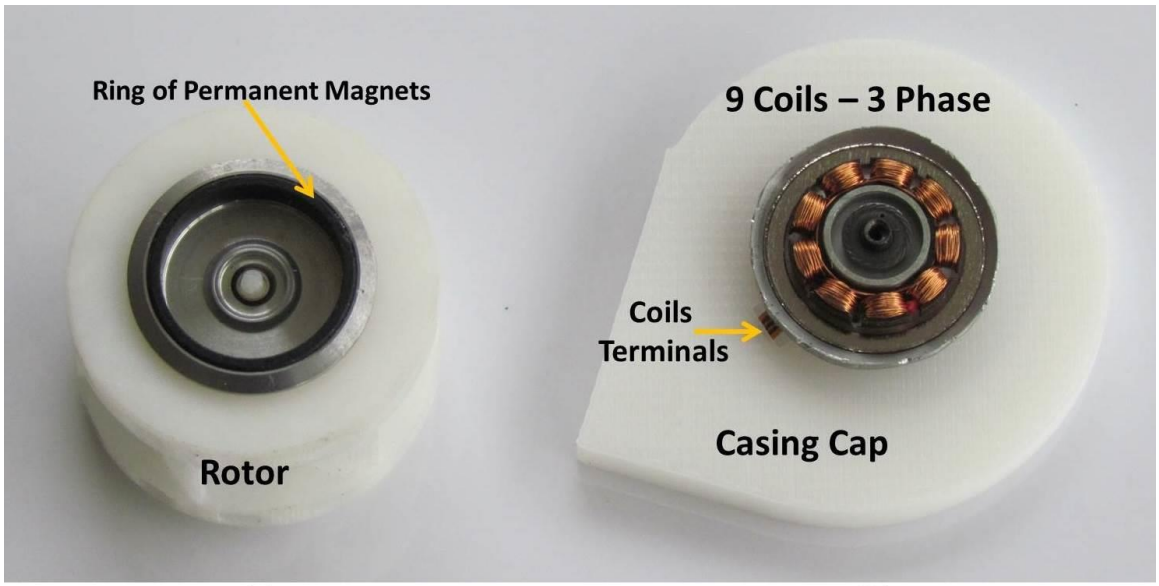

Figure 4.7 Ring of permanent magnets and coils assembled and bonded, on rotor and the turbine casing cap.

4.1.3 Energy Generation System

The novel design presented in this dissertation is supported by the CAD designs and the mathematical model developed in Chapter 3. The original size of the system was defined according to the requirement of small millimeter-sized applications, where the system could be integrated and used to support the operation of a larger system, such as a physiological system.

The geometries of the notched blade energy generation system were presented in Chapters 2 and 3, and the dimensions and configurations of the original model are shown in Table 4.1.

The notched blade generator is assembled in three steps: in the first step the rings of PMs are inserted and attached to the top and bottom of the rotor, the second step is the integration and union of coils in the turbine casing, and the third step is the

alignment, enclosing and sealing of all parts. Figure 4.7a and 4.9b show how the rotor and the ring of PM's magnets are assembled, while Figures 4.7b and 4.9a show how the coils and casing are joined together.

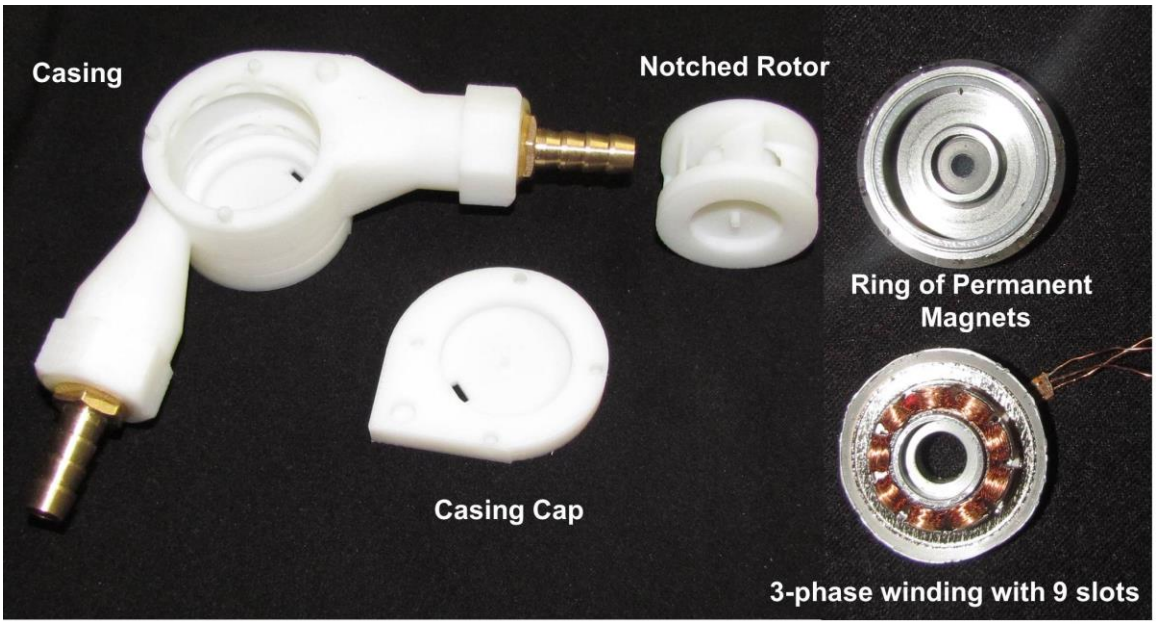

Figure 4.8 Components of the notched blade energy generation system.

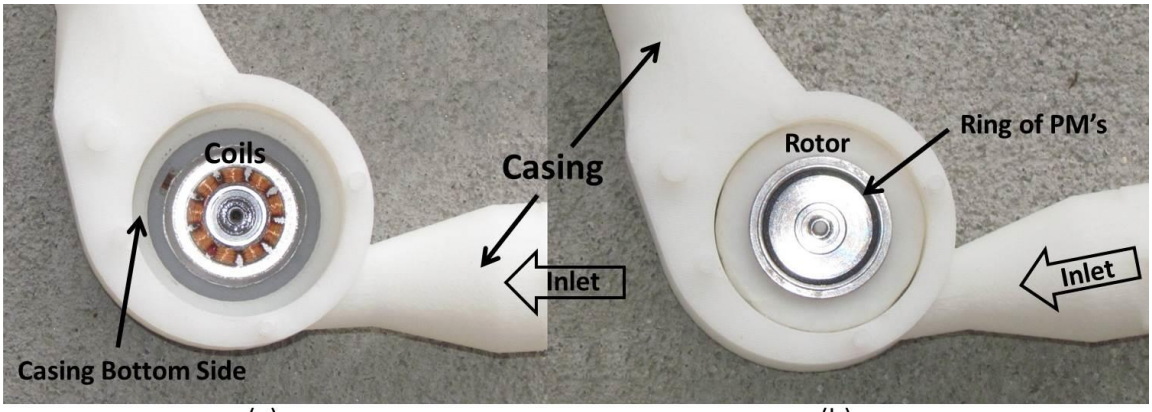

Figure 4.9 Final prototype assembled in separated parts.

Figure 4.8 shows all components of the final prototype before being assembled, and Figure 4.10 shows the notched blade generator, assembled and ready to be connected to a larger system in a particular application.

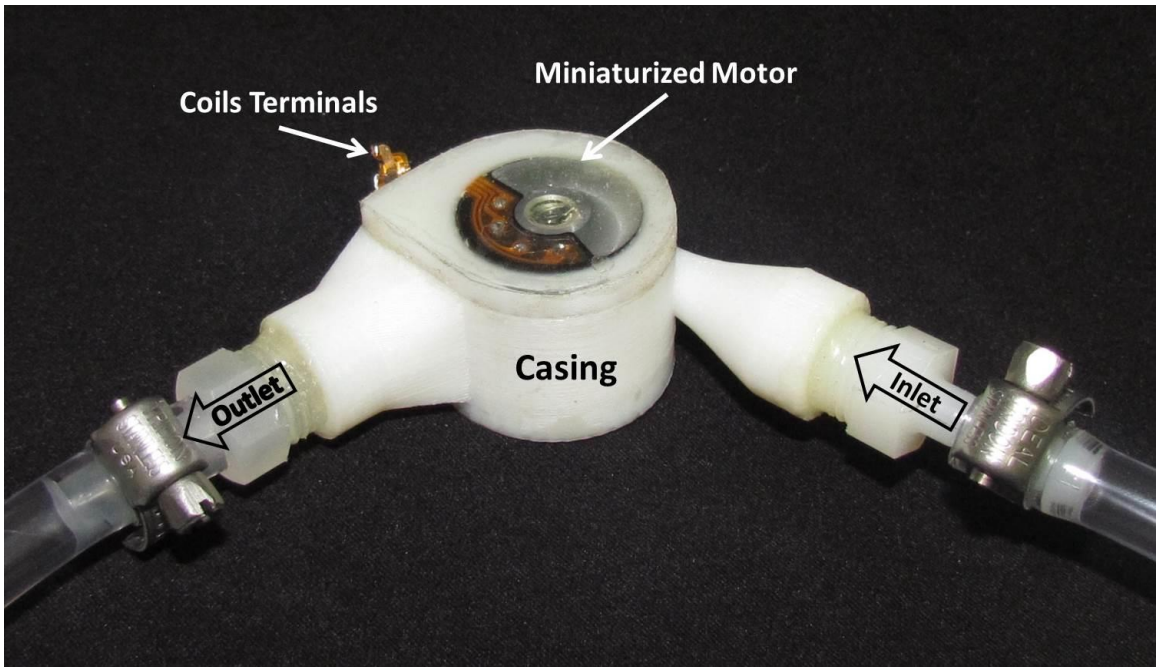

Figure 4.10 Notched blade generator assembled.

4.2 Energy Generation System Testing Results

As mentioned before, six different prototypes were built, but in this manuscript only the last three were taken into consideration. The three selected models have been simulated by using ANSYS Workbench V. 13.0, and the associated software to include geometry, mesh, pre-processing and post-processing. The simulation processes used the same solver control, output control, and data expressions, to maintain the same reference point for the analysis. The velocity and pressure behavior of the three models are shown in Figures 4.12, 4.13, and 4.14.

Voltage	RPM
0.505	1374
0.556	1580
0.564	1646
0.605	1685
0.611	1712
0.623	1752
0.684	1967
0.737	2116
0.743	2133
0.825	2360
0.892	2560
0.924	2654
0.985	2798
1.045	3007
1.056	3040
1.058	3070
1.102	3175
1.142	3283
1.169	3352
1.223	3509
1.241	3542
1.281	3673

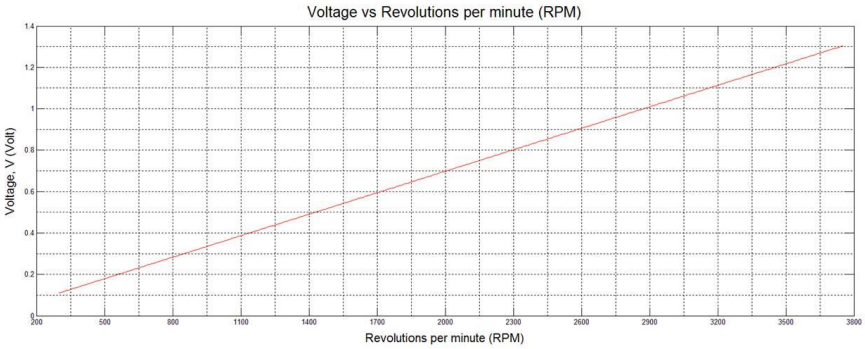

Figure 4.11 Characterization of a HDD motor used as PM-generator.

Figure 4.11 shows the characterization data and linearization of a small HDD motor used as PM-generator. The data of Figure 4.11 was collected at USF's AMBIR lab and is used in this dissertation to find the relationships between the voltage and angular velocity, and between the volume flow rate and angular velocity, when the HDD motor is assembled into the turbines and used as a motor-generator machine.

The characteristics of the three models are summarized in Table 4.2; and the testing results are shown in Table 4.3. The data points of voltage and volume flow rate in Table 4.3 were taken using the Extech 430 (part number EX430) True RMS Autoranging Multimeter and the OMEGA Digital Paddlewheel Meter FP2001-RE respectively. The volume flow meter was connected between the domestic water system and the turbine inlet to measure how many gallons per minute were entering the Turbine-generator system, and to use this meter as a flow regulator. The volume flow rate measured was between 0 and 4 gallons per minute. The maximum Q of the turbine was sufficient to move the motor/generator in a safe range of revolutions per minute,

without causing any damage to the internal structure of the generator's motor. The HDD motors used and assembled into the prototypes were designed to work at angular velocity of 5400 RPM [108]–[111].

4.3 Analysis of Results

The data analysis of three prototypes is presented in this section, to validate the miniaturized notched blade energy generation system, as an efficient and novel system, which converts mechanical energy to electricity. Traditional impulse turbines are not included in this analysis because the miniaturized system developed in this dissertation fulfills a different function compared to the impulse and reaction systems found and reported in the literature, such as was reported in Chapter 1.

The internal behavior of the turbines, when a fluid flows through the system, is shown in Figure 4.12, 4.13 and 4.14. These simulations shown the internal differences between the three turbine models and confirm the adaptability problems intern with the old models, when operating in a closed circulatory system. In contrast to the old models, Figures 4.12 and 4.13, the notched blade turbine system, Figure 4.14, shows several innovations, but the main novelty is the inclusion of a notch on each blade. As shown in Figure 4.14, the notches in the internal central edge of each blade, allows for continuous circulation of liquid inside of the rotor-chamber, and assures more interaction between fluid and the blades. In the new turbine, the fluid strikes the first blade and the notch redirects the fluid, to impact more than one blade.

Table 4.3 Volume flow rate vs. voltage produced by the turbine-generator machines. Lab testing results of three prototype models.

Prototype 1, Not notched 3.175X, 2.5-inch HDD motor		Prototype 2, Not notched 4X, 2.5-inch HDD motor		Prototype 3, Notched 3.175X, 2.5-inch HDD motor	
Volume Flow Rate Q (Gallons/Minute)	Voltage (V)	Volume Flow Rate Q (Gallons/Minute)	Voltage (V)	Volume Flow Rate Q (Gallons/Minute)	Voltage (V)
0.92	0.07	0.52	0.044	0.63	0.142
1.1	0.168	0.62	0.092	0.71	0.173
1.14	0.19	0.68	0.12	0.81	0.205
1.2	0.22	0.72	0.141	0.9	0.26
1.21	0.232	0.82	0.184	1.02	0.32
1.34	0.271	0.9	0.19	1.11	0.362
1.42	0.3	1	0.276	1.21	0.421
1.48	0.323	1.1	0.322	1.31	0.471
1.5	0.334	1.2	0.371	1.4	0.51
1.55	0.34	1.3	0.409	1.51	0.56
1.62	0.372	1.4	0.452	1.61	0.6
1.7	0.401	1.51	0.47	1.71	0.64
1.78	0.435	1.6	0.535	1.8	0.666
1.8	0.45	1.71	0.58	1.85	0.684
1.83	0.44	1.8	0.6	1.9	0.7
1.92	0.47	1.83	0.615	1.95	0.737
2	0.518	1.91	0.635	2	0.76
2.3	0.62	2	0.684	2.11	0.794
2.4	0.625	2.1	0.716	2.2	0.83
2.5	0.684	2.23	0.79	2.3	0.87
2.66	0.706	2.3	0.807	2.4	0.91
2.75	0.738	2.4	0.86	2.5	0.95
2.8	0.76	2.5	0.905	2.6	0.985
2.9	0.81	2.71	0.98	2.71	1.025
3	0.83	2.8	1	2.8	1.05
3.2	0.875	2.91	1.043	2.9	1.06
3.46	0.943	3.02	1.09	3	1.13
3.79	1.04	3.08	1.11	3.12	1.16
		3.13	1.14	3.2	1.185
		3.29	1.19	3.25	1.195
		3.3	1.195	3.3	1.125
		3.35	1.21	3.47	1.26
		3.43	1.24		

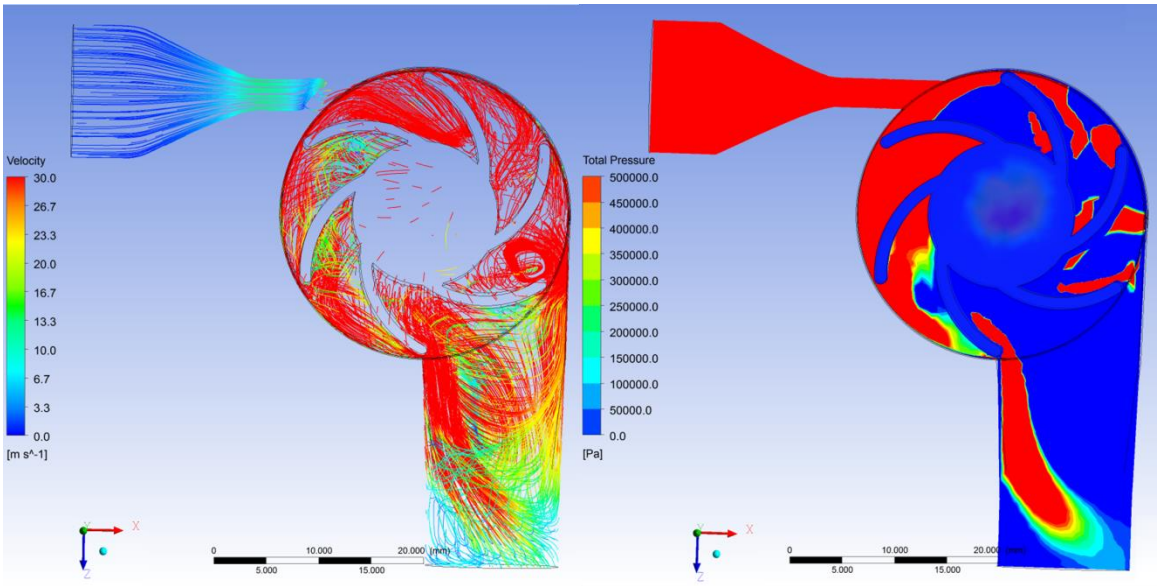

Figure 4.12 Not-notched model turbine simulations scale 3.175X. The left side - velocity behavior, and right side - internal pressure. Maximum and minimum values of velocity and pressure are defined in both simulations as red and blue respectively.

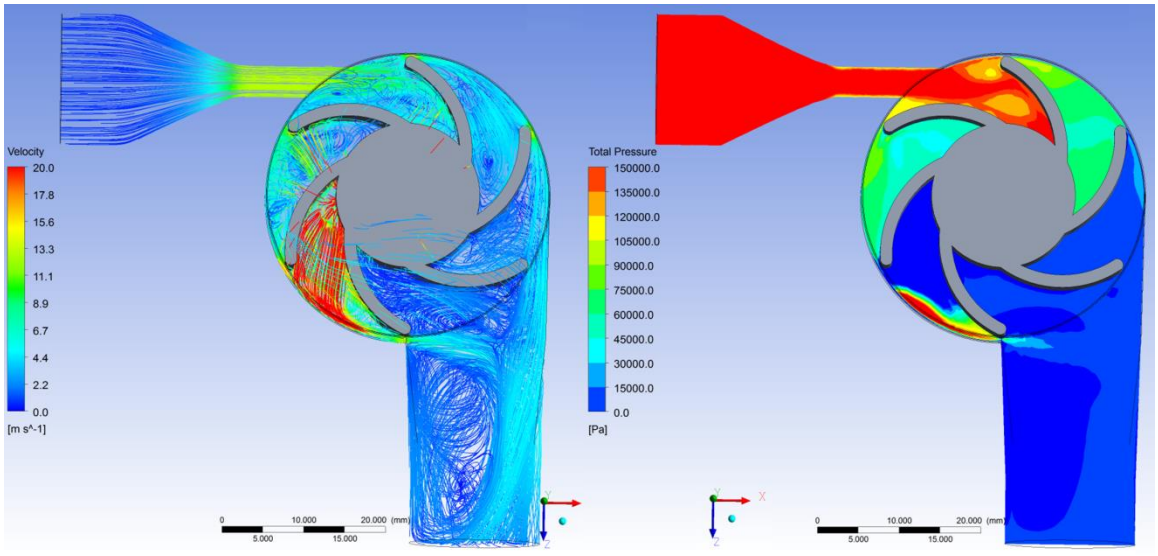

Figure 4.13 Not-notched model turbine simulations scale 4X. The left side shows the velocity behavior, and the internal pressure is shown in the right side. Maximum and minimum values of velocity and pressure are defined in both simulations as red and blue respectively.

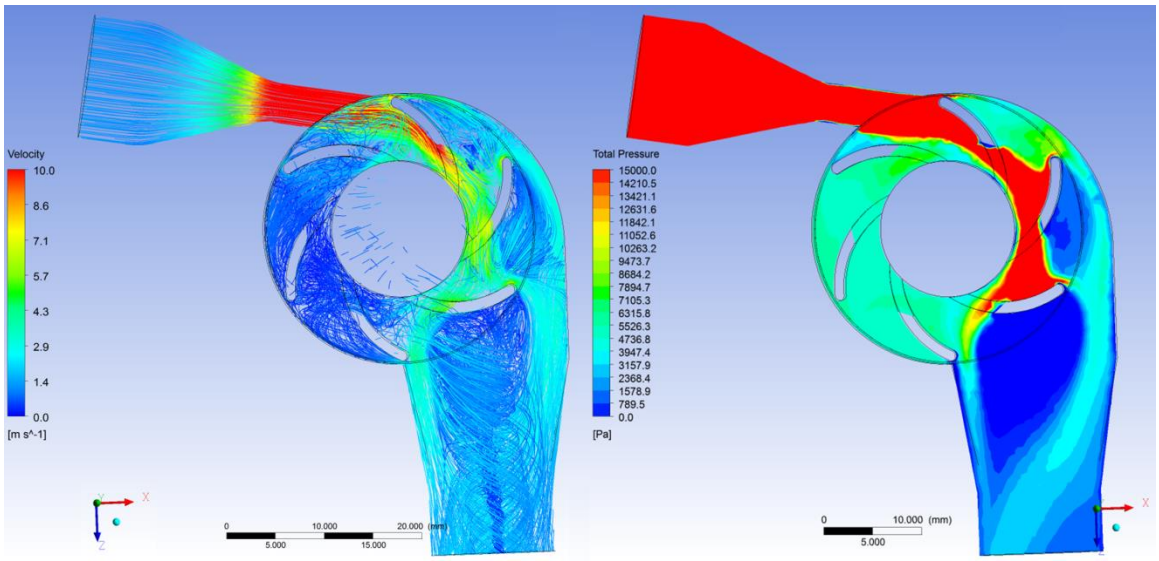

Figure 4.14 Notched model turbine simulations scale 3.175X. The left side shows the velocity behavior, and the internal pressure is shown in the right side. Maximum and minimum values of velocity and pressure are defined in both simulations as red and blue respectively.

The simulations in Figure 4.12, 4.13, and 4.14, show the impulse jet behavior on the first blade in the three prototyped models. Only in the notched system is most of the fluid directed clockwise, resulting in more than one blade being impacted and contributing to an increased rotor spin. The simulations of the notched turbine in Figure 4.14 show more interaction between the fluid and the blades than that of the simulations of the old turbine models where the blades were not notched. Figures 4.12 and 4.13 show the fluid impacting the first non-notched blade, producing only a single force impulse on the rotor, while the notched blade model, Figure 4.14, has a direct jet impact on the first blade, and an indirect impact on second and third blades. While this benefit is due to the notches in the blades, the blade curvature and casing shape also aid in the directed flow.

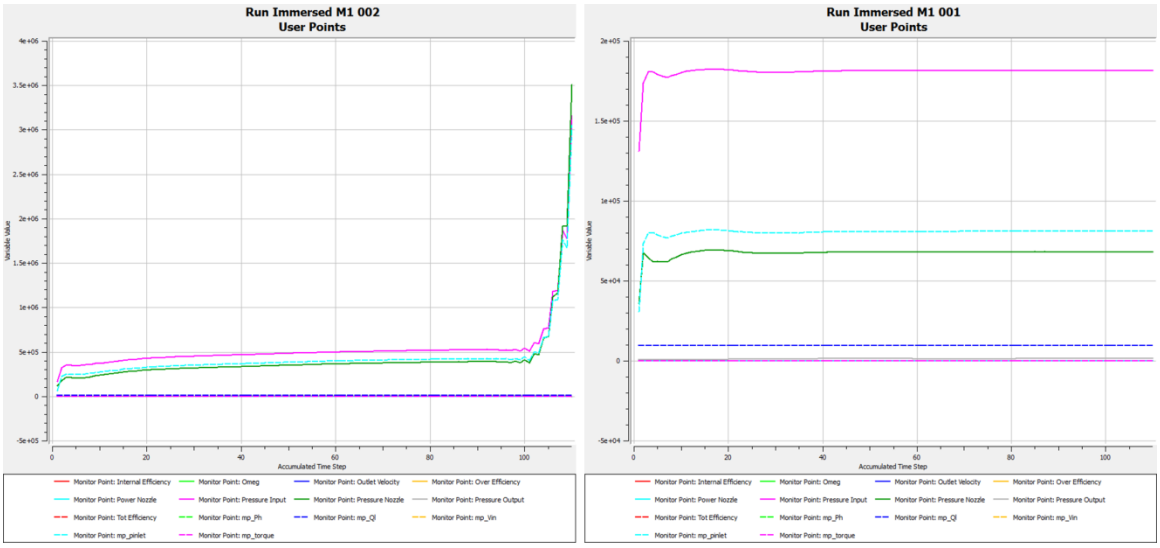

Figure 4.15 Turbine simulations time response parallel 1: systems behavior using volume flow rate Q=2.5 gallons per minute. (a) 3.175X Not-notched model; (b) 3.175X notched turbine model.

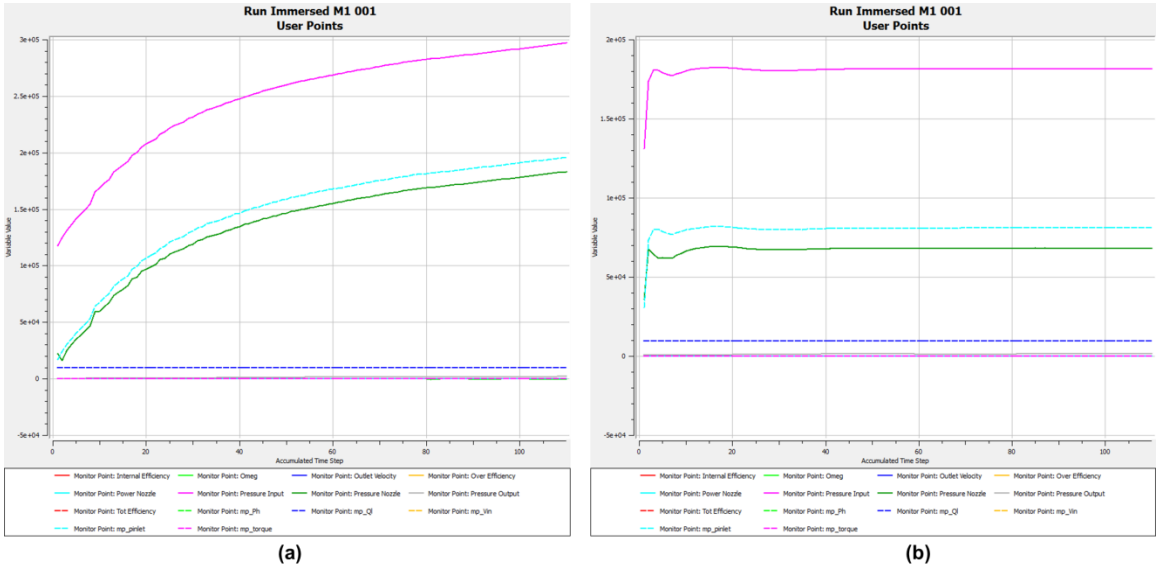

Figure 4.16 Turbine simulations time response parallel 2: systems behavior using volume flow rate Q=2.5 gallons per minute. (a) 4X Not-notched model; (b) 3.175X notched turbine model.

Other differences between models are in the transient response, which is immediate in the notched turbine, Figures 4.15b and 4.16b. Also, flow circulation

problems were detected in the old turbines because when the flow was interrupted, the turbine inlet pressure and the pressure in the first blade increased dramatically, causing vortices inside of the rotor blades, which could reduce the lifetime of the turbine system.

For organization purposes and to ease of comprehensions, the testing results of Voltage (V) vs. Volume Flow Rate (Q) and Voltage (V) vs. Angular Velocity (ω) of the three prototypes are drawn in the same graphics and are shown in Figures 4.17, and 4.18.

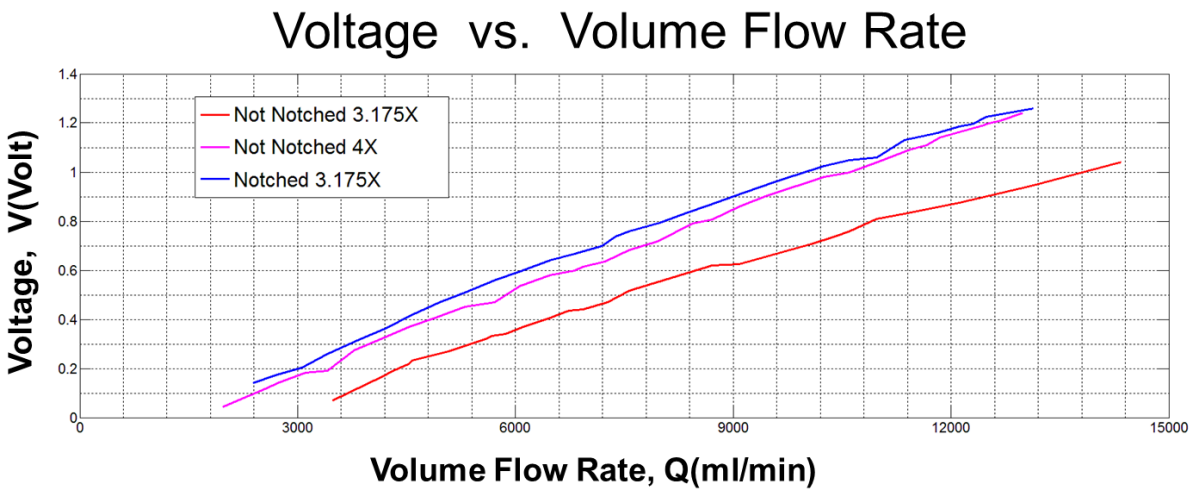

Figure 4.17 Volume flow rate (Q) vs. voltage, experimental results.

The analysis of the experimental data shown in Figures 4.17 and 4.18 validates the innovations developed on the final prototype. Using the same volume flow rate of the three models, an increase in voltage can be seen in the final prototype (notched model) when compared to the models without the notch. Also, to spin the rotor in the three prototypes, a higher volume flow rate is needed to spin the un-notched models, than in the notched model. Figure 4.17 shows the testing results and the relationship V vs. Q in the three models, and Figure 4.18 shows the relationship Q vs. ω in the three models. In summary, the simulation results, Figures 4.12 through 4.16, and the

experimental data shown in Table 4.3 and Figures 4.11, 4.17, and 4.18, validate the new notched blade energy generation system. These results show the benefits of the prototype, and its capability to produce electricity using water flow. Also, these analyses support the conclusion that the notched system is more efficient than previous models, developed in this dissertation process, and satisfies the minimal efficiency general standard of impulse turbines which reach an average of 70% efficiency.

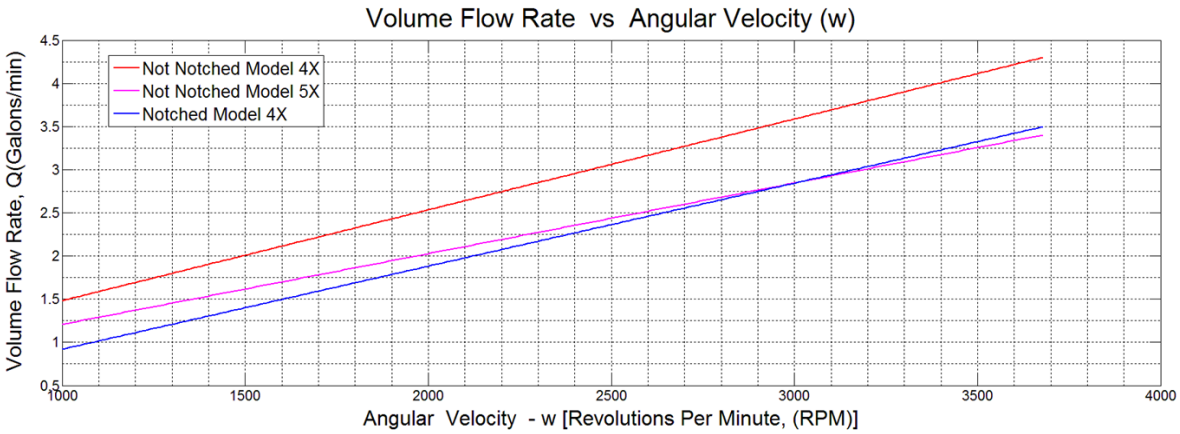

Figure 4.18 Volume flow rate (Q) vs. angular velocity (ω) , experimental results.

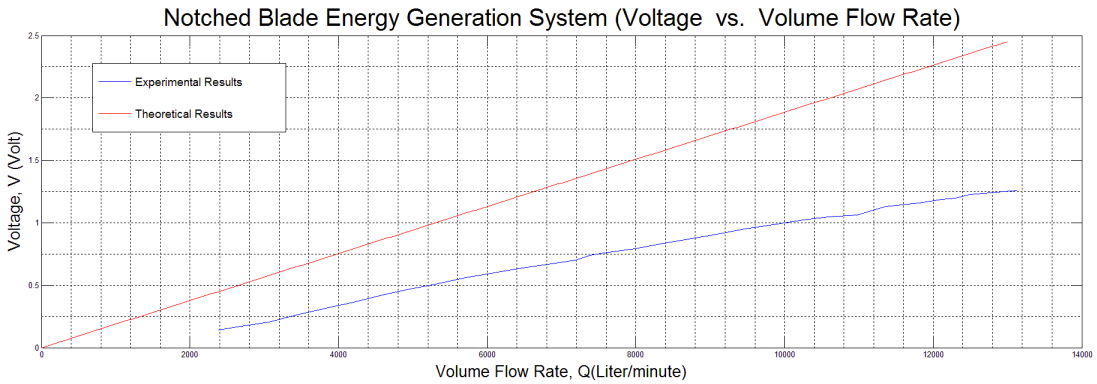

Figure 4.19 Voltage (v) vs. angular velocity (ω), experimental results.

The three prototypes tested could be used as energy generation systems, but only the final model, which is a cross-flow turbine energy generation system, can be used in closed fluid systems of constant flow. The notched blades prototype shown in Figures 4.5 and 4.10 has functionality aspects of impulse and reaction turbines. Therefore, in this specific case the curvature design of the blades guarantees that the jet stream from the nozzle is impacting the first blade on the given surface while it also guarantees that the pressure produced internally will further contribute to the spin of the rotor, increasing efficiency and the resulting power.

Figure 4.19 was developed to understand the difference between the theoretical calculations and the experimental data. The mathematical model developed in Chapter 3 was used to find the relationship between volume flow rate and the ideal voltage which must be produced by the notched blade energy generation system. The parameters of a 3.175X size model were used and the final relationship is shown in red on Figure 4.19. The experimental data of the notched blade energy generation prototype was used to complete Figure 4.19 and drawn in blue on this figure.

Under ideal conditions, the experimental (blue) and theoretical (red) results of Figure 4.19 should be close to being equal. The mathematical relationship of experimental to theoretical (blue line)/(red line) produces a result of 53%. This result has multiple causes, which are listed as follows:

a. The theoretical calculations were developed using a perfect model which didn't include the losses by structure, frictions, material, viscosity, and gravity.
b. The materials used to develop the prototypes, and the limitations of the 3D printer machines at USF labs created assembly problems.

c. The prototype quality was impacted by structural problems in the casing walls, and many tiny holes increased wall porosity and changed the internal behavior of the system.

d. The relationship between the inlet and outlet volume flow rate was affected by the porosity of the material, which became a considerable factor that adversely affected the efficiency of the system.

e. The materials, facilities and tools used presented limitations, but were sufficient to show proof of concept.

f. And finally, the HDD motors used as motor-generators which added friction, weight, forces and torques were not taken into account in the theoretical model resulting in an efficiency of 53% when compared with the experimental results.

The above analysis concluded this Chapter, and leads to the conclusions and future work.

CHAPTER 5: CONCLUSIONS AND FUTURE WORK

5.1 Summary and Contributions to the Field of Electrical Engineering

The overall research objective of this dissertation work was to investigate a novel miniaturized electrical generator system. Depending on the volume flow rate and the application power requirements, where the notched blade turbine energy generation system is to be installed, a single or a double motor frame (coils and permanent magnets) could be assembled on the same turbine. The double motor frame design increases the energy transformed. Also, the double combination of coils and permanent magnets could account for a more efficient system.

The preferred embodiment contains a cross-flow turbine design which can be installed and used in different orientations and positions; in contrast to the more standard turbine designs and energy generating systems, which only work in one position, and have limited orientations. The design has three novel and critical components:

a. The notched blade turbine rotor which was especially designed to be used in an immersed environment and minimized turbulence between blades and any opposing impulse forces.
b. A turbine casing designed to increase the jet impact and permit circulation inside of the turbine.
c. The third innovation is the adaptation and assembly of a brushless machine model, designed to provide the mechanism by which the system will convert

mechanical energy to electricity. The permanent magnet (PM) machine configuration (brushless machine) was inspired by the principles of operation and architecture of a micro hard drive disk motor.

Thus, this novel hybrid action-reaction turbine with notched blades and casing architecture designs has broadened the engineering contribution of my work well beyond the power and bio-medical fields. The system has potential uses not only in medical equipment, but in automotive applications, home appliances, and aquatic and ventilation systems. In addition, with small design modifications and utilization of biocompatible materials, this notched blade energy generation system can be used for in vivo systems and many other applications.

As this work has progressed and milestones were accomplished, the innovative design of my investigation has been submitted to undergo a patent process through the USF Patent Office.

In summary, the final result of this research is a miniaturized system capable of producing electrical energy by the use of a novel notched blade turbine. The turbine has an attached magnetic system that induces electric current in coils when a fluid rotates the turbine rotor. The shape and geometries of the notched blade energy generator system can be scaled to meet the power demands for several different applications such as home appliances, military devices, and bio-compatible devices in need of energy recharging.

5.2 Recommendation for Future Work and Emerging Projects

For any future work to be successful it is imperative to develop real size prototypes, using rigid, resistant and durable materials. It is also important that the prototypes be coated with a bio-compatible material that allows for in-vivo uses.

To improve the mathematical model equations developed in chapter 3, it is necessary to conduct a study of the interaction between the PMs and the stator coil slots. The analysis of the magnetic field and the effects produced by electromagnetic forces must be developed in a similar way as it is presented by Li Jiangtao in [104][100].

To complement the notched blade energy generation system and convert the system in a regulated power supply, a micro AC to DC converter could be designed and attached on the turbine casing.

As an added benefit to the current research, a levitation system of the rotor is being developed. A permanent-magnet configuration in the casing and the rotor will create the rotor levitation effect. This special characteristic could minimize friction inside of the turbine, reducing pressure through the turbine, as well as contribute to increase the rotor spin and efficiency.

REFERENCES

[1] J. Peirs, D. Reynaerts, and F. Verplaetsen, “A microturbine for electric power generation,” *Sens. Actuators Phys.*, vol. 113, no. 1, pp. 86–93, Jun. 2004.

[2] P. C.-P. Chao, C. I. Shao, C. X. Lu, and C. K. Sung, “A new energy harvest system with a hula-hoop transformer, micro-generator and interface energy-harvesting circuit,” *Microsyst. Technol.*, vol. 17, no. 5–7, pp. 1025–1036, Jun. 2011.

[3] J. Martinez-Quijada and S. Chowdhury, “A two-stator MEMS power generator for cardiac pacemakers,” in *IEEE International Symposium on Circuits and Systems, 2008. ISCAS 2008*, 2008, pp. 161–164.

[4] P. D. Mitcheson, “Analysis and Optimisation of Energy-Harvesting Micro-Generator Systems,” Imperial College, 2005.

[5] R. Yang, Y. Qin, C. Li, G. Zhu, and Z. L. Wang, “Converting Biomechanical Energy into Electricity by a Muscle-Movement-Driven Nanogenerator,” *Nano Lett.*, vol. 9, no. 3, pp. 1201–1205, Mar. 2009.

[6] Y. Nakanishi, S. Iio, Y. Takahashi, A. Kato, and T. Ikeda, “Development of a Simple Impulse Turbine for Nano Hydropower,” *J. Fluid Sci. Technol.*, vol. 4, no. 3, pp. 567–577, 2009.

[7] D. P. Arnold and M. G. Allen, “Fabrication of Microscale Rotating Magnetic Machines,” in *Multi-Wafer Rotating MEMS Machines*, J. Lang, Ed. Springer US, 2010, pp. 157–190.

[8] M. Bugge and G. Palmers, “Implantable device for utilization of the hydraulic energy of the heart,” RE4139422-Jun-2010.

[9] T. W. Piaget, B. Mi, L. E. Juffer, K. R. Maile, A. V. Chavan, and C. Zhang, “Implantable Medical Device with Internal Piezoelectric Energy Harvesting,” .

[10] B. Pless and J. A. Connor, “IMPLANTABLE POWER GENERATOR,” 2008020096321-Aug-2008.

[11] A. C. Fernandez-Pello, A. P. Pisano, K. Fu, D. C. Walther, A. Knobloch, F. Martinez, M. Senesky, C. Stoldt, R. Maboudian, S. Sanders, and D. Liepmann, “MEMS Rotary Engine Power System,” *IEEJ Trans. Sens. Micromachines*, vol. 123, no. 9, pp. 326–330, 2003.

[12] J. D. Jackson and R. F. Fox, “Classical electrodynamics,” *Am. J. Phys.*, vol. 67, p. 841, 1999.

[13] M. F. Iskander, *Electromagnetic fields and waves*. Prentice Hall Englewood Cliffs, 1992.

[14] A. Kovetz, *Electromagnetic theory*. Oxford University Press Oxford, 2000.

[15] Lorentz, F., Barstad, “CFD Analysis of a Pelton Turbine,” Norwegian University of Science and Technology, Department of Energy and Process Engineering, 2012.

[16] “CrossFlow Turbine Design,” *Scribd*. [Online]. Available: http://www.scribd.com/doc/117792063/CrossFlow-Turbine-Design. [Accessed: 11-Mar-2013].

[17] J.-C. Marongiu, F. Leboeuf, J. Caro, and E. Parkinson, “Free surface flows simulations in Pelton turbines using an hybrid SPH-ALE method,” *J. Hydraul. Res.*, vol. 48, no. sup1, pp. 40–49, 2010.

[18] A. Perrig, “Hydrodynamics of the free surface flow in Pelton turbine buckets,” *EPFL These*, no. 3715, 2007.

[19] B. R. Cobb and K. V. Sharp, “Impulse (Turgo and Pelton) turbine performance characteristics and their impact on pico-hydro installations,” *Renew. Energy*, vol. 50, pp. 959–964, Feb. 2013.

[20] H. Cabra and S. W. Thomas, “FABRICATION OF CROSS-FLOW BIO-MICRO-TURBINE.”: http://cap.ee.imperial.ac.uk/~pdm97/powermems/2010/poster-pdfs/183_Cabra_158.pdf

[21] Y. D. Choi, J. I. Lim, Y. T. Kim, and Y. H. Lee, “Performance and Internal Flow Characteristics of a Cross-Flow Hydro Turbine by the Shapes of Nozzle and Runner Blade,” *J. Fluid Sci. Technol.*, vol. 3, no. 3, pp. 398–409, 2008.

[22] S. Chalasani and J. M. Conrad, “A survey of energy harvesting sources for embedded systems,” in *IEEE Southeastcon, 2008*, 2008, pp. 442–447.

[23] M. Lossec, B. Multon, and H. Ben Ahmed, “Micro-kinetic generator: Modeling, energy conversion optimization and design considerations,” in *MELECON 2010 - 2010 15th IEEE Mediterranean Electrotechnical Conference*, 2010, pp. 1516–1521.

[24] A. S. Holmes, G. Hong, K. R. Pullen, and K. R. Buffard, “Axial-flow microturbine with electromagnetic generator: design, CFD simulation, and prototype demonstration,” presented at the Micro Electro Mechanical Systems, 2004. 17th IEEE International Conference on. (MEMS), 2004, pp. 568–571.

[25] B. Philippon, “Design of a film cooled MEMS micro turbine,” Massachusetts Institute of Technology, 2001.

[26] M.-C. Tsai and L.-Y. Hsu, “Design of a Miniature Axial-Flux Spindle Motor With Rhomboidal PCB Winding,” *IEEE Trans. Magn.*, vol. 42, no. 10, pp. 3488 –3490, Oct. 2006.

[27] B. S. Jeon, K. J. Park, S. J. Song, Y. C. Joo, and K. D. Min, “Design, fabrication, and testing of a MEMS microturbine,” *J. Mech. Sci. Technol.*, vol. 19, no. 2, pp. 682–691, Feb. 2005.

[28] “turbine :: History of water turbine technology -- Britannica Online Encyclopedia,” 31-Jan-2013. [Online]. Available: http://www.britannica.com/EBchecked/topic/609552/turbine/45676/History-of-water-turbine-technology. [Accessed: 31-Jan-2013].

[29] S. J. Williamson, B. H. Stark, and J. D. Booker, “Performance of a low-head pico-hydro Turgo turbine,” *Appl. Energy*, vol. 102, pp. 1114–1126, Feb. 2013.

[30] J. De Andrade, C. Curiel, F. Kenyery, O. Aguillón, A. Vásquez, and M. Asuaje, “Numerical Investigation of the Internal Flow in a Banki Turbine,” *Int. J. Rotating Mach.*, vol. 2011, pp. 1–12, 2011.

[31] J. Martinez-Quijada and S. Chowdhury, “Body-Motion Driven MEMS Generator for Implantable Biomedical Devices,” presented at the Electrical and Computer Engineering, 2007. CCECE 2007. Canadian Conference on, 2007, pp. 164–167.

[32] “turbine: History of water turbine technology - Britannica Online Encyclopedia,” 31-Jan-2013. [Online]. Available: http://www.britannica.com/EBchecked/topic/609552/turbine/45676/History-of-water-turbine-technology. [Accessed: 31-Jan-2013].

[33] M. Durali and M. I. of T. T. A. Program, *Design of small water turbines for farms and small communities*. Technology Adaptation Program, Massachusetts Institute of Technology, 1976.

[34] T. Ikeda, S. Ilo, and K. Tatsuno, “Performance of nano-hydraulic turbine utilizing waterfalls,” *Renew. Energy*, vol. 35, no. 1, pp. 293–300, 2010.

[35] T. Meier, *Mini hydropower for rural development: a new market-oriented approach to maximize electrification benefits with special focus on Indonesia*. Lit Verlag, 2001.

[36] K. Miyazaki, M. Takashiri, J. -i. Kurosaki, B. Lenoir, A. Dauscher, and H. Tsukamoto, “Development of a micro-generator based on Bi2Te3 thin films,” presented at the Thermoelectrics, 2007. ICT 2007. 26th International Conference on, 2007, pp. 294–299.

[37] WangWang, J. Liu, Song, and Z. L. Wang, “Integrated Nanogenerators in Biofluid,” *Nano Lett.*, vol. 7, no. 8, pp. 2475–2479, 2007.

[38] R. Cordero, A. Rivera, M. Neuman, R. Warrington, and E. Romero, “Micro-rotational electromagnetic generator for high speed applications,” presented at the 2012 IEEE 25th International Conference on Micro Electro Mechanical Systems (MEMS), 2012, pp. 1257 –1260.

[39] S. Kerzenmacher, J. Ducrée, R. Zengerle, and F. von Stetten, “An abiotically catalyzed glucose fuel cell for powering medical implants: Reconstructed manufacturing protocol and analysis of performance,” *J. Power Sources*, vol. 182, no. 1, pp. 66–75, Jul. 2008.

[40] Y. J. Chen, C. T. Pan, and Z. H. Liu, “Analysis of an in-plane micro-generator with various microcoil shapes,” *Microsyst. Technol.*, vol. 19, no. 1, pp. 43–52, Jan. 2013.

[41] J. Martinez-Quijada and S. Chowdhury, “Body-Motion Driven MEMS Generator for Implantable Biomedical Devices,” in *Electrical and Computer Engineering, 2007. CCECE 2007. Canadian Conference on*, 2007, pp. 164–167.

[42] C. R. Saha, T. O’Donnell, N. Wang, and P. McCloskey, “Electromagnetic generator for harvesting energy from human motion,” *Sens. Actuators Phys.*, vol. 147, no. 1, pp. 248–253, Sep. 2008.

[43] S. Kerzenmacher, J. Ducrée, R. Zengerle, and F. von Stetten, “Energy harvesting by implantable abiotically catalyzed glucose fuel cells,” *J. Power Sources*, vol. 182, no. 1, pp. 1–17, Jul. 2008.

[44] J. Lueke and W. A. Moussa, “MEMS-Based Power Generation Techniques for Implantable Biosensing Applications,” *Sensors*, vol. 11, no. 2, pp. 1433–1460, Jan. 2011.

[45] Z. Wang, “Energy harvesting for self-powered nanosystems,” *Nano Res.*, vol. 1, no. 1, pp. 1–8, Jul. 2008.

[46] F. Herrault, C.-H. Ji, and M. G. Allen, “Ultraminiaturized High-Speed Permanent-Magnet Generators for Milliwatt-Level Power Generation,” *J. Microelectromechanical Syst.*, vol. 17, no. 6, pp. 1376 –1387, Dec. 2008.

[47] L. Debnath, “The legacy of Leonhard Euler–a tricentennial tribute,” *Int. J. Math. Educ. Sci. Technol.*, vol. 40, no. 3, pp. 353–388, 2009.

[48] C.-S. Liu, P.-D. Lin, and M.-C. Tsai, “A miniature spindle motor with fluid dynamic bearings for portable storage device applications,” *Microsyst. Technol.*, vol. 15, no. 7, pp. 1001–1007, 2009.

[49] “[Micro and Precision Engineering Research Group] Microturbine for electric power generation.” [Online]. Available: http://www.mech.kuleuven.be/micro/topics/turbine/. [Accessed: 02-Apr-2013].

[50] N. Ghalichechian, A. Modafe, M. I. Beyaz, and R. Ghodssi, “Design, Fabrication, and Characterization of a Rotary Micromotor Supported on Microball Bearings,” *J. Microelectromechanical Syst.*, vol. 17, no. 3, pp. 632–642, 2008.

[51] Kinetron Company, “The 14-pole Micro Generator with Sm2Co17 magnet (MG205),” 04-Apr-2013. [Online]. Available: http://www.kinetron.nl/cms/publish/content/downloaddocument.asp?document_id=7. [Accessed: 04-Apr-2013].

[52] “Kinetron the micro energy company: the smallest micro-generators, micro-motors and micro-magnets in the world,” 04-Apr-2013. [Online]. Available: http://www.kinetron.nl. [Accessed: 04-Apr-2013].

[53] S. Das, D. P. Arnold, I. Zana, J. W. Park, M. G. Allen, and J. H. L. Lang, “Microfabricated high-speed axial-flux multiwatt permanent-magnet generators—Part I: Modeling,” *Microelectromechanical Syst. J. Of*, vol. 15, no. 5, pp. 1330–1350, 2006.

[54] D. P. Arnold, S. Das, J. W. Park, I. Zana, J. H. Lang, and M. G. Allen, “Microfabricated high-speed axial-flux multiwatt permanent-magnet generators—Part II: Design, fabrication, and testing,” *Microelectromechanical Syst. J. Of*, vol. 15, no. 5, pp. 1351–1363, 2006.

[55] R. Cordero, A. Rivera, M. Neuman, R. Warrington, and E. Romero, “Micro-rotational electromagnetic generator for high speed applications,” presented at the 2012 IEEE 25th International Conference on Micro Electro Mechanical Systems (MEMS), 2012, pp. 1257 –1260.

[56] M. S. Slaughter, M. A. Sobieski, D. Tamez, T. Horrell, J. Graham, P. S. Pappas, A. J. Tatooles, and J. LaRose, “HeartWare Miniature Axial-Flow Ventricular Assist Device,” *Tex. Heart Inst. J.*, vol. 36, no. 1, pp. 12–16, 2009.

[57] D. Timms, “A review of clinical ventricular assist devices,” *Med. Eng. Phys.*, vol. 33, no. 9, pp. 1041–1047, Nov. 2011.

[58] O. H. Frazier, C. Gemmato, T. J. Myers, I. D. Gregoric, B. Radovancevic, P. Loyalka, and B. Kar, “Initial Clinical Experience with the HeartMate® II Axial-Flow Left Ventricular Assist Device,” *Tex. Heart Inst. J.*, vol. 34, no. 3, pp. 275–281, 2007.

[59] “ABIOMED AB5000 Circulatory Support System - Texas Heart Institute - Heart Assist Devices.” [Online]. Available: http://texasheart.org/Research/Devices/abiomed_ab5000.cfm. [Accessed: 05-Apr-2013].

[60] D. J. Burke, E. Burke, F. Parsaie, V. Poirier, K. Butler, D. Thomas, L. Taylor, and T. Maher, “The HeartMate II: Design and Development of a Fully Sealed Axial Flow Left Ventricular Assist System,” *Artif. Organs*, vol. 25, no. 5, pp. 380–385, 2001.

[61] O. H. Frazier, N. A. Shah, T. J. Myers, K. D. Robertson, I. D. Gregoric, and R. Delgado, “Use of the Flowmaker (Jarvik 2000) left ventricular assist device for destination therapy and bridging to transplantation,” *Cardiology*, vol. 101, no. 1–3, pp. 111–116, 2004.

[62] S. Haj-Yahia, E. J. Birks, P. Rogers, C. Bowles, M. Hipkins, R. George, M. Amrani, M. Petrou, J. Pepper, and G. Dreyfus, “Midterm experience with the Jarvik 2000 axial flow left ventricular assist device,” *J. Thorac. Cardiovasc. Surg.*, vol. 134, no. 1, pp. 199–203, 2007.

[63] S. Takatani, “Progress of rotary blood pumps,” *Artif. Organs*, vol. 30, no. 5, pp. 317–321, 2006.

[64] K. E. Griffith and E. Jenkins, “Abiomed Impella® 2.5 patient transport: lessons learned,” *Perfusion*, vol. 25, no. 6, pp. 381–386, 2010.

[65] R. Krishnamani, D. DeNofrio, and M. A. Konstam, “Emerging ventricular assist devices for long-term cardiac support,” *Nat. Rev. Cardiol.*, vol. 7, no. 2, pp. 71–76, 2010.

[66] D. Timms, “A review of clinical ventricular assist devices,” *Med. Eng. Phys.*, vol. 33, no. 9, pp. 1041–1047, Nov. 2011.

[67] L. Zhang, E. I. Kapetanakis, R. H. Cooke, L. C. Sweet, and S. W. Boyce, “Bi-Ventricular Circulatory Support With the Abiomed AB5000 System in a Patient With Idiopathic Refractory Ventricular Fibrillation,” *Ann. Thorac. Surg.*, vol. 83, no. 1, pp. 298–300, Jan. 2007.

[68] “Circulatory & Ventricular Assist Devices - Center for Circulatory Support - University of Michigan Cardiac Surgery.” [Online]. Available: http://www.med.umich.edu/cardiac-surgery/patient/adult/ccs/vad.shtml. [Accessed: 05-Apr-2013].

[69] F. M. White, *Fluid Mechanics*. McGraw-Hill, 2010.

[70] S. L. Dixon, *Fluid mechanics, thermodynamics of turbomachinery*. Butterworth-Heinemann, 2005.

[71] R. H. Enns, “World of Motion,” in *It’s a Nonlinear World*, Springer New York, 2011, pp. 131–171.

[72] I. E. Idelchik, *Handbook of hydraulic resistance, 1994*. Begell House, Redding, CT, USA.

[73] H. Bruus, *Theoretical microfluidics*. Oxford University Press, USA, 2008.

[74] G. Ingram, *Basic Concepts in Turbomachinery*. Bookboon, 2009.

[75] M. Durali and M. I. of T. T. A. Program, “Design of Small Water Turbines for Farms and Small Communities,” 1976.

[76] O. ZIA, O. A. GHANI, S. T. WASIF, and Z. HAMID, “DESIGN, FABRICATION AND INSTALLATION OF A MICRO-HYDRO POWER PLANT,” 2010.

[77] J. L. Gordon, “Hydraulic turbine efficiency,” *Can. J. Civ. Eng.*, vol. 28, no. 2, pp. 238–253, 2001.

[78] H. Bruus, *Theoretical microfluidics*. Oxford University Press, USA, 2008.

[79] S. L. Dixon, *Fluid mechanics, thermodynamics of turbomachinery*. Butterworth-Heinemann, 2005.

[80] B. S. Massey, *Mechanics of fluids*, vol. 1. Taylor & Francis, 1998.

[81] F. M. White, *Fluid Mechanics*. McGraw-Hill, 2010.

[82] T. S. Desmukh, *Fluid Mechanics and Hydraulic Machines (A Lab Manual)*. Firewall Media, 2001.

[83] D. J. Griffiths and R. College, *Introduction to electrodynamics*, vol. 3. prentice Hall Upper Saddle River, NJ, 1999.

[84] A. Krawczyk and S. Wiak, *Electromagnetic fields in electrical engineering*, vol. 22. IOS Press, 2002.

[85] H. Polinder and M. J. Hoeijmakers, “Analytic calculation of the magnetic field in PM machines,” in *, Conference Record of the 1997 IEEE Industry Applications Conference, 1997. Thirty-Second IAS Annual Meeting, IAS ’97*, 1997, vol. 1, pp. 35–41 vol.1.

[86] D. L. Trumper, W. Kim, and M. E. Williams, “Design and analysis framework for linear permanent-magnet machines,” *IEEE Trans. Ind. Appl.*, vol. 32, no. 2, pp. 371–379, 1996.

[87] M. F. Iskander, *Electromagnetic fields and waves*. Prentice Hall Englewood Cliffs, 1992.

[88] A. Kovetz, *Electromagnetic theory*. Oxford University Press Oxford, 2000.

[89] A. Krawczyk and S. Wiak, *Electromagnetic fields in electrical engineering*, vol. 22. IOS Press, 2002.

[90] D. C. Hanselman, *Brushless permanent-magnet motor design*. McGraw-Hill New York, 1994.

[91] J. F. Gieras, R.-J. Wang, and M. J. Kamper, *Axial flux permanent magnet brushless machines*. Springer, 2008.

[92] J. F. Gieras, *Permanent Magnet Motor Technology: Design and Applications, Third Edition*. Taylor & Francis US, 2011.

[93] M. Humphries, *Rare earth elements: The global supply chain*. DIANE Publishing, 2010.

[94] T. Minowa, “Rare earth magnets: conservation of energy and the environment,” *Resour. Geol.*, vol. 58, no. 4, pp. 414–422, 2008.

[95] W. D. Jackson and G. Christiansen, “International strategic minerals inventory summary report; rare-earth oxides,” United States Geological Survey, CIR - 930-N, 1993.

[96] Z. Q. Zhu and C. C. Chan, “Electrical machine topologies and technologies for electric, hybrid, and fuel cell vehicles,” in *Vehicle Power and Propulsion Conference, 2008. VPPC’08. IEEE*, 2008, pp. 1–6.

[97] K. T. Chau, null, and C. Liu, “Overview of Permanent-Magnet Brushless Drives for Electric and Hybrid Electric Vehicles,” *IEEE Trans. Ind. Electron.*, vol. 55, no. 6, pp. 2246–2257, June.

[98] F. M. White, *Fluid Mechanics*. McGraw-Hill, 2010.

[99] S. L. Dixon, *Fluid mechanics, thermodynamics of turbomachinery*. Butterworth-Heinemann, 2005.

[100] J. L. Gordon, “Hydraulic turbine efficiency,” *Can. J. Civ. Eng.*, vol. 28, no. 2, pp. 238–253, 2001.

[101] A. Perrig, “Hydrodynamics of the free surface flow in Pelton turbine buckets,” *EPFL These*, no. 3715, 2007.

[102] “Hydropower,” 11-Oct-2013. [Online]. Available: http://www.eaton.com/Eaton/ProductsbyMarket/Energy/Hydropower/index.htm. [Accessed: 11-Oct-2013].

[103] J. R. Bumby and R. Martin, “Axial-flux permanent-magnet air-cored generator for small-scale wind turbines,” *Electr. Power Appl. IEE Proc. -*, vol. 152, no. 5, pp. 1065–1075, 2005.

[104] D. W. Novotny, *Vector Control and Dynamics of AC Drives*. Oxford University Press, 1996.

[105] A. M. EL-Refaie and T. M. Jahns, “Optimal flux weakening in surface PM machines using concentrated windings,” in *Conference Record of the 2004 IEEE Industry Applications Conference, 2004. 39th IAS Annual Meeting*, 2004, vol. 2, pp. 1038–1047 vol.2.

[106] J. Y. Chen, C. V. Nayar, and L. Xu, “Design and finite-element analysis of an outer-rotor permanent-magnet generator for directly coupled wind turbines,” *IEEE Trans. Magn.*, vol. 36, no. 5, pp. 3802–3809, 2000.

[107] Y. A. Cengel and J. M. Cimbala, “Fluid Dynamics: Fundamentals and Applications,” *Seoul Korea McGraw-Hill Korea*, 2006.

[108] B. Chao, “Hard Disk Drive Spindle Motor System Design For Data Recording With Ultrahigh TPI,” pp. 5123–5128, Nov.

[109] D.-K. Jang and J.-H. Chang, “Development of a new spindle motor for a hard disk drive,” pp. 1601–1606, Sep. 2013.

[110] Z. J. Liu, C. Bi, Q. D. Zhang, M. A. Jabbar, and T. S. Low, “Electromagnetic design for hard disk drive spindle motors with fluid film lubricated bearings,” pp. 3893 –3895, Sep. 1996.

[111] J. F. Gieras, *Permanent Magnet Motor Technology: Design and Applications, Third Edition*. Taylor & Francis US, 2011.

APPENDICES

Appendix A Retrospective of the Design Changes and Justifications

Hydraulic turbines extract energy from the gravitational potential of fluids (water) sources, or from the kinetic energy of flowing liquids, or through of a combination of the two. There are two broad categories of turbines, reaction and impulse turbines. The first one acts on a charge of pressure in the flow of the fluid to move the turbine. The reaction turbines require a design complex, because the efficiency depends of very high level of precision in the gap between the rotor and its casing. The second one, the impulse turbine, is a system moved by the impact of a fluid jet on the concave surface of the blades. The impulse turbines are easy to build and assemble. In this dissertation, impulse and reaction effects are combined to form a kind of impulse-reaction turbine. This turbine combines the impulse of the flow, from nozzle, striking the turbine blades, and the reactive force produced on the blades in rotation, when the fluid through the rotor chamber, changes the direction.

The requirements stated in this project demand a combination of characteristics of impulse and reaction turbine, extracting of the impulse turbine, the simple construction and the jet impacting over blades, and from the reaction turbine, the precision and the use of pressure to move the rotor.

A.1 Turbine System Designs

An impulse Michell Banki turbine was the original model proposed to develop this project, but simulations, lab tests and theoretical analysis shown that this specific kind of turbines do not work on applications where is required complete conditions of immersion. An impulse turbine uses the absolute velocity at inlet (jet velocity) from nozzle to move the rotor by the change in the kinetic energy. Also, the rotor of a Pelton

and others impulse turbines work at atmospheric pressure (the rotor chamber is at atmospheric pressure), and without immersed rotor. In general an impulse turbine such as the reported and the commercial models don't have the shape characteristics, to be used in close flow systems, where the energy conversion demands a full rotor immersion. Also, these kinds of turbines need to be fixed in a place, and only works in a specific position and orientation. On the other hand, a reaction turbine has fixed blades and moving blades, and the energy is generated by the pressure inside the rotor chamber, which must kept full of fluid at all times.

Four generations of designs to realize a notched blade energy generator were developed. The First Generation → approach using simple Banki turbine with traditional blade (non-notched) rotor, cylindrical magnets with axial orientation, and coils; The Second Generation → approach using simple Pelton turbine with traditional curved blade (air) and external notched blade (water) rotor, ring magnets, and winding coils; Third Generation → approach using novel internal notched blade rotor, ring magnets, and winding coils; Fourth Generation → approach using novel internal notched blade rotor, ring magnets, winding coils, and casing innovations. The design of the four generation of turbine was presented in Chapter 3 and analyzed in Chapter 4. The keys findings in the first generation,

a. Inlet pressure too high to spin rotor at adequate speed to produce energy (low velocity)
b. Casing inlet too large
c. Design not efficient enough to generate high rotor spin for energy generation

The approach findings in the first generation are listed as follow,

d. Alter casing and blades in second generation

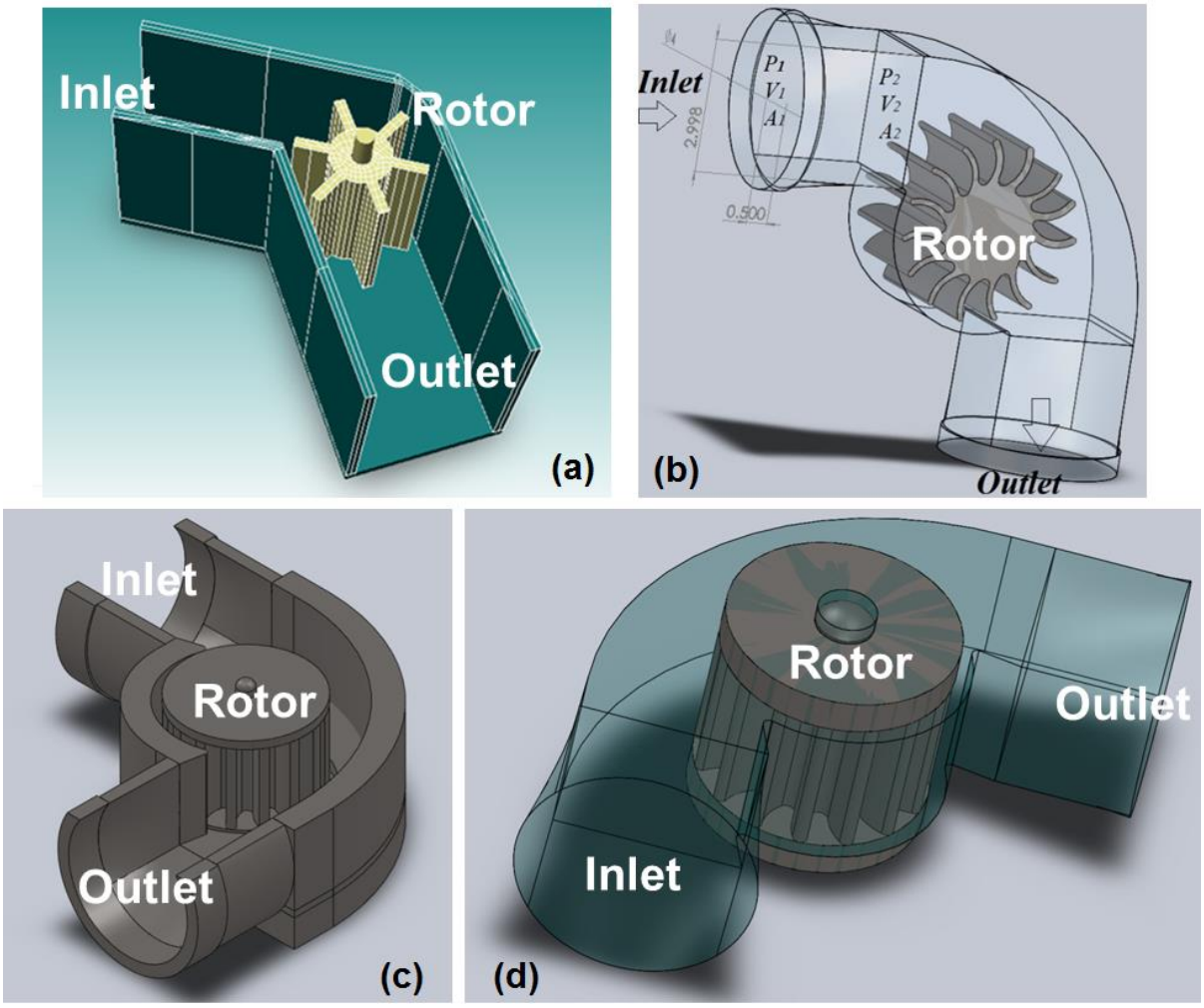

Figure A.1 Turbines first generation.

The key findings in the second turbine generation,

a. Casing inlet nozzle was adequately designed to create high inlet velocity
b. External notched blade did not provide jet stream continuity for rotor impact to create high angular velocity

The approach findings in the second generation,

c. To increase rotor speed and create cross flow conditions (continuous flow) in third generation.

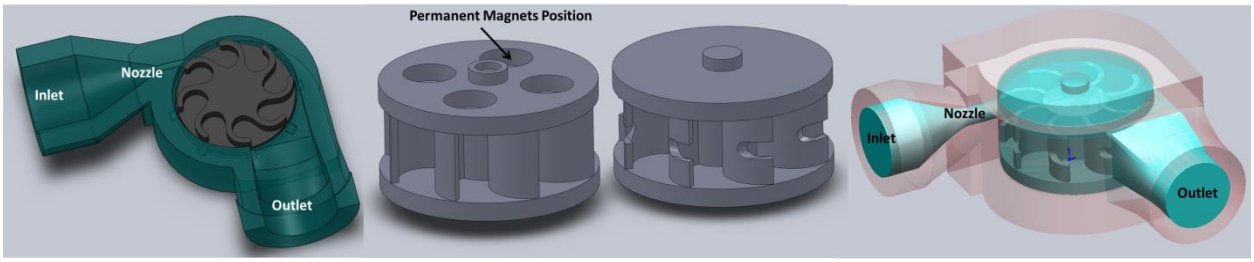

Figure A.2 Turbines second generation.

The key findings in the third turbine generation,

a. An internal notched blade vs. an external notched blade creates cross flow characteristics
b. This generation created vortices between blades
c. Applied fluid

The approach findings in the third generation,

d. To reduce vortices, increase system efficiency, and create favorable impulse-reaction conditions for power generation in fourth generation (final design).

The first models used in the development of this dissertation works are shown in Figure A.1. Rotors, holders, and coils designs are shown in Figures A.2, A.3, and A.4, while different models of permanent magnets, shown in Figure A.5, were part of the simulation and analysis. Also, previous models design were simulated and analyzed in transient state, most of them having a good performance when air or fluid were used, but when the steady state was included in the simulations, a reduction of rotor speed was the final result, with values close to zero and a poor mechanical power, insufficient to be converted to electrical energy, and to be used as power supply of electronic devices.

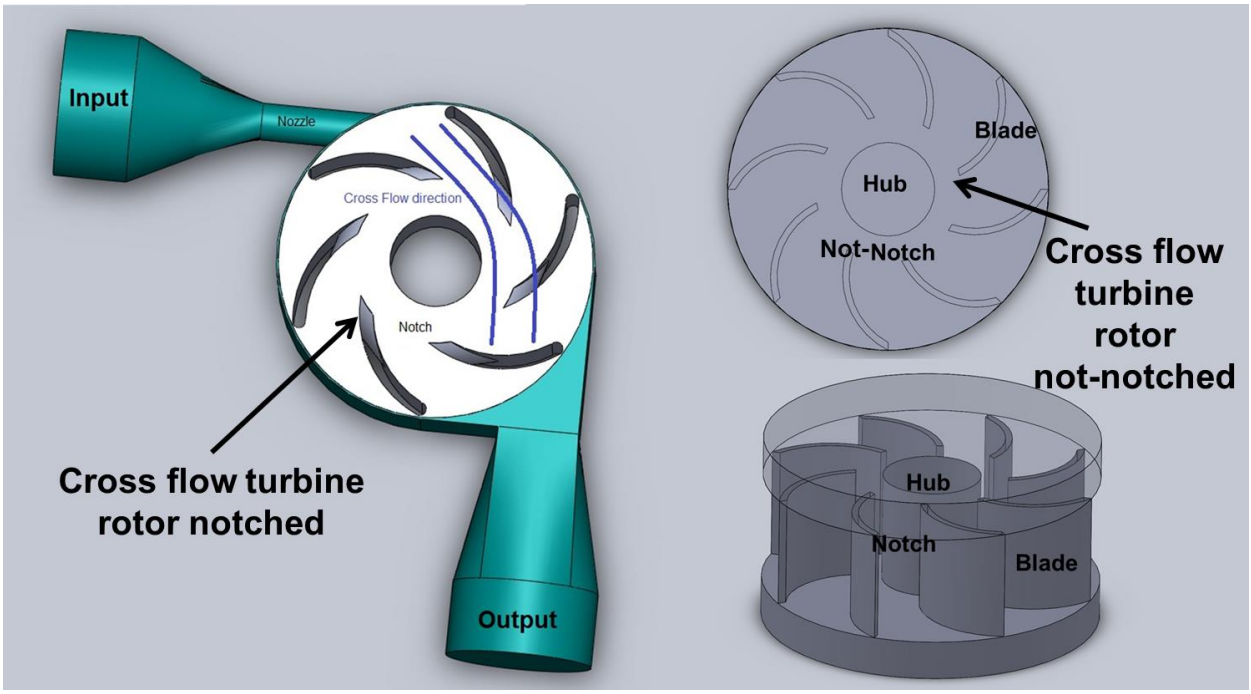

Figure A.3 Turbines third generation.

In the case of systems using air to move the turbine system, the results were different, and those depended of the rotor shape and the area impacted by the jet. In those cases, the efficiency in the cross flow rotor designs is reduced, while uniform and curved blades with proximity of nano meter to the walls holder, produced a good response and power efficiency, keeping the rotation and the induction of energy in the system.

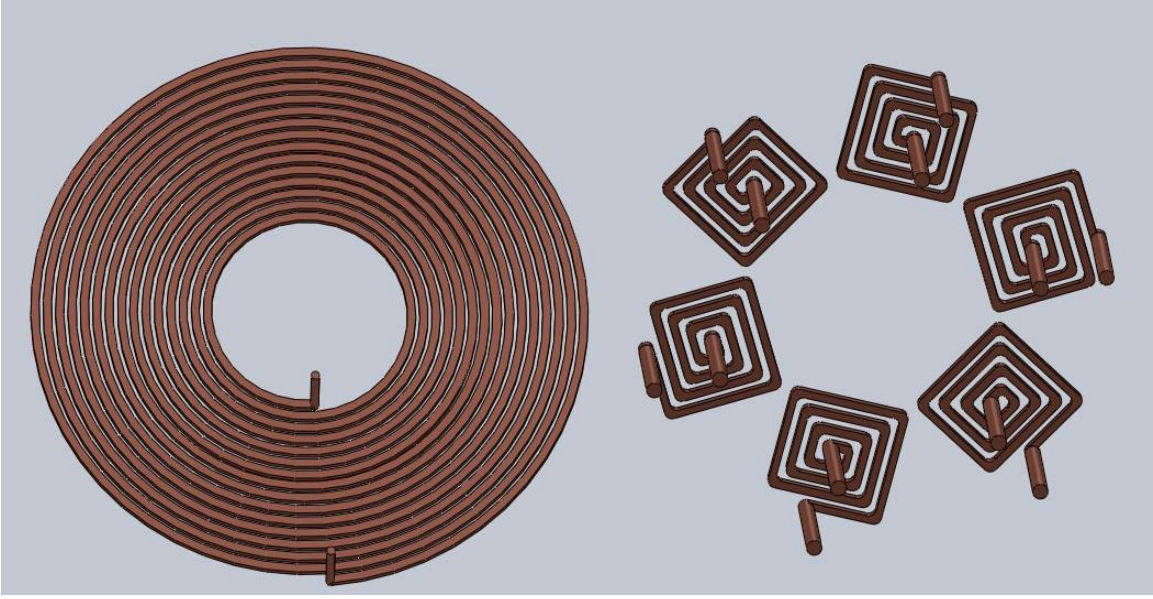

Figure A.4 Initial coils model designs.

Previous permanent magnets and coils configurations used, analyzed and simulated are shown in Figures A.4, A.5, and A.6.

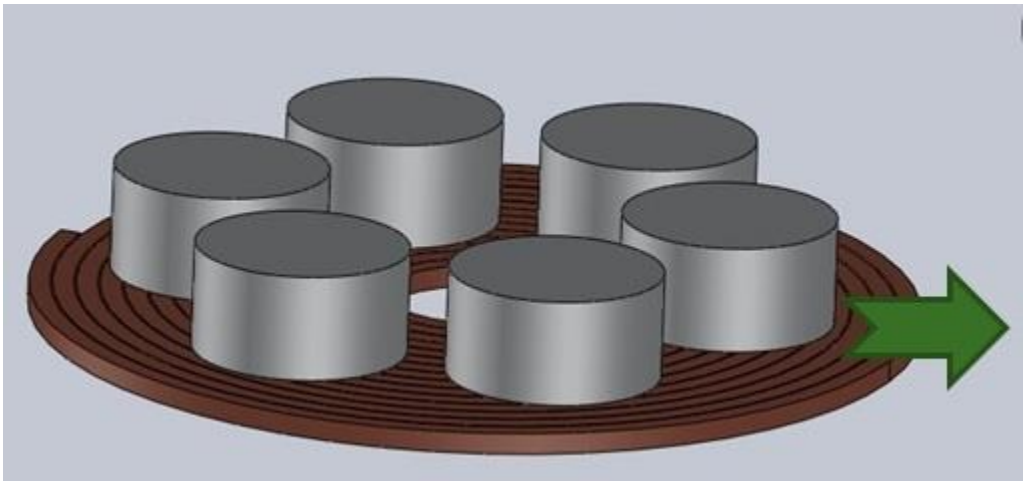

Figure A.5 The previous coils designs and permanent magnets designs.

Appendix B Copyright Permissions

B.1 Permission for Use of Figure 1.1

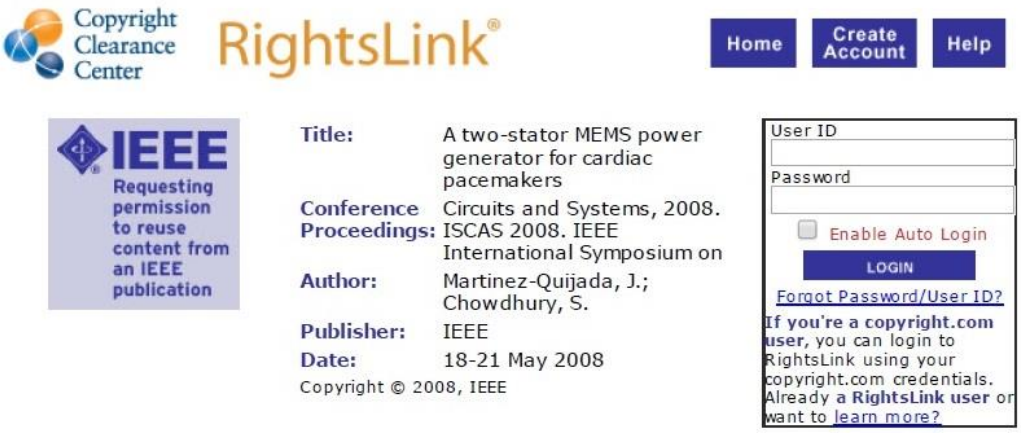

Thesis / Dissertation Reuse

The IEEE does not require individuals working on a thesis to obtain a formal reuse license, however, you may print out this statement to be used as a permission grant:

Requirements to be followed when using any portion (e.g., figure, graph, table, or textual material) of an IEEE copyrighted paper in a thesis:

1) In the case of textual material (e.g., using short quotes or referring to the work within these papers) users must give full credit to the original source (author, paper, publication) followed by the IEEE copyright line © 2011 IEEE.
2) In the case of illustrations or tabular material, we require that the copyright line © [Year of original publication] IEEE appear prominently with each reprinted figure and/or table.
3) If a substantial portion of the original paper is to be used, and if you are not the senior author, also obtain the senior author's approval.

Requirements to be followed when using an entire IEEE copyrighted paper in a thesis:

1) The following IEEE copyright/ credit notice should be placed prominently in the references: © [year of original publication] IEEE. Reprinted, with permission, from [author names, paper title, IEEE publication title, and month/year of publication]
2) Only the accepted version of an IEEE copyrighted paper can be used when posting the paper or your thesis on-line.
3) In placing the thesis on the author's university website, please display the following message in a prominent place on the website: In reference to IEEE copyrighted material which is used with permission in this thesis, the IEEE does not endorse any of [university/educational entity's name goes here]'s products or services. Internal or personal use of this material is permitted. If interested in reprinting/republishing IEEE copyrighted material for advertising or promotional purposes or for creating new collective works for resale or redistribution, please go to http://www.ieee.org/publications_standards/publications/rights/rights_link.html to learn how to obtain a License from RightsLink.

If applicable, University Microfilms and/or ProQuest Library, or the Archives of Canada may supply single copies of the dissertation.

BACK CLOSE WINDOW

B.2 Permission for Use of Figure 1.2

ELSEVIER LICENSE
TERMS AND CONDITIONS

Mar 29, 2014

This is a License Agreement between Henry Cabra ("You") and Elsevier ("Elsevier") provided by Copyright Clearance Center ("CCC"). The license consists of your order details, the terms and conditions provided by Elsevier, and the payment terms and conditions.

All payments must be made in full to CCC. For payment instructions, please see information listed at the bottom of this form.

Supplier	Elsevier Limited The Boulevard,Langford Lane Kidlington,Oxford,OX5 1GB,UK
Registered Company Number	1982084
Customer name	Henry Cabra
Customer address	30229 Swinford Ln. Wesley Chapel, FL 33543
License number	3358360933207
License date	Mar 29, 2014
Licensed content publisher	Elsevier
Licensed content publication	Sensors and Actuators A: Physical
Licensed content title	A microturbine for electric power generation
Licensed content author	Jan Peirs,Dominiek Reynaerts,Filip Verplaetsen
Licensed content date	15 June 2004
Licensed content volume number	113

Licensed content issue number	1
Number of pages	8
Start Page	86
End Page	93
Type of Use	reuse in a thesis/dissertation
Intended publisher of new work	other
Portion	figures/tables/illustrations
Number of figures/tables/illustrations	2
Format	electronic
Are you the author of this Elsevier article?	No
Will you be translating?	No
Title of your thesis/dissertation	Design, Simulation, Prototype, and Testing of a Notched Blade Energy Generation System
Expected completion date	Apr 2014
Estimated size (number of pages)	130
Elsevier VAT number	GB 494 6272 12
Permissions price	0.00 USD
VAT/Local Sales Tax	0.00 USD / 0.00 GBP
Total	0.00 USD
Terms and Conditions	

INTRODUCTION

1. The publisher for this copyrighted material is Elsevier. Byclicking "accept" in connection with completing this licensingtransaction, you agree that the following terms and conditions apply to thistransaction (along with the Billing and Payment terms and conditionsestablished by Copyright

Clearance Center, Inc. ("CCC"), at the timethat you opened your Rightslink account and that are available at any time at http://myaccount.copyright.com).

GENERAL TERMS

2. Elsevier hereby grants you permission to reproduce the aforementionedmaterial subject to the terms and conditions indicated.

3. Acknowledgement: If any part of the material to be used (for example,figures) has appeared in our publication with credit or acknowledgement toanother source, permission must also be sought from that source. If suchpermission is not obtained then that material may not be included in yourpublication/copies. Suitable acknowledgement to the source must be made, eitheras a footnote or in a reference list at the end of your publication, asfollows:

"Reprinted from Publication title, Vol /edition number, Author(s), Title ofarticle / title of chapter, Pages No., Copyright (Year), with permission fromElsevier [OR APPLICABLE SOCIETY COPYRIGHT OWNER]." Also Lancet special credit -"Reprinted from The Lancet, Vol. number, Author(s), Title of article, PagesNo., Copyright (Year), with permission from Elsevier."

4. Reproduction of this material is confined to the purpose and/or media forwhich permission is hereby given.

5. Altering/Modifying Material: Not Permitted. However figures andillustrations may be altered/adapted minimally to serve your work. Any otherabbreviations, additions, deletions and/or any other alterations shall be madeonly with prior written authorization of Elsevier Ltd. (Please contact Elsevierat permissions@elsevier.com)

6. If the permission fee for the requested use of our material is waived inthis instance, please be advised that your future requests for Elseviermaterials may attract a fee.

7. Reservation of Rights: Publisher reserves all rights not specificallygranted in the combination of (i) the license details provided by you andaccepted in the course of this licensing transaction, (ii) these terms andconditions and (iii) CCC's Billing and Payment terms and conditions.

8. License Contingent Upon Payment: While you may exercise the rightslicensed immediately upon issuance of the license at the end of the licensingprocess for the transaction, provided that you have disclosed complete andaccurate details of your proposed use, no license is finally effective unlessand until full payment is received from you (either by publisher or by CCC) asprovided in CCC's Billing and Payment terms and conditions. If fullpayment is not received on a timely basis, then any license preliminarilygranted shall be deemed automatically revoked and shall be void as if nevergranted. Further, in the event that you breach any of these terms andconditions or any of CCC's Billing and Payment terms and conditions, thelicense is automatically revoked and shall be void as if never granted. Use of materials as described in a revoked license, as well as any use of thematerials beyond the scope of an unrevoked license, may constitute copyrightinfringement and publisher reserves the right to take any and all action toprotect its copyright in the materials.

9. Warranties: Publisher makes no representations or warranties with respectto the licensed material.

10. Indemnity: You hereby indemnify and agree to hold harmless publisher andCCC, and their respective officers, directors, employees and agents, from andagainst any and all claims arising out of your use of the licensed materialother than as specifically authorized pursuant to this license.

11. No Transfer of License: This license is personal to you and may not besublicensed, assigned, or transferred by you to any other person withoutpublisher's written permission.

12. No Amendment Except in Writing: This license may not be amended exceptin a writing signed by both parties (or, in the case of publisher, by CCC onpublisher's behalf).

13. Objection to Contrary Terms: Publisher hereby objects to any termscontained in any purchase order, acknowledgment, check endorsement or otherwriting prepared by you, which terms are inconsistent with these terms andconditions or CCC's Billing and Payment terms and conditions. These termsand conditions, together with CCC's Billing and Payment terms and conditions(which are incorporated herein), comprise the entire agreement between you andpublisher (and CCC) concerning this licensing transaction. In the eventof any conflict between your obligations established by these terms andconditions and those established by CCC's Billing and Payment terms andconditions, these terms and conditions shall control.

14. Revocation: Elsevier or Copyright Clearance Center may deny thepermissions described in this License at their sole discretion, for any reasonor no reason, with a full refund payable to you. Notice of such denialwill be made using the contact information provided by you. Failure toreceive such notice will not alter or invalidate the denial. In no eventwill Elsevier or Copyright Clearance Center be responsible or liable for anycosts, expenses or damage incurred by you as a result of a denial of yourpermission request, other than a refund of the amount(s) paid by you toElsevier and/or Copyright Clearance Center for denied permissions.

LIMITED LICENSE

The following terms and conditions apply only to specific license types:

15. **Translation**: This permission is granted fornon-exclusive world **English** rights only unless yourlicense was granted for translation rights. If you licensed translation rightsyou may only translate this content into the languages you requested. Aprofessional translator must perform all translations and reproduce the contentword for word preserving the integrity of the article. If this license is tore-use 1 or 2 figures then permission is granted for non-exclusive world rightsin all languages.

16. **Posting licensed content on any Website**: The followingterms and conditions apply as follows: Licensing material from an Elsevierjournal: All content posted to the web site must maintain the copyright informationline on the bottom of each image; A hyper-text must be included to the Homepageof the journal from which you are licensing at http://www.sciencedirect.com/science/journal/xxxxx orthe Elsevier homepage for books at http://www.elsevier.com; CentralStorage: This license does not include permission for a scanned version of thematerial to be stored in a central repository such as that provided byHeron/XanEdu.

Licensing material from an Elsevier book: A hyper-text link must be includedto the Elsevier homepage at http://www.elsevier.com . Allcontent posted to the web site must maintain the copyright information line onthe bottom of each image.

Posting licensed content on Electronic reserve: In addition to the above the following clausesare applicable: The web site must be password-protected and made available onlyto bona fide students registered on a relevant course. This permission isgranted for 1 year only. You may obtain a new license for future websiteposting.

For journal authors: the following clauses are applicable inaddition to the above: Permission granted is limited to the author acceptedmanuscript version* of your paper.

***Accepted Author Manuscript (AAM) Definition:** An accepted authormanuscript (AAM) is the author's version of the manuscript of an article thathas been accepted for publication and which may include any author-incorporatedchanges suggested through the processes of submission processing, peer review,and editor-author communications. AAMs do not include other publishervalue-added contributions such as copy-editing, formatting, technicalenhancements and (if relevant) pagination.

You are not allowed to download and post the published journal article (whetherPDF or HTML, proof or final version), nor may you scan the printed edition tocreate an electronic version. A hyper-text must be included to the Homepage ofthe journal from which you are licensing at

http://www.sciencedirect.com/science/journal/xxxxx. As part of our normal production process, you will receive an e-mail noticewhen your article appears on Elsevier's online service ScienceDirect(www.sciencedirect.com). That e-mail will include the article's Digital ObjectIdentifier (DOI). This number provides the electronic link to the publishedarticle and should be included in the posting of your personal version. We askthat you wait until you receive this e-mail and have the DOI to do any posting.

Posting to a repository: Authorsmay post their AAM immediately to their employer's institutional repository forinternal use only and may make their manuscript publically available after thejournal-specific embargo period has ended.

Please also refer to Elsevier'sArticle Posting Policy for further information.

18. **For book authors** the following clauses are applicable in addition tothe above: Authors are permitted to place a briefsummary of their work online only.. You are notallowed to download and post the published electronic version of your chapter,nor may you scan the printed edition to create an electronic version. Posting to a repository: Authors arepermitted to post a summary of their chapter only in their institution'srepository.

20. **Thesis/Dissertation**: If your license is for use in athesis/dissertation your thesis may be submitted to your institution in eitherprint or electronic form. Should your thesis be published commercially, pleasereapply for permission. These requirements include permission for the Libraryand Archives of Canada to supply single copies, on demand, of the completethesis and include permission for UMI to supply single copies, on demand, ofthe complete thesis. Should your thesis be published commercially, pleasereapply for permission.

Elsevier Open Access Terms andConditions

Make Payment To:
Copyright Clearance Center
Dept 001
P.O. Box 843006
Boston, MA 02284-3006

For suggestions or comments regarding this order, contact RightsLink Customer Support: customercare@copyright.com or +1-877-622-5543 (toll free in the US) or +1-978-646-2777.

Gratis licenses (referencing $0 in the Total field) are free. Please retain this printable license for your reference. No payment is required.

B.3 Permission for Use of Figure 1.3

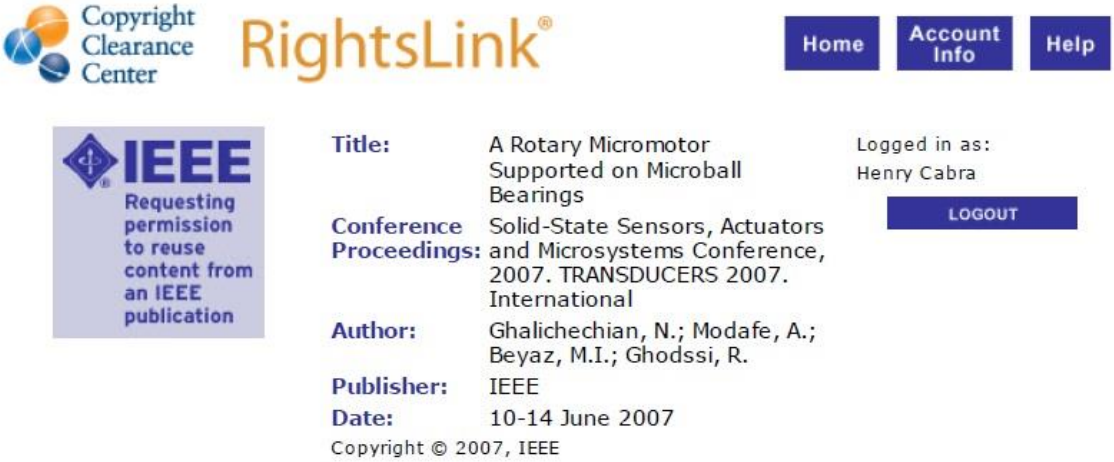

Copyright Clearance Center RightsLink®

Home | Account Info | Help

IEEE Requesting permission to reuse content from an IEEE publication

Title:	A Rotary Micromotor Supported on Microball Bearings
Conference Proceedings:	Solid-State Sensors, Actuators and Microsystems Conference, 2007. TRANSDUCERS 2007. International
Author:	Ghalichechian, N.; Modafe, A.; Beyaz, M.I.; Ghodssi, R.
Publisher:	IEEE
Date:	10-14 June 2007

Copyright © 2007, IEEE

Logged in as: Henry Cabra

LOGOUT

Thesis / Dissertation Reuse

The IEEE does not require individuals working on a thesis to obtain a formal reuse license, however, you may print out this statement to be used as a permission grant:

Requirements to be followed when using any portion (e.g., figure, graph, table, or textual material) of an IEEE copyrighted paper in a thesis:

1) In the case of textual material (e.g., using short quotes or referring to the work within these papers) users must give full credit to the original source (author, paper, publication) followed by the IEEE copyright line © 2011 IEEE.
2) In the case of illustrations or tabular material, we require that the copyright line © [Year of original publication] IEEE appear prominently with each reprinted figure and/or table.
3) If a substantial portion of the original paper is to be used, and if you are not the senior author, also obtain the senior author's approval.

Requirements to be followed when using an entire IEEE copyrighted paper in a thesis:

1) The following IEEE copyright/ credit notice should be placed prominently in the references: © [year of original publication] IEEE. Reprinted, with permission, from [author names, paper title, IEEE publication title, and month/year of publication]
2) Only the accepted version of an IEEE copyrighted paper can be used when posting the paper or your thesis on-line.
3) In placing the thesis on the author's university website, please display the following message in a prominent place on the website: In reference to IEEE copyrighted material which is used with permission in this thesis, the IEEE does not endorse any of [university/educational entity's name goes here]'s products or services. Internal or personal use of this material is permitted. If interested in reprinting/republishing IEEE copyrighted material for advertising or promotional purposes or for creating new collective works for resale or redistribution, please go to http://www.ieee.org/publications_standards/publications/rights/rights_link.html to learn how to obtain a License from RightsLink.

If applicable, University Microfilms and/or ProQuest Library, or the Archives of Canada may supply single copies of the dissertation.

BACK | CLOSE WINDOW

B.4 Permission for Use of Figure 1.6

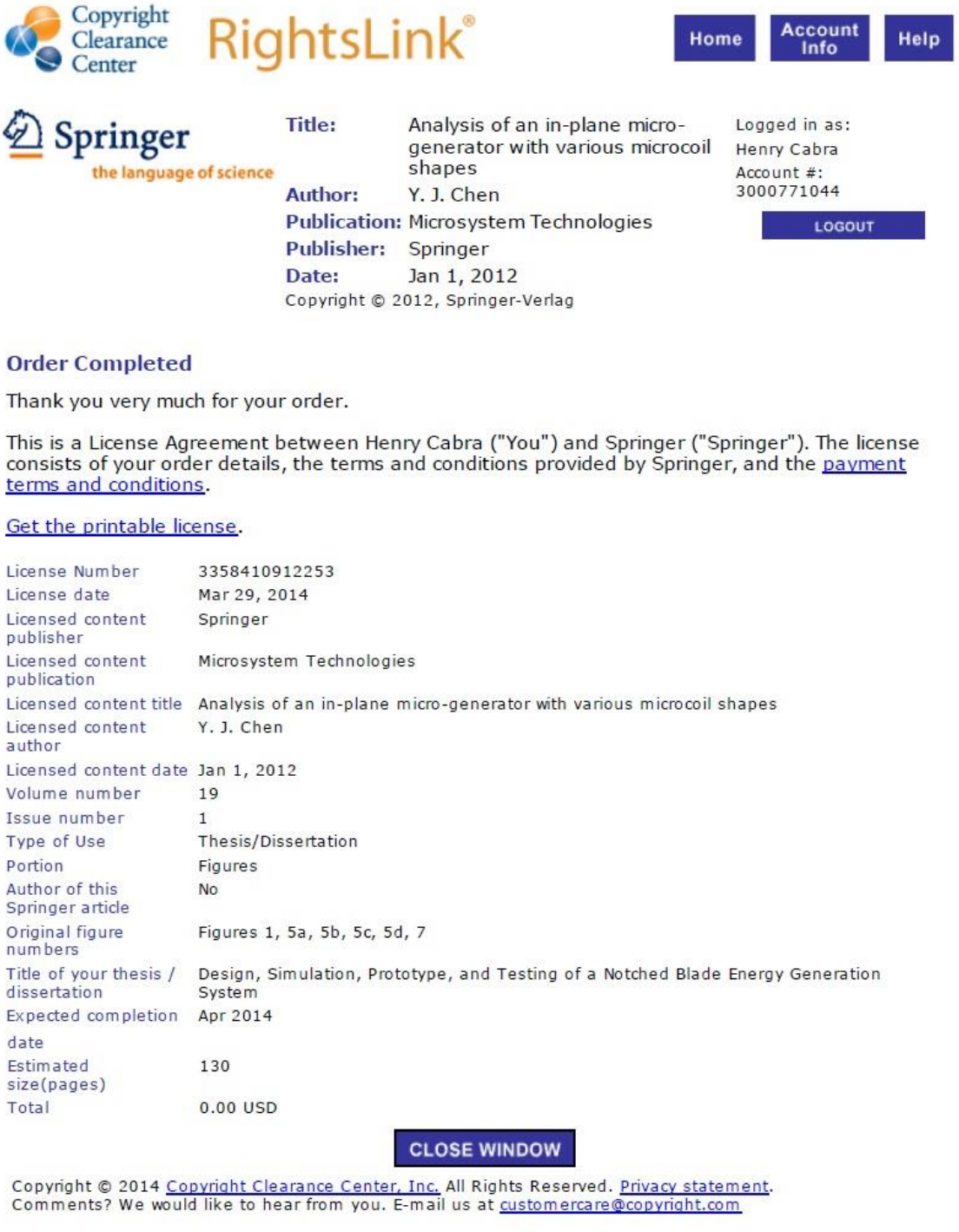

Copyright Clearance Center RightsLink®

Home | Account Info | Help

Springer
the language of science

Title:	Analysis of an in-plane micro-generator with various microcoil shapes
Author:	Y. J. Chen
Publication:	Microsystem Technologies
Publisher:	Springer
Date:	Jan 1, 2012

Copyright © 2012, Springer-Verlag

Logged in as:
Henry Cabra
Account #:
3000771044

LOGOUT

Order Completed

Thank you very much for your order.

This is a License Agreement between Henry Cabra ("You") and Springer ("Springer"). The license consists of your order details, the terms and conditions provided by Springer, and the payment terms and conditions.

Get the printable license.

License Number	3358410912253
License date	Mar 29, 2014
Licensed content publisher	Springer
Licensed content publication	Microsystem Technologies
Licensed content title	Analysis of an in-plane micro-generator with various microcoil shapes
Licensed content author	Y. J. Chen
Licensed content date	Jan 1, 2012
Volume number	19
Issue number	1
Type of Use	Thesis/Dissertation
Portion	Figures
Author of this Springer article	No
Original figure numbers	Figures 1, 5a, 5b, 5c, 5d, 7
Title of your thesis / dissertation	Design, Simulation, Prototype, and Testing of a Notched Blade Energy Generation System
Expected completion date	Apr 2014
Estimated size(pages)	130
Total	0.00 USD

CLOSE WINDOW

Copyright © 2014 Copyright Clearance Center, Inc. All Rights Reserved. Privacy statement.
Comments? We would like to hear from you. E-mail us at customercare@copyright.com

B.5 Permission for Use of Figure 1.7

Copyright Clearance Center RightsLink®

Home | Account Info | Help

IEEE Requesting permission to reuse content from an IEEE publication

Title:	Microfabricated High-Speed Axial-Flux Multiwatt Permanent-Magnet Generators—Part I: Modeling
Author:	Das, S.; Arnold, D.P.; Zana, Iulica; Jin-Woo Park; Allen, M.G.; Lang, Jeffrey H.
Publication:	Microelectromechanical Systems, IEEE/ASME Journal of
Publisher:	IEEE
Date:	Oct 2006

Copyright © 2006, IEEE

Logged in as:
Henry Cabra
Account #:
3000771044
LOGOUT

Thesis / Dissertation Reuse

The IEEE does not require individuals working on a thesis to obtain a formal reuse license, however, you may print out this statement to be used as a permission grant:

Requirements to be followed when using any portion (e.g., figure, graph, table, or textual material) of an IEEE copyrighted paper in a thesis:

1) In the case of textual material (e.g., using short quotes or referring to the work within these papers) users must give full credit to the original source (author, paper, publication) followed by the IEEE copyright line © 2011 IEEE.
2) In the case of illustrations or tabular material, we require that the copyright line © [Year of original publication] IEEE appear prominently with each reprinted figure and/or table.
3) If a substantial portion of the original paper is to be used, and if you are not the senior author, also obtain the senior author's approval.

Requirements to be followed when using an entire IEEE copyrighted paper in a thesis:

1) The following IEEE copyright/ credit notice should be placed prominently in the references: © [year of original publication] IEEE. Reprinted, with permission, from [author names, paper title, IEEE publication title, and month/year of publication]
2) Only the accepted version of an IEEE copyrighted paper can be used when posting the paper or your thesis on-line.
3) In placing the thesis on the author's university website, please display the following message in a prominent place on the website: In reference to IEEE copyrighted material which is used with permission in this thesis, the IEEE does not endorse any of [university/educational entity's name goes here]'s products or services. Internal or personal use of this material is permitted. If interested in reprinting/republishing IEEE copyrighted material for advertising or promotional purposes or for creating new collective works for resale or redistribution, please go to http://www.ieee.org/publications_standards/publications/rights/rights_link.html to learn how to obtain a License from RightsLink.

If applicable, University Microfilms and/or ProQuest Library, or the Archives of Canada may supply single copies of the dissertation.

BACK | CLOSE WINDOW

B.6 Permission for Use of Figure 1.8

Copyright Clearance Center RightsLink®

Home | Account Info | Help

IEEE Requesting permission to reuse content from an IEEE publication

Title:	Micro-rotational electromagnetic generator for high speed applications
Conference Proceedings:	Micro Electro Mechanical Systems (MEMS), 2012 IEEE 25th International Conference on
Author:	Cordero, R.; Rivera, A.; Neuman, M.; Warrington, R.; Romero, E.
Publisher:	IEEE
Date:	Jan. 29 2012-Feb. 2 2012

Copyright © 2012, IEEE

Logged in as:
Henry Cabra
Account #:
3000771044

LOGOUT

Thesis / Dissertation Reuse

The IEEE does not require individuals working on a thesis to obtain a formal reuse license, however, you may print out this statement to be used as a permission grant:

Requirements to be followed when using any portion (e.g., figure, graph, table, or textual material) of an IEEE copyrighted paper in a thesis:

1) In the case of textual material (e.g., using short quotes or referring to the work within these papers) users must give full credit to the original source (author, paper, publication) followed by the IEEE copyright line © 2011 IEEE.
2) In the case of illustrations or tabular material, we require that the copyright line © [Year of original publication] IEEE appear prominently with each reprinted figure and/or table.
3) If a substantial portion of the original paper is to be used, and if you are not the senior author, also obtain the senior author's approval.

Requirements to be followed when using an entire IEEE copyrighted paper in a thesis:

1) The following IEEE copyright/ credit notice should be placed prominently in the references: © [year of original publication] IEEE. Reprinted, with permission, from [author names, paper title, IEEE publication title, and month/year of publication]
2) Only the accepted version of an IEEE copyrighted paper can be used when posting the paper or your thesis on-line.
3) In placing the thesis on the author's university website, please display the following message in a prominent place on the website: In reference to IEEE copyrighted material which is used with permission in this thesis, the IEEE does not endorse any of [university/educational entity's name goes here]'s products or services. Internal or personal use of this material is permitted. If interested in reprinting/republishing IEEE copyrighted material for advertising or promotional purposes or for creating new collective works for resale or redistribution, please go to http://www.ieee.org/publications_standards/publications/rights/rights_link.html to learn how to obtain a License from RightsLink.

If applicable, University Microfilms and/or ProQuest Library, or the Archives of Canada may supply single copies of the dissertation.

BACK | CLOSE WINDOW

Copyright © 2014 Copyright Clearance Center, Inc. All Rights Reserved. Privacy statement.
Comments? We would like to hear from you. E-mail us at customercare@copyright.com

B.7 Permission for Use of Figures 1.9a and 1.9b

ELSEVIER LICENSE
TERMS AND CONDITIONS

Mar 29, 2014

This is a License Agreement between Henry Cabra ("You") and Elsevier ("Elsevier") provided by Copyright Clearance Center ("CCC"). The license consists of your order details, the terms and conditions provided by Elsevier, and the payment terms and conditions.

All payments must be made in full to CCC. For payment instructions, please see information listed at the bottom of this form.

Supplier	Elsevier Limited The Boulevard,Langford Lane Kidlington,Oxford,OX5 1GB,UK
Registered Company Number	1982084
Customer name	Henry Cabra
Customer address	30229 Swinford Ln. Wesley Chapel, FL 33543
License number	3358420481423
License date	Mar 29, 2014
Licensed content publisher	Elsevier
Licensed content publication	Medical Engineering & Physics
Licensed content title	A review of clinical ventricular assist devices
Licensed content author	Daniel Timms
Licensed content date	November 2011
Licensed content volume number	33

Licensed content issue number	9
Number of pages	7
Start Page	1041
End Page	1047
Type of Use	reuse in a thesis/dissertation
Intended publisher of new work	other
Portion	figures/tables/illustrations
Number of figures/tables/illustrations	2
Format	electronic
Are you the author of this Elsevier article?	No
Will you be translating?	No
Title of your thesis/dissertation	Design, Simulation, Prototype, and Testing of a Notched Blade Energy Generation System
Expected completion date	Apr 2014
Estimated size (number of pages)	130
Elsevier VAT number	GB 494 6272 12
Permissions price	0.00 USD
VAT/Local Sales Tax	0.00 USD / 0.00 GBP
Total	0.00 USD
Terms and Conditions	

INTRODUCTION

1. The publisher for this copyrighted material is Elsevier. Byclicking "accept" in connection with completing this licensingtransaction, you agree that the following terms and conditions apply to thistransaction (along with the Billing and Payment terms and conditionsestablished by Copyright

Clearance Center, Inc. ("CCC"), at the timethat you opened your Rightslink account and that are available at any time at http://myaccount.copyright.com).

GENERAL TERMS

2. Elsevier hereby grants you permission to reproduce the aforementionedmaterial subject to the terms and conditions indicated.

3. Acknowledgement: If any part of the material to be used (for example,figures) has appeared in our publication with credit or acknowledgement toanother source, permission must also be sought from that source. If suchpermission is not obtained then that material may not be included in yourpublication/copies. Suitable acknowledgement to the source must be made, eitheras a footnote or in a reference list at the end of your publication, asfollows:

"Reprinted from Publication title, Vol /edition number, Author(s), Title ofarticle / title of chapter, Pages No., Copyright (Year), with permission fromElsevier [OR APPLICABLE SOCIETY COPYRIGHT OWNER]." Also Lancet special credit -"Reprinted from The Lancet, Vol. number, Author(s), Title of article, PagesNo., Copyright (Year), with permission from Elsevier."

4. Reproduction of this material is confined to the purpose and/or media forwhich permission is hereby given.

5. Altering/Modifying Material: Not Permitted. However figures andillustrations may be altered/adapted minimally to serve your work. Any otherabbreviations, additions, deletions and/or any other alterations shall be madeonly with prior written authorization of Elsevier Ltd. (Please contact Elsevierat permissions@elsevier.com)

6. If the permission fee for the requested use of our material is waived inthis instance, please be advised that your future requests for Elseviermaterials may attract a fee.

7. Reservation of Rights: Publisher reserves all rights not specificallygranted in the combination of (i) the license details provided by you andaccepted in the course of this licensing transaction, (ii) these terms andconditions and (iii) CCC's Billing and Payment terms and conditions.

8. License Contingent Upon Payment: While you may exercise the rightslicensed immediately upon issuance of the license at the end of the licensingprocess for the transaction, provided that you have disclosed complete andaccurate details of your proposed use, no license is finally effective unlessand until full payment is received from you (either by publisher or by CCC) asprovided in CCC's Billing and Payment terms and conditions. If fullpayment is not received on a timely basis, then any license preliminarilygranted shall be deemed automatically revoked and shall be void as if nevergranted. Further, in the event that you breach any of these terms andconditions or any of CCC's Billing and Payment terms and conditions, thelicense is automatically revoked and shall be void as if never granted. Use of materials as described in a revoked license, as well as any use of thematerials beyond the scope of an unrevoked license, may constitute copyrightinfringement and publisher reserves the right to take any and all action toprotect its copyright in the materials.

9. Warranties: Publisher makes no representations or warranties with respectto the licensed material.

10. Indemnity: You hereby indemnify and agree to hold harmless publisher andCCC, and their respective officers, directors, employees and agents, from andagainst any and all claims arising out of your use of the licensed materialother than as specifically authorized pursuant to this license.

11. No Transfer of License: This license is personal to you and may not besublicensed, assigned, or transferred by you to any other person withoutpublisher's written permission.

12. No Amendment Except in Writing: This license may not be amended exceptin a writing signed by both parties (or, in the case of publisher, by CCC onpublisher's behalf).

13. Objection to Contrary Terms: Publisher hereby objects to any termscontained in any purchase order, acknowledgment, check endorsement or otherwriting prepared by you, which terms are inconsistent with these terms andconditions or CCC's Billing and Payment terms and conditions. These termsand conditions, together with CCC's Billing and Payment terms and conditions(which are incorporated herein), comprise the entire agreement between you andpublisher (and CCC) concerning this licensing transaction. In the eventof any conflict between your obligations established by these terms andconditions and those established by CCC's Billing and Payment terms andconditions, these terms and conditions shall control.

14. Revocation: Elsevier or Copyright Clearance Center may deny thepermissions described in this License at their sole discretion, for any reasonor no reason, with a full refund payable to you. Notice of such denialwill be made using the contact information provided by you. Failure toreceive such notice will not alter or invalidate the denial. In no eventwill Elsevier or Copyright Clearance Center be responsible or liable for anycosts, expenses or damage incurred by you as a result of a denial of yourpermission request, other than a refund of the amount(s) paid by you toElsevier and/or Copyright Clearance Center for denied permissions.

LIMITED LICENSE

The following terms and conditions apply only to specific license types:

15. **Translation**: This permission is granted fornon-exclusive world **English** rights only unless yourlicense was granted for translation rights. If you licensed translation rightsyou may only translate this content into the languages you requested. Aprofessional translator must perform all translations and reproduce the contentword for word preserving the integrity of the article. If this license is tore-use 1 or 2 figures then permission is granted for non-exclusive world rightsin all languages.

16. **Posting licensed content on any Website**: The followingterms and conditions apply as follows: Licensing material from an Elsevierjournal: All content posted to the web site must maintain the copyright informationline on the bottom of each image; A hyper-text must be included to the Homepageof the journal from which you are licensing at http://www.sciencedirect.com/science/journal/xxxxx orthe Elsevier homepage for books at http://www.elsevier.com; CentralStorage: This license does not include permission for a scanned version of thematerial to be stored in a central repository such as that provided byHeron/XanEdu.

Licensing material from an Elsevier book: A hyper-text link must be includedto the Elsevier homepage at http://www.elsevier.com . Allcontent posted to the web site must maintain the copyright information line onthe bottom of each image.

Posting licensed content on Electronic reserve: In addition to the above the following clausesare applicable: The web site must be password-protected and made available onlyto bona fide students registered on a relevant course. This permission isgranted for 1 year only. You may obtain a new license for future websiteposting.

For journal authors: the following clauses are applicable inaddition to the above: Permission granted is limited to the author acceptedmanuscript version* of your paper.

***Accepted Author Manuscript (AAM) Definition:** An accepted authormanuscript (AAM) is the author's version of the manuscript of an article thathas been accepted for publication and which may include any author-incorporatedchanges suggested through the processes of submission processing, peer review,and editor-author communications. AAMs do not include other publishervalue-added contributions such as copy-editing, formatting, technicalenhancements and (if relevant) pagination.

You are not allowed to download and post the published journal article (whetherPDF or HTML, proof or final version), nor may you scan the printed edition tocreate an electronic version. A hyper-text must be included to the Homepage ofthe journal from which you are licensing at

http://www.sciencedirect.com/science/journal/xxxxx. As part of our normal production process, you will receive an e-mail noticewhen your article appears on Elsevier's online service ScienceDirect(www.sciencedirect.com). That e-mail will include the article's Digital ObjectIdentifier (DOI). This number provides the electronic link to the publishedarticle and should be included in the posting of your personal version. We askthat you wait until you receive this e-mail and have the DOI to do any posting.

Posting to a repository: Authorsmay post their AAM immediately to their employer's institutional repository forinternal use only and may make their manuscript publically available after thejournal-specific embargo period has ended.

Please also refer to Elsevier'sArticle Posting Policy for further information.

18. **For book authors** the following clauses are applicable in addition tothe above: Authors are permitted to place a briefsummary of their work online only.. You are notallowed to download and post the published electronic version of your chapter,nor may you scan the printed edition to create an electronic version. Posting to a repository: Authors arepermitted to post a summary of their chapter only in their institution'srepository.

20. **Thesis/Dissertation**: If your license is for use in athesis/dissertation your thesis may be submitted to your institution in eitherprint or electronic form. Should your thesis be published commercially, pleasereapply for permission. These requirements include permission for the Libraryand Archives of Canada to supply single copies, on demand, of the completethesis and include permission for UMI to supply single copies, on demand, ofthe complete thesis. Should your thesis be published commercially, pleasereapply for permission.

Elsevier Open Access Terms andConditions

CC BY NC SA: For non-commercialpurposes you may distribute and copy the article, create extracts, abstractsand other revised versions, adaptations or derivative works of or from anarticle (such as a translation), to include in a collective work (such as ananthology), to text and data mine the article and license new adaptations or creationsunder identical terms without permission from Elsevier

CC BY NC ND: For non-commercialpurposes you may distribute and copy the article and include it in a collectivework (such as an anthology), provided you do not alter or modify the article,without permission from Elsevier

Any commercial reuse of Open Access articles published with a CC BY NC SA or CC BY NC NDlicense requires permission from Elsevier and will be subject to a fee.

Commercial reuse includes:

- Promotional purposes (advertising or marketing)
- Commercial exploitation (e.g. a product forsale or loan)
- Systematic distribution (for a fee or free ofcharge)

Please refer to Elsevier'sOpen Access Policy for further information.

21. **Other Conditions**:

v1.7

If you would like to pay for this license now, please remit this license along with your payment made payable to "COPYRIGHT CLEARANCE CENTER" otherwise you will be invoiced within 48 hours of the license date. Payment should be in the form of a check or money order referencing your account number and this invoice number RLNK501264184. Once you receive your invoice for this order, you may pay your invoice by credit card. Please follow instructions provided at that time.

Make Payment To:
Copyright Clearance Center
Dept 001
P.O. Box 843006
Boston, MA 02284-3006

For suggestions or comments regarding this order, contact RightsLink Customer Support: customercare@copyright.com or +1-877-622-5543 (toll free in the US) or +1-978-646-2777.

Gratis licenses (referencing $0 in the Total field) are free. Please retain this printable license for your reference. No payment is required.

B.8 Permission for Use of Figure 1.9c

ELSEVIER LICENSE
TERMS AND CONDITIONS

Mar 29, 2014

This is a License Agreement between Henry Cabra ("You") and Elsevier ("Elsevier") provided by Copyright Clearance Center ("CCC"). The license consists of your order details, the terms and conditions provided by Elsevier, and the payment terms and conditions.

All payments must be made in full to CCC. For payment instructions, please see information listed at the bottom of this form.

Supplier	Elsevier Limited The Boulevard,Langford Lane Kidlington,Oxford,OX5 1GB,UK
Registered Company Number	1982084
Customer name	Henry Cabra
Customer address	30229 Swinford Ln. Wesley Chapel, FL 33543
License number	3358431503988
License date	Mar 29, 2014
Licensed content publisher	Elsevier
Licensed content publication	The Annals of Thoracic Surgery
Licensed content title	Bi-Ventricular Circulatory Support With the Abiomed AB5000 System in a Patient With Idiopathic Refractory Ventricular Fibrillation
Licensed content author	Li Zhang,Emmanouil I. Kapetanakis,Richard H. Cooke,Leslie C. Sweet,Steven W. Boyce

Licensed content date	January 2007
Licensed content volume number	83
Licensed content issue number	1
Number of pages	3
Start Page	298
End Page	300
Type of Use	reuse in a thesis/dissertation
Intended publisher of new work	other
Portion	figures/tables/illustrations
Number of figures/tables/illustrations	1
Format	electronic
Are you the author of this Elsevier article?	No
Will you be translating?	No
Title of your thesis/dissertation	Design, Simulation, Prototype, and Testing of a Notched Blade Energy Generation System
Expected completion date	Apr 2014
Estimated size (number of pages)	130
Elsevier VAT number	GB 494 6272 12
Permissions price	0.00 USD
VAT/Local Sales Tax	0.00 USD / 0.00 GBP
Total	0.00 USD
Terms and Conditions	

INTRODUCTION

1. The publisher for this copyrighted material is Elsevier. Byclicking "accept" in connection with completing this licensingtransaction, you agree that the following terms and conditions apply to thistransaction (along with the Billing and Payment terms and conditionsestablished by Copyright

Clearance Center, Inc. ("CCC"), at the timethat you opened your Rightslink account and that are available at any time at http://myaccount.copyright.com).

GENERAL TERMS

2. Elsevier hereby grants you permission to reproduce the aforementionedmaterial subject to the terms and conditions indicated.

3. Acknowledgement: If any part of the material to be used (for example,figures) has appeared in our publication with credit or acknowledgement toanother source, permission must also be sought from that source. If suchpermission is not obtained then that material may not be included in yourpublication/copies. Suitable acknowledgement to the source must be made, eitheras a footnote or in a reference list at the end of your publication, asfollows:

"Reprinted from Publication title, Vol /edition number, Author(s), Title ofarticle / title of chapter, Pages No., Copyright (Year), with permission fromElsevier [OR APPLICABLE SOCIETY COPYRIGHT OWNER]." Also Lancet special credit -"Reprinted from The Lancet, Vol. number, Author(s), Title of article, PagesNo., Copyright (Year), with permission from Elsevier."

4. Reproduction of this material is confined to the purpose and/or media forwhich permission is hereby given.

5. Altering/Modifying Material: Not Permitted. However figures andillustrations may be altered/adapted minimally to serve your work. Any otherabbreviations, additions, deletions and/or any other alterations shall be madeonly with prior written authorization of Elsevier Ltd. (Please contact Elsevierat permissions@elsevier.com)

6. If the permission fee for the requested use of our material is waived inthis instance, please be advised that your future requests for Elseviermaterials may attract a fee.

7. Reservation of Rights: Publisher reserves all rights not specificallygranted in the combination of (i) the license details provided by you andaccepted in the course of this licensing transaction, (ii) these terms andconditions and (iii) CCC's Billing and Payment terms and conditions.

8. License Contingent Upon Payment: While you may exercise the rightslicensed immediately upon issuance of the license at the end of the licensingprocess for the transaction, provided that you have disclosed complete andaccurate details of your proposed use, no license is finally effective unlessand until full payment is received from you (either by publisher or by CCC) asprovided in CCC's Billing and Payment terms and conditions. If fullpayment is not received on a timely basis, then any license preliminarilygranted shall be deemed automatically revoked and shall be void as if nevergranted. Further, in the event that you breach any of these terms andconditions or any of CCC's Billing and Payment terms and conditions, thelicense is automatically revoked and shall be void as if never granted. Use of materials as described in a revoked license, as well as any use of thematerials beyond the scope of an unrevoked license, may constitute copyrightinfringement and publisher reserves the right to take any and all action toprotect its copyright in the materials.

9. Warranties: Publisher makes no representations or warranties with respectto the licensed material.

10. Indemnity: You hereby indemnify and agree to hold harmless publisher andCCC, and their respective officers, directors, employees and agents, from andagainst any and all claims arising out of your use of the licensed materialother than as specifically authorized pursuant to this license.

11. No Transfer of License: This license is personal to you and may not besublicensed, assigned, or transferred by you to any other person withoutpublisher's written permission.

12. No Amendment Except in Writing: This license may not be amended exceptin a writing signed by both parties (or, in the case of publisher, by CCC onpublisher's behalf).

13. Objection to Contrary Terms: Publisher hereby objects to any termscontained in any purchase order, acknowledgment, check endorsement or otherwriting prepared by you, which terms are inconsistent with these terms andconditions or CCC's Billing and Payment terms and conditions. These termsand conditions, together with CCC's Billing and Payment terms and conditions(which are incorporated herein), comprise the entire agreement between you andpublisher (and CCC) concerning this licensing transaction. In the eventof any conflict between your obligations established by these terms andconditions and those established by CCC's Billing and Payment terms andconditions, these terms and conditions shall control.

14. Revocation: Elsevier or Copyright Clearance Center may deny thepermissions described in this License at their sole discretion, for any reasonor no reason, with a full refund payable to you. Notice of such denialwill be made using the contact information provided by you. Failure toreceive such notice will not alter or invalidate the denial. In no eventwill Elsevier or Copyright Clearance Center be responsible or liable for anycosts, expenses or damage incurred by you as a result of a denial of yourpermission request, other than a refund of the amount(s) paid by you toElsevier and/or Copyright Clearance Center for denied permissions.

LIMITED LICENSE

The following terms and conditions apply only to specific license types:

15. **Translation**: This permission is granted fornon-exclusive world **English** rights only unless yourlicense was granted for translation rights. If you licensed translation rightsyou may only translate this content into the languages you requested. Aprofessional translator must perform all translations and reproduce the contentword for word preserving the integrity of the article. If this license is tore-use 1 or 2 figures then permission is granted for non-exclusive world rightsin all languages.

16. **Posting licensed content on any Website**: The followingterms and conditions apply as follows: Licensing material from an Elsevierjournal: All content posted to the web site must maintain the copyright informationline on the bottom of each image; A hyper-text must be included to the Homepageof the journal from which you are licensing at http://www.sciencedirect.com/science/journal/xxxxx orthe Elsevier homepage for books at http://www.elsevier.com; CentralStorage: This license does not include permission for a scanned version of thematerial to be stored in a central repository such as that provided byHeron/XanEdu.

Licensing material from an Elsevier book: A hyper-text link must be includedto the Elsevier homepage at http://www.elsevier.com . Allcontent posted to the web site must maintain the copyright information line onthe bottom of each image.

Posting licensed content on Electronic reserve: In addition to the above the following clausesare applicable: The web site must be password-protected and made available onlyto bona fide students registered on a relevant course. This permission isgranted for 1 year only. You may obtain a new license for future websiteposting.

For journal authors: the following clauses are applicable inaddition to the above: Permission granted is limited to the author acceptedmanuscript version* of your paper.

***Accepted Author Manuscript (AAM) Definition:** An accepted authormanuscript (AAM) is the author's version of the manuscript of an article thathas been accepted for publication and which may include any author-incorporatedchanges suggested through the processes of submission processing, peer review,and editor-author communications. AAMs do not include other publishervalue-added contributions such as copy-editing, formatting, technicalenhancements and (if relevant) pagination.

You are not allowed to download and post the published journal article (whetherPDF or HTML, proof or final version), nor may you scan the printed edition tocreate an electronic version. A hyper-text must be included to the Homepage ofthe journal from which you are licensing at

http://www.sciencedirect.com/science/journal/xxxxx. As part of our normal production process, you will receive an e-mail noticewhen your article appears on Elsevier's online service ScienceDirect(www.sciencedirect.com). That e-mail will include the article's Digital ObjectIdentifier (DOI). This number provides the electronic link to the publishedarticle and should be included in the posting of your personal version. We askthat you wait until you receive this e-mail and have the DOI to do any posting.

Posting to a repository: Authorsmay post their AAM immediately to their employer's institutional repository forinternal use only and may make their manuscript publically available after thejournal-specific embargo period has ended.

Please also refer to Elsevier'sArticle Posting Policy for further information.

18. **For book authors** the following clauses are applicable in addition tothe above: Authors are permitted to place a briefsummary of their work online only.. You are notallowed to download and post the published electronic version of your chapter,nor may you scan the printed edition to create an electronic version. Posting to a repository: Authors arepermitted to post a summary of their chapter only in their institution'srepository.

20. **Thesis/Dissertation**: If your license is for use in athesis/dissertation your thesis may be submitted to your institution in eitherprint or electronic form. Should your thesis be published commercially, pleasereapply for permission. These requirements include permission for the Libraryand Archives of Canada to supply single copies, on demand, of the completethesis and include permission for UMI to supply single copies, on demand, ofthe complete thesis. Should your thesis be published commercially, pleasereapply for permission.

Elsevier Open Access Terms andConditions

CC BY NC SA: For non-commercialpurposes you may distribute and copy the article, create extracts, abstractsand other revised versions, adaptations or derivative works of or from anarticle (such as a translation), to include in a collective work (such as ananthology), to text and data mine the article and license new adaptations or creationsunder identical terms without permission from Elsevier

CC BY NC ND: For non-commercialpurposes you may distribute and copy the article and include it in a collectivework (such as an anthology), provided you do not alter or modify the article,without permission from Elsevier

Any commercial reuse of Open Access articles published with a CC BY NC SA or CC BY NC NDlicense requires permission from Elsevier and will be subject to a fee.

Commercial reuse includes:

- Promotional purposes (advertising or marketing)
- Commercial exploitation (e.g. a product forsale or loan)
- Systematic distribution (for a fee or free ofcharge)

Please refer to Elsevier'sOpen Access Policy for further information.

21. **Other Conditions**:

v1.7

If you would like to pay for this license now, please remit this license along with your payment made payable to "COPYRIGHT CLEARANCE CENTER" otherwise you will be invoiced within 48 hours of the license date. Payment should be in the form of a check or money order referencing your account number and this invoice number RLNK501264184. Once you receive your invoice for this order, you may pay your invoice by credit card. Please follow instructions provided at that time.

Make Payment To:
Copyright Clearance Center
Dept 001
P.O. Box 843006
Boston, MA 02284-3006

For suggestions or comments regarding this order, contact RightsLink Customer Support: customercare@copyright.com or +1-877-622-5543 (toll free in the US) or +1-978-646-2777.

Gratis licenses (referencing $0 in the Total field) are free. Please retain this printable license for your reference. No payment is required.

B.9 Permission for Use of Table 2.2

JOHN WILEY AND SONS LICENSE TERMS AND CONDITIONS

Mar 30, 2014

This is a License Agreement between Henry Cabra ("You") and John Wiley and Sons ("John Wiley and Sons") provided by Copyright Clearance Center ("CCC"). The license consists of your order details, the terms and conditions provided by John Wiley and Sons, and the payment terms and conditions.

All payments must be made in full to CCC. For payment instructions, please see information listed at the bottom of this form.

License Number	3358791266153
License date	Mar 30, 2014
Licensed content publisher	John Wiley and Sons
Licensed content publication	Resource Geology
Licensed content title	Rare Earth Magnets: Conservation of Energy and the Environment
Licensed copyright line	© 2008 The Author Journal compilation © 2008 The Society of Resource Geology
Licensed content author	Takehisa Minowa
Licensed content date	Nov 2, 2008
Start page	414
End page	422
Type of use	Dissertation/Thesis
Requestor type	University/Academic
Format	Electronic

Portion	Figure/table
Number of figures/tables	1
Original Wiley figure/table number(s)	Table 1
Will you be translating?	No
Title of your thesis / dissertation	Design, Simulation, Prototype, and Testing of a Notched Blade Energy Generation System
Expected completion date	Apr 2014
Expected size (number of pages)	130
Total	0.00 USD

Terms and Conditions

Terms and Conditions are not available at this time.

If you would like to pay for this license now, please remit this license along with your payment made payable to "COPYRIGHT CLEARANCE CENTER" otherwise you will be invoiced within 48 hours of the license date. Payment should be in the form of a check or money order referencing your account number and this invoice number RLNK501264433. Once you receive your invoice for this order, you may pay your invoice by credit card. Please follow instructions provided at that time.

Make Payment To:
Copyright Clearance Center
Dept 001
P.O. Box 843006
Boston, MA 02284-3006

For suggestions or comments regarding this order, contact RightsLink Customer Support: customercare@copyright.com or +1-877-622-5543 (toll free in the US) or +1-978-646-2777.

Gratis licenses (referencing $0 in the Total field) are free. Please retain this printable license for your reference. No payment is required.

ABOUT THE AUTHOR

Henry Cabra received his bachelor degree in Electronic Engineering from Universidad Pontificia Bolivariana, Medellín, Colombia in 1994. He then received his MA degree in Communication and Technological Innovation, Instituto Latinoamericano de La Comunicación Educativa (ILCE), México, 2007, and master degree in electrical engineering from the University of South Florida in Tampa, Florida in 2009. During his graduate studies, he conducted research with the Advanced Materials and Biocompatible Interfaces Research (AMBIR) Group, where he worked as a research assistant with Dr. Sylvia Thomas, Assistant professor in the Department of Electrical Engineering. His current research focuses on creating greener and less invasive bio compatible devices and technologies to harvest energy.